WILLIAM & MARY

CHARTERED 1693

Dissertations, Theses, and Masters Projects   Theses, Dissertations, & Master Projects

2010

Hadron structure from holographic QCD

Zainul Abidin
College of William & Mary - Arts & Sciences

Follow this and additional works at: https://scholarworks.wm.edu/etd

Part of the Nuclear Commons

NOTE TO USERS

This reproduction is the best copy available.

UMI®

HADRON STRUCTURE FROM HOLOGRAPHIC QCD

Zainul Abidin

Parepare, Indonesia

Master of Science, College of William and Mary, 2006
Bachelor of Science, Institut Teknologi Bandung, 2004

A Dissertation presented to the Graduate Faculty
of the College of William and Mary in Candidacy for the Degree of
Doctor of Philosophy

Department of Physics

The College of William and Mary
August 2010

APPROVAL PAGE

This Dissertation is submitted in partial fulfillment of
the requirements for the degree of

Doctor of Philosophy

_____

Zainul Abidin

Approved by the Committee, April 2010
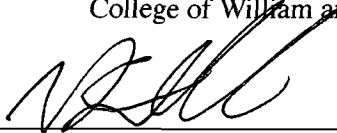
_____
Committee Chair
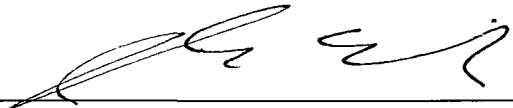Professor Carl E. Carlson, Physics
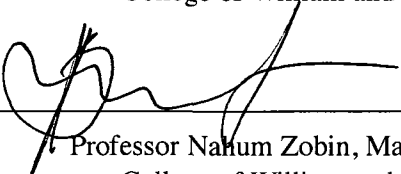College of William and Mary

_____
Associate Professor Todd Averett, Physics
College of William and Mary

_____
Assistant Professor William Detmold, Physics
College of William and Mary

_____
Assistant Professor Joshua Erlich, Physics
College of William and Mary

_____
Professor Nahum Zobin, Mathematics
College of William and Mary

ABSTRACT PAGE

The AdS/CFT correspondence relates a strongly coupled gauge theory in four dimensional space-time with a weakly coupled gravity theory in five dimensional space-time. This correspondence provides a way to access the strongly coupled regime of a gauge theory via a perturbative approach in its gravity dual theory. In this dissertation, the gravity dual of Quantum Chromodynamics(QCD) is discussed. The so-called bottom-up approach (AdS/QCD) successfully reproduces the low energy observables at 10-20% accuracy.

An AdS/QCD model with two flavors of quarks is considered, assuming isospin symmetry. Pions and rho mesons masses and decay constants are obtained. We calculate the stress tensor, or energy-momentum tensor, form factors. Mesons appear strikingly more compact measured by the gravitational form factor than by the electromagnetic form factor.

Extension of the model to three flavors of quarks, incorporating quarks with differing masses (including the strange quark), is also considered. Dynamical properties of mesons such as electromagnetic form factors, strangeness-changing form factors, and gravitational form factors are obtained from 3-point function calculations. The results agree well with experimental data (when available) and with calculations from other methods (when available).

Electromagnetic and gravitational form factors for baryons are calculated, in a scheme where the baryons are treated as independent particles in AdS space. The form factors were calculated both in the case of so called hard-wall and soft-wall model. The simplest fermion Lagrangian for the five dimensional curved space does not contribute to the F_2 form factor unless one adds a Pauli term, which also contributes to the F_1 form factor.

TABLE OF CONTENTS

LIST OF TABLES

LIST OF FIGURES

DEDICATION

I present this dissertation in honor of my beloved parents, Badaruddin A. B. and Haliah Rasyid. Their support has been indispensable in shaping my life until now.

ACKNOWLEDGMENTS

I would like to express my gratitude to Prof. Carl Carlson for his guidance and inspiration over the years. My first interaction with him is when I was his TA for electricity and magnetism class during my first semester in William and Mary. I asked to become his RA student the next summer, and I worked with him ever since. We worked on six paper together during my five year as a graduate student.

I would like to thank members of theoretical high energy particle physics, and theoretical nuclear and hadronic physics groups. Especially to Prof. Erlich for interesting and enlightening discussion on AdS/CFT. Prof. Sher for his willingness to become my annual review committee. I also would like to thank all the committee members of my Ph.D. defense. Physics department staff, especially Paula for reminding me every year to register and to do my annual review.

Finally, I would like to thank my current roommates Bo Zhang and Agus Ananda. My previous roommates Hendra and Jong Tan. Finally, to all Indonesian student who has been in William and Mary, Wirawan, Herry, Reinard, Yudistira, and Adithya. I wish you all a life long and prosper.

CHAPTER 1

Introduction

Until the early 1940s, only a few elementary particles were known: photons, electrons, muons, protons, and neutrons. Subsequent observations, from cosmic ray and particle accelerators, show the existence of a large number of new particles. Most of these new particles, together with protons and neutrons are classified as hadrons. These are particles that can interact through the so-called strong force (interaction), a force that was previously proposed to explain how positively charge protons packed together in the atomic nucleus overcoming their electromagnetic repulsion. Other non-strongly-interacting particles such as electron, muon, tau, and neutrinos, belong to a different classification called leptons. Furthermore, the observed hadrons can be classified into two groups: mesons which are hadrons with integer spin and baryons with half-integer spin.

The observed regularity in hadrons mass spectra suggested that hadrons are not elementary objects but are made of constituent particles with spin-1/2 called quarks, bound by strong interactions. According to the quark model [1], every meson is made of a quark and an anti-quark, while every baryon is made of three quarks. Up through the 1960's only three types (or flavors) of quarks were known: up, down, and strange, although some had suggested the existence of the fourth flavor, the charm quark. The up quark carries an

electric charge of 2/3 (of a proton charge), while the down and the strange quark carry a charge of $-1/3$. To each quark flavor there is an anti-quark with opposite charge. The concrete evidence for the existence of quarks came in 1968, from scattering experiments at high momentum transfer at the Stanford Linear Accelerator Center. This quark model among other things successfully predicts new hadronic states and explains the strength of electromagnetic and weak-interaction transitions among different hadrons.

Despite the phenomenological success, the quark model seems to violate Fermi-Dirac statistics, which states that fermions should be described by totally anti-symmetric wave functions. As an example, consider a Δ^{++} hadron, which is a hadron with spin-3/2 and made of three up quarks. The ground state should be in the zero angular momentum state, that is, a spatially symmetric wave function. Also, the only way to obtain spin-3/2 from three spin-1/2 particles is that the spin of the three quarks align in the same direction, which can only be in a symmetric combination. Hence, overall, we have a totally symmetric wave function. One way out of this dilemma is to introduce an additional degree of freedom. This degree of freedom is called color, and each quark in the Δ^{++} is assigned different color in an anti-symmetric combination.

It was generally believed that the theory of strong interactions may not be described by a perturbative method. However, experimental measurements in a process called deep inelastic electron-proton scattering, reveal that certain functions, which parametrize the cross-sections, become dependent only on a single variable at high momentum transfer. This behavior known as "Bjorken scaling" [2], with the single variable dependence called "Bjorken x". One way to understand Bjorken scaling is to assume that the point-like electron scattered off almost-free point-like constituents. Hence, it appears that although quarks are not free particles, their interaction is quite weak at short distances. This diminishing strength of the strong interaction is known as asymptotic freedom. The discovery of asymptotic freedom subsequently established quantum chromodynamics (QCD) as the theory of the strong interaction. This is in contrast with the theory of quantum electrody-

namics (QED), in which the coupling strength increases at short distances.

In the case of QED, intuitively, the increase of the coupling strength at short distances can be understood as analogous to the screening effect in dielectric materials. Pairs of virtual electrons and positrons created in the surrounding of any electrically charge particles screen the bare electric charges. In the case of QCD, the decrease of coupling strength at shorter distance should be understood as anti-screening effects.

The fact that at large distance (low energy) we observe hadrons but not individually free quarks leads physicists to hypothesize color confinement, i. e., quarks are confined in colorless hadrons. As the two quarks that form a meson are separated from one another, the force between them remains finite, hence the energy required to separate the two quarks to infinity is infinite. Instead, at some separation with sufficient energy, another quark-anti-quark pair will be produced.

Apparently, the perturbative method as in QED is not possible for QCD at large distances. In this regime, solving QCD is a big challenge. One approach is by introducing an effective Lagrangian guided by symmetry assumptions, expecting that it reproduces many of the properties of QCD. Instead of using the coupling strength as the expansion parameter, the smallness of the mass of the pions to the mass of typical hadrons is used as the expansion parameter. This approach is known as chiral perturbation theory [3], since the perturbation is performed around the massless pion limit, which is believed to be associated with massless quark limit, where the QCD Lagrangian has symmetry known as chiral symmetry.

A different perturbation expansion was proposed by t ' Hooft in 1974 [4]. He noticed that QCD simplified when number of quark colors, N_C, becomes large. The real world, where $N_C = 3$, can be obtained by performing perturbation in power of N_C^{-1}. Although, the expansion parameter, $N_C^{-1} = 1/3$, is not as small as the expansion parameter in QED, $\alpha_{QED} = 1/137$, perturbation theory is still useful in the analysis of hadronic processes. Detailed calculations show that the leading order contributions to the amplitude of a par-

ticular process are the planar diagrams with a minimum number of quark loops [5, 6]. A meson in the large N_C limit can be viewed as two quark lines connected by dense sheet of gluons. This description resembles a string moving in space-time and sweeping out a world-sheet.

Preceding QCD as the theory of strong interactions, string theory was introduced to describe the large number of hadrons that were discovered around 1960's. The idea of string theory is that the various hadrons are the excitation modes of vibrating strings. This stringy description of hadrons among other things successfully explains Regge behavior of the hadron spectrum, that is the mass of a hadron with a given spin satisfies $m^2 \sim TJ$, with J is the spin and T is a constant. This Regge behavior can be reproduced by the properties of a rotating relativistic string, with tension T. However, in the early 1970's the theory of Quantum Chromodynamics emerges and is generally recognized as the correct theory of hadrons, with hadrons described as composite particles made of quarks. Subsequently, string theory is no longer identified as a theory of hadrons. Instead, it was suggested that string theory should be identified as a theory of quantum gravity. In the 1990's Polchinski introduced the concept of D-branes [7]. Dp-branes can be viewed as p-dimensional hypersurfaces where open strings can end. The letter "D" stands for Dirichlet and the "brane" is as in membrane.

In 1997, by examining type IIB string theory with stack of N coincident D3-Brane, J. M. Maldacena conjectured relations between a weakly-coupled gravity theory in an anti-de Sitter (AdS_5) space and a strongly-coupled $SU(N)$ gauge theory in a flat 4-dimensional space [8]. The gauge theory also turns out to be conformal, that is, the coupling strength of the theory does not change with energy scale. In addition, it is super-symmetric, that is, the theory is symmetric under a particular transformation of fermion into boson fields and vice versa.

The duality becomes a very promising tool to access the strong regimes of a gauge theory from its weakly coupled gravity dual. However, QCD is neither conformal, nor

supersymmetric. Inspired by the original AdS/CFT (conformal field theory) correspondence, a plethora of models have been proposed for the dual of QCD. Model building applications of the strong-weak duality to QCD can be classified in two categories. The first, dubbed as top-down models, start from string theory in ten dimensional space, constructing a D-brane configuration to reproduce a QCD like theory [9, 10, 11, 12]. The second, dubbed as bottom-up models, anticipates the five dimensional Lagrangian, based on simplicity and symmetry arguments [13, 14, 15].

Progress in computer technology open the possibility to approach the strong coupling regime of QCD numerically, using the lattice gauge calculations. Four dimensional space-time is represented by set of lattice points with as small as possible a lattice spacing. This approach requires intense calculation by a cluster of computers. However, at present, extrapolation to the chiral limit is still difficult. In order to perform the extrapolation, another method is used, such as the chiral perturbation theory.

In this dissertation, some properties of low energy QCD are calculated using the bottom-up AdS/QCD correspondence. Remarkable agreement with experimental data and other methods is obtained.

The organization of the rest of this dissertation is as follows: for the rest of this chapter, the theory of QCD is reviewed, an introduction to the extra-dimensional space with anti-de Sitter geometry is provided, some basic knowledge in AdS/CFT correspondence is given, finally the bottom-up AdS/QCD model is discussed. In the next few chapters applications of the AdS/QCD model are presented to obtain some dynamical properties of hadrons, such as the gravitational form factors, electromagnetic form factors, and strangeness changing form factors. Chapter 2 contains the application of AdS/QCD in obtaining gravitational form factors for vector mesons. Similar application of the correspondence in obtaining the gravitational form factors for pion and axial-vector mesons is presented in Chapter 3. Generalization of the model to include the strange meson is discussed in Chapter 4. In Chapter 5, the spatial density of energy-momentum tensor is calculated

for rho meson based on theoretical AdS/QCD results, and for nucleon based on semi-empirical results. In Chapter 6, the AdS/QCD correspondence application to the nucleon is considered. We also calculate the electromagnetic and the gravitational form factors of proton and neutron.

1.1 Theory of Quantum Chromodynamics

Quantum chromodynamics is a non-Abelian, $SU(3)_C$, gauge theory. The letter 'C' stands for color, while the number three in $SU(3)_C$ represents number of colors. Quarks are in the fundamental representation of the gauge symmetry. Gluons, the force carriers, are in the adjoint representation. The Lagrangian is given by

$$\mathcal{L} = -\frac{1}{4}G^a_{\mu\nu}G^{a\mu\nu} + \sum_f^{N_f} \bar{\psi}_f \left(i\gamma^\mu\partial_\mu + g_s\gamma^\mu G^a_\mu T^a - m_f\right)\psi_f, \tag{1.1}$$

where

$$G^a_{\mu\nu} = \partial_\mu G^a_\nu - \partial_\nu G^a_\mu + g_s f^{abc}G^b_\mu G^c_\nu. \tag{1.2}$$

There are N_f different flavors of quarks, each represented by a Dirac fermion field, ψ_f with mass m_f. Greek letters represent the space time index $\mu = 0, 1, 2, 3$. The Dirac matrices, γ^μ, satisfy the anti-commutation relations

$$\{\gamma^\mu, \gamma^\nu\} = 2\eta^{\mu\nu} \times \mathbf{1}_{4\times4}. \tag{1.3}$$

where $\eta^{\mu\nu} = \mathrm{diag}(1, -1, -1, -1)$.

A distinctive feature of non-Abelian gauge theory compared to the Abelian one is that the gluon field, denoted by G^a_μ, may interact with other gluons. This is apparent in the last term of equation (1.2). The QCD coupling constant is given by g_s, often written in the form of $\alpha_s = g_s^2/(4\pi)$. The $SU(3)_C$ generators and structure constants are denoted by T^a and f^{abc} respectively; the group index a runs from one to eight. The normalization

condition for the SU(3)$_C$ generators in the fundamental representation is given by

$$\text{Tr}(T^a T^b) = \frac{\delta^{ab}}{2}.$$ (1.4)

In addition to SU(3)$_C$ color symmetry, QCD also has approximate SU(3)$_F$ flavor symmetry. The generators of SU(3)$_F$ will be denoted by t^a, to distinguish them.

1.1.1 Symmetries of QCD

The QCD Lagrangian (1.1) constructed based on gauge invariance. Of course, it is also Lorentz invariant as well as symmetric under parity, charge conjugation and time reversal transformations separately. The possibility of adding terms of higher dimensional operators is eliminated by imposing renormalizability. As a gauge invariance theory, the Lagrangian (1.1) is invariant under local symmetry transformations

$$\psi_f \quad \rightarrow \quad U(x)\psi_f \,,$$
$$G_\mu^a T^a \quad \rightarrow \quad U(x)G_\mu^a T^a U^\dagger(x) + ig^{-1}U(x)\partial_\mu U^\dagger(x) \,,$$ (1.5)

where $U(x)$ is an element of SU(3)$_C$.

If the mass of different quark flavors were identical, QCD will also be invariant under global vectorial flavor symmetry. It is currently believed that there are six flavors of quarks. Three of the quarks denoted by charm, bottom, and top are heavy compared to QCD confinement scale, $\Lambda_{\text{QCD}} \sim 300$ MeV and they are far from identical in mass. However, up, down and strange quarks are light enough that SU(3)$_F$ symmetry is useful. Different quark flavors can be combined into a column matrix,

$$\psi = \begin{pmatrix} u \\ d \\ s \end{pmatrix} \underset{SU(3)_F}{\rightarrow} \psi' = U_V \psi = \exp\left(-i\theta_V^a t^a\right)\psi \,,$$ (1.6)

where each component represents a Dirac spinor and the color index is implicit. The symmetry would be manifest as mass degeneracy of hadron SU(3) multiplet. The QCD

Lagrangian is also invariant under global U(1) symmetry

$$\psi \rightarrow \exp(-i\theta)\psi, \qquad (1.7)$$

which gives rise to baryon number conservation. The associated currents for these symmetries can be written as

$$J^\mu = \bar{\psi}\gamma^\mu\psi, \qquad J^{a\mu} = \bar{\psi}\gamma^\mu t^a\psi, \qquad (1.8)$$

the iso-singlet and the iso-octet currents, respectively. The relative difference of the strange quark mass from the up and down quark masses breaks the $SU(3)_F$ symmetry significantly. While predictions of the $SU(3)_F$ hold only to about 30%, those of $SU(2)_F$ isospin subgroup hold to about 1%.

The fermion field can be split into left and right handed chirality as follows

$$\psi_L = \frac{1 - \gamma^5}{2}\psi, \qquad (1.9)$$

$$\psi_R = \frac{1 + \gamma^5}{2}\psi. \qquad (1.10)$$

where $\gamma^5 \equiv i\gamma^0\gamma^1\gamma^2\gamma^3$. If quarks were massless, the QCD Lagrangian will also be invariant under separate left and right global flavor symmetry

$$\psi_L \rightarrow U_L\psi_L, \qquad \psi_R \rightarrow U_R\psi_R. \qquad (1.11)$$

Separating the SU(3) and the U(1) part of the U(3) transformation, the symmetry of massless QCD Lagrangian can be written as $SU(3)_L \times SU(3)_R \times U(1)_L \times U(1)_R$. Conserved currents associated with these symmetries are $J_{L,R}^\mu = \bar{\psi}_{L,R}\gamma^\mu\psi_{L,R}$ and $J_{L,R}^{a\mu} = \bar{\psi}_{L,R}\gamma^\mu t^a\psi_{L,R}$. The sums of left and right handed currents give equation (1.8). In addition, the difference of right and left handed currents give axial-vector currents

$$J_A^\mu = \bar{\psi}\gamma^\mu\gamma^5\psi, \qquad J_A^{a\mu} = \bar{\psi}\gamma^\mu\gamma^5 t^a\psi. \qquad (1.12)$$

This symmetry must be broken, otherwise, we should have observed doubling in the hadrons spectrum, that is, for every positive parity state there is a negative parity state with

the same mass. Nambu and Jona-Lasinio hypothesized that the axial-vector symmetries are broken spontaneously, that is, although the QCD Lagrangian is symmetric under the axial-vector transformation, the QCD ground state is not.

In the theory of superconductivity, pairs of electrons with opposite spins form scalar bound states which condense in the ground state of a metal. In QCD, pairs of quark and anti-quarks are created from the vacuum and condense. This condensation of quark-anti-quark pairs can be explicitly expressed as the non-vanishing vacuum expectation value of the quark bilinear operator,

$$\langle 0|\bar{\psi}\psi|0\rangle = \langle 0|\bar{\psi}_L\psi_R + \bar{\psi}_R\psi_L|0\rangle \neq 0 . \tag{1.13}$$

The QCD vacuum breaks the full $U(3)_L \times U(3)_R$ symmetry down to diagonal subgroup, $U(3)_V$.

Goldstone's theorem states that for every spontaneously broken continuous symmetry there exists a massless spinless particle. Such particles are referred as Nambu-Goldstone bosons or simply Goldstone bosons. This implies that there are nine Goldstone bosons, for nine generators of the broken axial symmetry, $i.e.$, eight from $SU(3)_A$ and one from $U(1)_A$. The nine Goldstone bosons should be the pseudo-scalar octet: π^+, π^-, π^0, $K^+, K^-, K^0, \bar{K}^0, \eta_8$, which correspond to: $u\bar{d}, d\bar{u}, u\bar{u}-d\bar{d}, u\bar{s}, s\bar{u}, d\bar{s}, s\bar{d}, u\bar{u}+d\bar{d}-2s\bar{s}$ quark–anti-quark pairs, respectively; and a pseudo-scalar singlet η_0 which corresponds to a $u\bar{u} + d\bar{d} + s\bar{s}$ quark–anti-quark pair.

It turns out that, although $U(1)_A$ is a symmetry of the classical QCD action, it is not a symmetry of the full quantum theory, since certain quantum corrections (a triangle diagram in which the current couples to two gluons through a quark loop) introduce anomalous terms. The anomaly prevents the iso-singlet axial-vector current from being conserved; instead it satisfies

$$\partial_\mu J_A^\mu = \frac{3\alpha_s}{8\pi}\epsilon^{\mu\nu\alpha\beta}G_{\mu\nu}^a G_{\alpha\beta}^a . \tag{1.14}$$

This prevents the η_0 meson from being a Goldstone boson. Thus, we may expect that the pseudo-scalars octet are massless in the limit of massless quarks, but not necessarily for η_0. The exception is when $N_F \ll N_C$, the triangle diagram that leads to the $U(1)_A$ anomaly is suppressed by $1/N_C$, hence, restoring $U(3)_A$ symmetry [6]. In reality, although they are light compared to typical hadrons, none of the pseudo-scalars are massless. The $SU(3)_L \times SU(3)_R$ symmetry must be broken, explicitly, by quark mass terms. The observed pseudo-scalars: pions(140 MeV), kaons(496 MeV), and η(549 MeV) are light, compared to typical hadrons mass at around 1 GeV. The η(549 MeV) and η'(960 MeV) are a mixture of η_0 and η_8, with η' mostly η_0.

The eight Goldstone bosons are coupled to the broken axial-vector currents through

$$\langle 0|J_{A\mu}^a(0)|\pi^b(p)\rangle = if^a\delta^{ab}p_\mu, \qquad a,b = 1,2,\ldots,8. \tag{1.15}$$

where the constants, f^{ab}, are also known as the decay constants of the corresponding pseudo-scalars. The usual notations for pseudo-scalar mesons can be written as $\pi^0 = \pi^3$, $\pi^\pm = (\pi^1 \mp i\pi^2)/\sqrt{2}$, $K^\pm = (\pi^4 \mp i\pi^5)/\sqrt{2}$, $K^0(\bar{K}^0) = (\pi^6 \mp i\pi^7)/\sqrt{2}$, and $\eta_8 = \pi^8$. By taking the divergence and imposing the conservation of the axial-vector currents, we obtain $p^2 = 0$ for on-shell pions. Thus, we obtain massless pseudo-scalars as required by Goldstone's theorem.

Restoring the quark mass terms, the axial-vector currents are no longer exactly conserved. The masses of the pseudo-scalar mesons, the decay constants, the masses of the quarks and the quark condensates are related through Gell-Mann–Oakes-Renner relations

$$\begin{aligned}
f_\pi^2 m_\pi^2 &= m_q\langle 0|\bar{u}u + \bar{d}d|0\rangle \\
f_K^2 m_K^2 &= \frac{m_u + m_s}{2}\langle 0|\bar{u}u + \bar{s}s|0\rangle \\
f_\eta^2 m_\eta^2 &= \frac{m_q}{3}\langle 0|\bar{u}u + \bar{d}d|0\rangle + \frac{4m_s}{3}\langle 0|\bar{s}s|0\rangle
\end{aligned} \tag{1.16}$$

where equality for the up and the down quark's mass is assumed, $m_q = m_u = m_d$, but not with the strange quark's mass, $m_s \neq m_q$.

1.1.2 Asymptotic Freedom

The perturbative method is applicable to the so-called hard processes, since QCD is asymptotically free, that is, the coupling constant is diminishing for higher energy (shorter distance). One can calculate amplitudes of various processes such as quark-quark scattering, by utilizing the Feynman rules of QCD. The amplitude should be dominated by tree level diagrams.

Up to one loop corrections, the dependence of the QCD coupling strength on energy scale is given by [16]

$$\alpha_s(Q^2) = \frac{\alpha_s(\mu^2)}{1 + \alpha_s(\mu^2) \frac{b_0}{4\pi} \ln(Q^2/\mu^2)} . \tag{1.17}$$

where $Q^2 = \mu^2$ is an arbitrary renormalization point. The constant b_0 is related to color and flavor degrees of freedom by

$$b_0 = \left(\frac{11}{3} N_C - \frac{2}{3} N_F \right) . \tag{1.18}$$

We see that as long as $N_F < 11 N_C/2$, the coupling constant is diminishing as Q^2 is increasing.

We can further define the parameter Λ_{QCD}, via

$$\ln \Lambda^2_{\text{QCD}} = \ln \mu^2 - \frac{4\pi}{\alpha_s(\mu) \, b_0} . \tag{1.19}$$

Then, rewrite QCD coupling constant as

$$\alpha_s(Q^2) = \frac{4\pi}{b_0 \, \ln(Q^2/\Lambda^2_{\text{QCD}})} . \tag{1.20}$$

The coupling constant becomes infinite at $Q^2 = \Lambda^2_{\text{QCD}}$. However, one should note that the perturbative approach, which is how equation (1.17) is derived, breaks down for large α_s. Even so, the parameter Λ_{QCD} is still a useful measure of where the QCD coupling constant becomes large. In fact, the quark masses and Λ_{QCD} are the entire set of parameters of the theory.

The physical reason for the behavior of α_s can be described as follows. Quark–antiquark vacuum polarization shields the color charge, just as the case with electric charge in QED. However, in QCD, gluons also carry color charge and they themselves can emit other gluons. Hence, the charge is no longer located at definite point in space but spread out in space due to gluon emission and absorption. Further from the source, or at smaller Q^2, we see more charge. Closer to the source, or at larger Q^2, it become less likely to see the charge. It turns out that, in QCD, this effect overcomes the shielding effect by the quark–anti-quark vacuum polarization.

The rate of change of the coupling constant with renormalization scale, is usually represented in terms of a β function as

$$\beta(g_s) = \mu \frac{\partial g_s}{\partial \mu} = \frac{g_s^3}{16\pi^2} \left(-\frac{11}{3} N_C + \frac{2}{3} N_F \right) . \tag{1.21}$$

A vanishing β function corresponds to a conformal gauge theory, in which the coupling strength does not change with energy scale. A negative β function, which is the case in QCD, means that the coupling constant decreases when the energy scale increases, and increases when energy scale decreases. The second equality in the above equation is for QCD up to one-loop.

1.1.3 Deep Inelastic Lepton-Hadron Scattering

Evidence for asymptotic freedom comes from a process called deep inelastic scattering. The process can be described as follows. Consider an electron scattered off a proton, exchanging one photon, with final hadrons unobserved (we sum over all possible hadronic final states). The unpolarized differential cross section of the process is given by

$$\frac{d\sigma}{d\Omega dE'} = \left(\frac{d\sigma}{d\Omega} \right)_{\text{Mott}} \left[\frac{1}{M_p} F_1(x, Q^2) \tan^2 \frac{\theta}{2} + \frac{xM_p}{Q^2} F_2(x, Q^2) \right] . \tag{1.22}$$

where θ is the scattering angle in the laboratory frame. $F_1(x, Q^2)$ and $F_2(x, Q^2)$ are Lorentz invariant structure functions, which carry the strong-interaction information of

the proton. The structure functions depend on $Q^2 = -q^2$, the 4-momentum transfer squared in the laboratory frame, and scaling variable

$$x = \frac{Q^2}{2p \cdot q} = \frac{Q^2}{2M_p\nu}, \tag{1.23}$$

where $p = (M_p, \vec{0})$ is the target proton momentum (M_p is the proton mass), and $q = (\nu, \vec{q})$ is the photon momentum in the laboratory frame ($\nu = E - E'$, where E and E' are the energy of the incoming and outgoing electron, respectively). The Mott differential cross section is given by

$$\left(\frac{d\sigma}{d\Omega}\right)_{\text{Mott}} = \frac{\alpha_e^2 \cos^2(\theta/2)}{4E^2 \sin^4(\theta/2)}. \tag{1.24}$$

This is the differential cross section for elastic scattering of a relativistic electron from a point-like spinless particle with recoil effect neglected.

Bjorken scaling is the statement that in the large Q^2 limit with x fixed, the F_i's are functions of x only. The simplest way to obtain Bjorken scaling behavior is by assuming that the proton was a point-like particle. The scattering cross section for elastic electron-proton scattering would be given by

$$\frac{d\sigma}{d\Omega} = \left(\frac{d\sigma}{d\Omega}\right)_{\text{Mott}} \left[\frac{Q^2}{2M_p^2} \tan^2 \frac{\theta}{2} + 1\right] \frac{E'}{E}, \tag{1.25}$$

which can be rewritten as

$$\frac{d\sigma}{d\Omega dE'} = \left(\frac{d\sigma}{d\Omega}\right)_{\text{Mott}} \left[\frac{Q^2}{2M_p^2} \tan^2 \frac{\theta}{2} + 1\right] \delta\left(\nu - \frac{Q^2}{2M_p}\right). \tag{1.26}$$

Thus, the corresponding structure functions would be

$$\begin{aligned}
\frac{1}{M_p} F_1(x, Q^2) &= \frac{Q^2}{2M_p^2} \delta\left(\nu - \frac{Q^2}{2M_p}\right), \\
\frac{xM_p}{Q^2} F_2(x, Q^2) &= \delta\left(\nu - \frac{Q^2}{2M_p}\right),
\end{aligned} \tag{1.27}$$

yielding,

$$\begin{aligned}
F_1(x, Q^2) &= x\delta(1 - x), \\
F_2(x, Q^2) &= 2\delta(1 - x),
\end{aligned} \tag{1.28}$$

which dependent upon a single variable x. That is the most elementary Bjorken scaling.

In spite of the fact that the above assumption is too simple, it suggests the existence of free point-like constituents inside the proton, *i.e.*, quarks. Assume that the photon struck an almost free point-like quark. In the limit of large Q^2, the quark momentum transverse to the proton can be ignored. Hence, the momentum of the i-th quark can be written as

$$p_i = x_i p \tag{1.29}$$

where p is the target proton momentum.

Thus, defining $\nu_i \equiv p_i \cdot q / m_i = \nu$ and $m_i = x_i M_p$, one obtains the structure function for the i-th parton

$$
\begin{aligned}
\frac{1}{m_i} F_1^{(i)}(x_i, Q^2) &= \frac{e_i^2 Q^2}{2m_i^2} \delta\left(\nu_i - \frac{Q^2}{2m_i}\right), \\
&= \frac{e_i^2}{M_p} \delta(x_i - x).
\end{aligned} \tag{1.30}
$$

Now, let $f(x_i) dx_i$ be the probability of i-th quark carries momentum fraction between x_i and $x_i + dx_i$. The corresponding structure functions for the hadron becomes

$$\frac{1}{M_p} F_1(x, Q^2) = \sum_{i=1}^{N} \int_0^1 dx_i f(x_i) \frac{F_1^{(i)}(x_i, Q^2)}{m_i} = \sum_{i=1}^{N} e_i^2 \frac{f(x)}{M_p}, \tag{1.31}$$

Similarly for F_2. In summary, we obtain

$$
\begin{aligned}
F_1 &= \sum_{i=1}^{N} e_i^2 f(x), \\
F_2 &= 2 \sum_{i=1}^{N} e_i^2 x f(x).
\end{aligned} \tag{1.32}
$$

I.e., from a point-like quark assumption, we have obtained Bjorken scaling. The function $f(x)$ is usually referred as the parton distribution function.

1.2 Anti-de Sitter Space

Five dimensional anti-de Sitter space (AdS$_5$) can be realized as a hyperboloid

$$X_0^2 - X_1^2 - X_2^2 - X_3^2 - X_4^2 + X_5^2 = R^2, \tag{1.33}$$

embedded in six dimensional space with metric,

$$ds_6^2 = dX_0^2 - dX_1^2 - dX_2^2 - dX_3^2 - dX_4^2 + dX_5^2. \tag{1.34}$$

A "Lorentz" transformation,

$$X^m \to \Lambda_n^m X^n, \quad \Lambda G \Lambda^T = G, \quad G = diag(1, -1, -1, -1, -1, 1), \tag{1.35}$$

where $m, n = 0, 1, \ldots, 5$, and $\Lambda_n^m \in$ SO(4,2), moves a point in the hyperboloid into another point which is also in the hyperboloid. Furthermore, the transformation preserves distance in the the sense of equation (1.34).

Let us write four of the embedding coordinates as $X_\mu = (X_0, X_1, X_2, X_3)$ and the other two as

$$U = X_4 + X_5, \qquad V = X_4 - X_5. \tag{1.36}$$

The hyperboloid can be parametrized by five dimensional coordinates (x^μ, z) as follows,

$$X^\mu = \frac{Rx^\mu}{z}, \qquad V = \frac{R^2}{z}. \tag{1.37}$$

The AdS metric becomes

$$ds^2 = \frac{R^2}{z^2} \left(\eta_{\mu\nu} dx^\mu dx^\nu - dz^2 \right), \qquad 0 < z < \infty, \tag{1.38}$$

where $\eta_{\mu\nu} =$ diag$(1, -1, -1, -1)$. One should note, however, that this parametrization does not cover the entire hyperboloid. In this parametrization, the boundary at $z = 0$ is four dimensional Minkowski space $x^\mu = (t, \vec{x})$, while at $z = \infty$, we have a single point, since the metric in x^μ directions vanishes in the limit $z \to \infty$.

Anti-de Sitter space is a space with constant curvature. The curvature is described by a quantity called the Ricci scalar,

$$\mathcal{R} = g^{MN}\mathcal{R}^L{}_{MLN}\,, \qquad M, N, L = \mu, z\,, \tag{1.39}$$

where $\mathcal{R}^L{}_{MPN}$ is the Riemann tensor defined as follows

$$\mathcal{R}^L{}_{MPN} = \partial_N \Gamma^L_{MP} - \partial_P \Gamma^L_{MN} + \Gamma^L_{MR}\Gamma^R_{NP} - \Gamma^L_{MN}\Gamma^R_{PR}\,. \tag{1.40}$$

The Christoffel symbols Γ^L_{MN} related to the metric of the space via,

$$\Gamma^L_{MN} = \frac{1}{2}g^{LP}\left(\partial_N g_{MP} + \partial_M g_{PN} - \partial_P g_{MN}\right)\,. \tag{1.41}$$

In particular for AdS$_5$ space, $g_{MN} = \eta_{MN}/z^2$, where $\eta_{MN} = \text{diag}\,(1, -1, -1, -1, -1)$. The resulting Ricci curvature is $\mathcal{R} = -20/R^2$.

Now, consider a field theory defined in x^μ space, $i.e.$, flat four dimensional space. For example, the action for free massless scalar field is given by

$$S = \int d^4x\,(\partial\phi)^2 \tag{1.42}$$

It is invariant under scaling $x^\mu \to \lambda x^\mu$, and $\phi \to \lambda^{-1}\phi$. Field ϕ has energy dimension one, and x has inverse energy dimension. On the AdS side, this symmetry should correspond to a symmetry of the metric. Notice that the metric (1.38) is invariant under scaling, $x^\mu \to \lambda x^\mu$ and $z \to \lambda z$, simultaneously. The implication is that in the AdS$_5$/CFT$_4$ correspondence, a different value of z represents a field theory with different energy scale. From now on, the boundary at $z = 0$ will be referred as ultraviolet boundary, and the boundary at $z = \infty$ will be referred as infrared boundary. Later, in order to simulate confinement in QCD, a cutoff at $z = z_0$ is introduced. In addition, the AdS radius R will be set to one.

Let me end this section by mentioning another AdS metric

$$ds^2 = \frac{R^2}{z^2}\left(f(z)dt^2 - d\vec{x}^2 - \frac{dz^2}{f(z)}\right)\,, \tag{1.43}$$

where $f(z) = 1 - (z/z_h)^4$. This is the black-hole AdS metric, with the event horizon at $z = z_h$. One can check that the Ricci curvature for this metric is also $\mathcal{R} = -20/R^2$.

1.3 The holographic QCD

AdS/CFT was originally motivated by heuristic arguments. Although the correspondence has not yet been proven rigorously, it has been tested extensively, and there is no reason to believe that it fails.

One of the motivations for the duality comes from matching symmetries of the four dimensional conformal field theory with the symmetries of five dimensional AdS space. In the CFT side, we have fifteen generators. Ten of them come from the generators of the usual Lorentz transformation, one comes from the generator of scaling transformation, and the rest come from the so-called special conformal transformations. Overall, they satisfy an $SO(4,2)$ algebra, which is, as mentioned previously, also the isometry of the AdS_5.

The conjecture of Maldacena can be stated as follows:

> $\mathcal{N} = 4$ U(N) super-Yang-Mills in four dimensions is dual to type IIB superstring theory on $AdS_5 \times S_5$,

Duality means that the two seemingly different theories can be considered as two different points of view to describe the same physical system. In this case, in one point of view, D-branes are considered as hypersurfaces where open strings can end, while in the other, the D-branes are considered as non-trivial solutions of a gravitational theory.

Parameters of the string theory and the gauge theory are related as follows

$$\frac{R^4}{\alpha'^2} = g_{YM}^2 N \,, \tag{1.44}$$

where α' is the inverse string tension, R is the AdS radius, and g_{YM} is the coupling constant of the super-Yang-Mills. The limit $R/\sqrt{\alpha'} \to \infty$ is taken. In this limit, the string

theory can be approximated by a supergravity theory. Later, only the AdS$_5$ geometry is considered; the extra five dimensions with geometry S_5 will be dropped. The isometry of S_5 is SO(6), which matches the so-called R-symmetry describing how the scalar fields are rotated among themselves and the fermion fields are rotated among themselves in the $\mathcal{N} = 4$ super Yang-Mills. Dropping the S_5 corresponds to removing the $R-$symmetry of the model.

1.3.1 AdS/CFT dictionary

The precise relation between gravity theory in AdS$_5$ and CFT$_4$ is that the generating functional in CFT, with a source $\phi^0(x)$ for operator $\mathcal{O}(x)$, is equal to partition function in AdS$_5$ with field content $\phi(x, z)$, which approaches $\phi^0(x)$ up to some factor of z at UV-boundary. This statement can be expressed as [17]

$$\left\langle \exp\left(i \int d^4x \phi^0(x)\mathcal{O}(x)\right) \right\rangle = \exp\left(iS_{AdS}\right)\Big|_{\phi(x,\varepsilon)=z^\lambda\phi^0(x)}. \tag{1.45}$$

In the right hand side of the equality, the classical approximation for the partition function is used. The AdS action is evaluated using the classical solution. Utilizing the correspondence, one can calculate n-point correlator of the operator,

$$\langle 0|\mathcal{TO}(x_1)\dots\mathcal{O}(x_n)|0\rangle = \frac{(-i)^n \delta^n e^{iS_{AdS}}}{\delta\phi^0(x_1)\dots\delta\phi^0(x_n)}\Big|_{\phi^0=0}. \tag{1.46}$$

As an example, consider a massless scalar field in AdS$_5$,

$$S = \frac{1}{2}\int d^5x \sqrt{g}\, g^{MN}\partial_M\phi\partial_N\phi. \tag{1.47}$$

where g is the determinant of the AdS metric. Field ϕ satisfies,

$$-z^3\partial_z\left(\frac{1}{z^3}\partial_z\phi\right) + \partial^\mu\partial_\mu\phi = 0. \tag{1.48}$$

The action, evaluated on the solution of the equation of motion, can be written as a surface integral

$$S = \frac{1}{2}\int d^4x \frac{1}{z^3}\phi\partial_z\phi\Big|_{z\to 0}. \tag{1.49}$$

where the AdS radius has been set to one. Note that there is no surface term at $z = \infty$, since the metric in the x^μ direction vanish as $z \to \infty$.

First, let us assume that ϕ only depends on z. The solution can be expressed as

$$\phi(z) = c_1 + c_2 z^4 \tag{1.50}$$

We can identify c_1, the boundary value at $z = 0$, as ϕ^0, the source for some CFT operator $\mathcal{O}$. Using the correspondence (1.46), and the five dimensional action (1.49), one can identify the vacuum expectation value of the operator, $\langle \mathcal{O} \rangle = 2c_2$.

Turning on the dependency of ϕ on x, the solution can be written as [17]

$$\phi(x, z) = \int d^4x' K(x, x'; z) \phi^0(x'), \tag{1.51}$$

where

$$K(x, x'; z) = c_3 \times \frac{z^4}{\left((x - x')^2 - z^2\right)^4}. \tag{1.52}$$

which can be verified by substituting (1.52) into (1.48). One can check that this solution satisfies $\phi(x, z \to 0) = \phi^0(x)$, by noting that $K(x, x'; z \to 0)$ behaves like a delta function. The action (1.49) becomes

$$S = 2c_3 \int d^4x\, d^4x' \frac{\phi^0(x)\phi^0(x')}{(x - x')^8}. \tag{1.53}$$

Again using the correspondence (1.46), one obtains the 2-point correlator

$$\langle \mathcal{O}(x_1)\mathcal{O}(x_2) \rangle \propto \frac{1}{|x_1 - x_2|^8}, \tag{1.54}$$

which implies that the CFT operator $\mathcal{O}$ has mass dimension $\Delta = 4$. For a scalar field ϕ with mass m_5, similar analysis yields [17],

$$\Delta = 2 + \sqrt{4 + m_5^2}. \tag{1.55}$$

In general for a $p-$form operator, the mass of the corresponding five dimensional field satisfies [17]

$$m_5^2 = (\Delta - p)(\Delta + p - 4). \tag{1.56}$$

1.3.2 Bottom-up: AdS/QCD

The correspondence involves an SU(N) gauge theory which has supersymmetry as well as conformal symmetry. Quantum chromodynamics, an SU(3) gauge theory, has neither of these symmetries. Hence, some sort of departure from the original string theory setup is required. First of all, these modifications should break supersymmetry. As for the running of the coupling constant, we might assume that the QCD coupling does not run for a small enough region of energy. This is one of the approximations that is used in the AdS/QCD bottom-up approach.

The bottom-up AdS/QCD model can be described as follows [13, 14]. Instead of starting with a setup of D-branes in ten dimensional spacetime, we anticipated what the five dimensional Lagrangian would be, based on symmetry arguments and simplicity. We want to reproduce most of QCD properties. Here, let us consider QCD with two flavors of quarks. A generalization to three flavors will be discussed Chapter 4. In the two-flavor model, a gauge theory with SU(2)$_L$×SU(2)$_R$ symmetry is introduced in the AdS side to reproduce the approximate global SU(2)$_L$×SU(2)$_R$ symmetry of QCD. A cutoff is introduced in the AdS geometry to reproduce the confinement of QCD. The AdS metric becomes

$$ds^2 = \frac{1}{z^2} \left(dt^2 - d\vec{x}^2 - dz^2 \right) , \qquad 0 < z < z_0. \tag{1.57}$$

where we have set AdS radius to one.

In the previous section, we have discussed that an operator $\mathcal{O}$ in the four dimensional theory corresponds to a field ϕ in the five dimensional theory. There are an infinite number of five dimensional fields corresponding to an infinite number of operators in QCD. However, there are only several crucial operators involved in the dynamics of spontaneously broken SU(2)$_L$×SU(2)$_R$ symmetry. One of these crucial operators is the quark bilinear $\bar{\psi}_L \psi_R$, whose non-vanishing expectation value breaks the full symmetry down to SU(2)$_V$. The corresponding five dimensional field should be a scalar field, X, which

transforms as bifundamental. The conserved current operators of the $SU(2)_L \times SU(2)_R$ symmetry, $J^\mu_{(L)}$ and $J^\mu_{(R)}$, correspond to the gauge fields, L_μ and R_μ, respectively. We will also be interested in the stress tensor operator, $T_{\mu\nu}$, which corresponds to the perturbation of the AdS metric, $g_{\mu\nu} = (\eta_{\mu\nu} + h_{\mu\nu})/z^2$. The operators and fields correspondence are summarized in Table 1.1

TABLE 1.1: Operator/field of the model

$\mathcal{O}(x)$	$\phi(x, z)$	Δ	m_5^2
$\bar{\psi}_L \gamma^\mu t^a \psi_L$	L_μ	3	0
$\bar{\psi}_R \gamma^\mu t^a \psi_R$	R_μ	3	0
$\bar{\psi}_L^\alpha \psi_R^\beta$	$(2/z)X^{\alpha\beta}$	3	-3
$T_{\mu\nu}$	$h_{\mu\nu}$	4	0

The simplest possible gauge invariant five dimensional Lagrangian constructed out of these fields is given by

$$S_{5D} = \int d^5x \sqrt{g} \left\{ \text{Tr}\left[|DX|^2 + 3|X|^2 - \frac{1}{4g_5^2}(F_{(L)}^2 + F_{(R)}^2) \right] \right\}, \qquad (1.58)$$

where the covariant derivative is defined by $D^M X = \partial^M X - iL^M X + iXR^M$, while the field strength is defined by $F_{MN}^{(L)} = \partial_M L_N - \partial_N L_M - i[L_M, L_N]$ and analogously for $F_{MN}^{(R)}$. The gauge field is $L_M = L_M^a t^a$, where t^a is the generator of SU(2). The bifundamental scalar field X can be written in terms of pseudo-scalar field $\pi(x, z)$ and scalar field $X_0(z)$,

$$X(x, z) = X_0(z) \exp\left(i2\pi^a t^a \right). \qquad (1.59)$$

When assuming isospin symmetry, one can take X_0 as a multiple of the identity, and one doesn't have to worry about the ordering. Solving the equation of motion for $X_0(z)$, one obtains

$$X_0(z) = \frac{1}{2} \left(\zeta M z + \frac{1}{\zeta} \Sigma z^3 \right), \qquad (1.60)$$

where $M^{\alpha\beta} = m_q \delta^{\alpha\beta}$ can be identified as the quark mass matrix, sourcing the bilinear operator $\bar{\psi}^\alpha \psi^\beta$ and $\Sigma^{\alpha\beta} = \sigma_q \delta^{\alpha\beta}$ as the vacuum expectation value of the quark bilinear

operator. The rescaling factor, $\zeta = \sqrt{N_C}/(2\pi)$, will be discussed below [18, 19, 20]. For later convenience, let us define $v(z) = (\zeta m_q z + \sigma_q z^3/\zeta)$. As shown later in Chapter 4, this model automatically reproduces the Gell-Mann–Oakes–Renner relations.

1.3.3 Meson Mass and Decay Constant

We will give some technical details here in the introduction. Since the AdS geometry is cut at z_0, a boundary condition has to be specified. A simple gauge invariant boundary condition, $F_{z\mu}(z_0) = 0$, is used, which is nothing but the Neumann boundary condition, $\partial_z L_\mu(z_0) = \partial_z R_\mu(z_0) = 0$, in the $L_z = R_z = 0$ gauge. The boundary condition for the π field will follow from the equation of motion. Hadrons will appear as normalizable modes satisfying this boundary condition. The vector field, axial-vector field, pseudo-scalar field will give rise to vector mesons, axial-vector mesons, and the pseudo-scalar meson, respectively.

Define $V = (L + R)/2$ and $A = (L - R)/2$, and one obtains the equation of motion for the vector field

$$\left(\partial_z(\frac{1}{z}\partial_z V_\mu^a(q,z)) + \frac{q^2}{z}V_\mu^a\right)_\perp = 0. \tag{1.61}$$

where q^μ is the momentum, that is the Fourier conjugate of the coordinate x^μ. For the axial sector, one obtains

$$\partial_z\left(\frac{1}{z}\partial_z A_{\nu\perp}^a\right) + \frac{q^2}{z}A_{\nu\perp}^a - \frac{g_5^2 v^2}{z^3}A_{\nu\perp}^a = 0, \tag{1.62}$$

$$\partial_z\left(\frac{1}{z}\partial_z \phi^a\right) + \frac{g_5^2 v^2}{z^3}(\pi^a - \phi^a) = 0, \tag{1.63}$$

$$-q^2\partial_z\phi^a + \frac{g_5^2 v^2}{z^2}\partial_z\pi^a = 0, \tag{1.64}$$

where ϕ^a is the longitudinal part of A_μ^a, defined by $A_{\mu\|}^a = \partial_\mu\phi^a$. The boundary conditions at z_0 are Neumann for the $V_{\mu\perp}$, $A_{\mu\perp}$, and ϕ fields, while for the π field the boundary condition follows from equation of motion, which is also Neumann. The value of the fields in the $z \to 0$ limit will be identified as the source for the corresponding operators.

Each of the fields can be written in terms of its boundary value multiplying a profile function, which is usually called the bulk-to-boundary propagator. Hence,

$$
\begin{aligned}
V^a_{\mu\perp}(q,z) &= \mathcal{V}(q^2,z)\, V^{0a}_{\mu\perp}(q)\,, \\
A^a_{\mu\perp}(q,z) &= \mathcal{A}(q^2,z)\, A^{0a}_{\mu\perp}(q)\,, \\
A^a_{\mu\parallel}(q,z) &= \phi(q^2,z)\, A^{0a}_{\mu\parallel}(q)\,, \\
\pi(q,z)^a &= \frac{-iq^\mu}{q^2}\pi(q^2,z)A^{0a}_{\mu\parallel}(q)\,.
\end{aligned}
\tag{1.65}
$$

Note that due to isospin symmetry, the bulk-to-boundary propagators are free of any flavor index. For the vector field the solution is

$$
\mathcal{V}(q^2,z) = \frac{\pi}{2}qz\left(\frac{Y_0(qz_0)}{J_0(qz_0)}J_1(qz) - Y_1(qz)\right) \quad q^2 > 0.
\tag{1.66}
$$

The other bulk-to-boundary propagators can be calculated numerically.

Evaluating the action on the solution gives,

$$
\begin{aligned}
S_{5D} = \int \frac{d^4q}{(2\pi)^4}\, & \left(\frac{-1}{2g_5^2}\right) P_T^{\mu\nu} V^a_{\mu\perp}(q,z)\frac{\partial_z V^a_{\nu\perp}(q,z)}{z}\bigg|_{z\to 0} \\
& + \left(\frac{-1}{2g_5^2}\right) P_T^{\mu\nu} A^a_{\mu\perp}(q,z)\frac{\partial_z A^a_{\nu\perp}(q,z)}{z}\bigg|_{z\to 0} \\
& + \left(\frac{-1}{2g_5^2}\right) P_L^{\mu\nu} A^a_{\mu\parallel}(q,z)\frac{\partial_z A^a_{\nu\parallel}(q,z)}{z}\bigg|_{z\to 0} \\
& + \frac{v(z)^2}{2z^3}\pi^a(q,z)\partial_z\pi^a(q,z)\big|_{z\to 0}\,,
\end{aligned}
\tag{1.67}
$$

where $P_T^{\mu\nu} = (\eta^{\mu\nu} - q^\mu q^\nu/q^2)$ and $P_L^{\mu\nu} = q^\mu q^\nu/q^2$ are the transverse and the longitudinal projectors, respectively. Performing functional derivatives with respect to the sources, one can obtain n-point correlators of the current operators.

The n-th Kaluza-Klein modes of mesons can be obtain from the normalizable modes of (1.61-1.64). The normalizable wave functions are denoted by $\psi_n(z)$, $\psi_n^{a_1}$, and $\phi_n(z)$ (or $\pi_n(z)$) for the rho mesons, the a_1-mesons, and the pions, respectively. The eigenvalues, $q^2 = m_n^2$, are identified as the mass of the corresponding mesons in the n-th Kaluza-Klein state. These normalizable wave functions satisfy Neumann boundary condition at $z = z_0$

and vanish at $z = 0$. The wave functions for the rho mesons and the a_1 mesons normalize as $\int (dz/z)\psi_n{}^2 = 1$, while the wave functions of the pions normalize as

$$\int_\varepsilon^{z_0} dz \, \frac{z}{g_5^2 v(z)^2} \partial_z \phi_n(z) \partial_z \phi_m(z) = \frac{\delta_{nm}}{m_n^2} \, . \tag{1.68}$$

Using this normalization, the dimension of the normalizable pion modes is different from the dimension of the bulk-to-boundary propagator. We use it because it is well behaved for the ground state in the chiral limit (despite the $1/m_n^2$ in the right-hand-side).

The bulk-to-boundary propagator can be written as infinite sum over normalizable wave functions. For the transverse vector bulk-to-boundary propagator, we have

$$\mathcal{V}(q^2, z) = -\sum_n \frac{(\partial_z \psi_n(\varepsilon)/\varepsilon) \, \psi_n(z)}{q^2 - m_n^2} \tag{1.69}$$

where $\varepsilon \to 0$. An analogous expression can be obtained for the transverse axial bulk-to-boundary propagator. For the longitudinal part and the pseudoscalar, we have

$$\begin{aligned}
\phi(q^2, z) &= \sum_n \frac{m_n^2 (\partial_z \phi_n(\varepsilon)/\varepsilon) \phi_n(z)}{q^2 - m_n^2} \, , \\
\pi(q^2, z) &= \sum_n \frac{m_n^2 (\partial_z \pi_n(\varepsilon)/\varepsilon) \pi_n(z)}{q^2 - m_n^2} \, .
\end{aligned} \tag{1.70}$$

The wave function for the pion can be obtained numerically. For vector meson, the wave function is given by Bessel function,

$$\psi_n(z) = \frac{\sqrt{2} z J_1(z m_n)}{z_0 J_1(z_0 m_n)} \, , \tag{1.71}$$

where the mass of the vector meson in the n-th Kaluza-Klein state is given by the root of Bessel function, $J_0(m_n z_0) = 0$.

Performing functional derivative twice on the action (1.67), one obtains the 2-point function. In particular, for the vector field

$$\begin{aligned}
i \int d^4 x e^{iqx} \left\langle 0 \left| \mathcal{T} J_\perp^{\mu a}(x) J_\perp^{\nu b}(0) \right| 0 \right\rangle &= -P_T^{\mu\nu} \delta^{ab} \frac{\partial_z \mathcal{V}(q^2, \varepsilon)}{g_5^2 \varepsilon} \, , \\
&= -P_T^{\mu\nu} \frac{Q^2}{2g_5^2} \ln(Q^2) \tag{1.72}
\end{aligned}$$

where the last equality is for large $Q^2 = -q^2$ and the contact term has been dropped. This can be compared with the QCD calculation, in the limit of large Q^2, where the leading order contribution comes from the quark bubble diagram. This matching fits one of the parameters of the model, $g_5^2 = 12\pi^2/N_C = 4\pi^2$.

From the 2-point functions, one can extract F^ρ, the vector meson decay constant, and f^π, the pion decay constant. They are defined via the following matrix elements

$$\langle 0|J_\mu^a(0)|\rho_n^b(p,\lambda)\rangle = F_n^\rho \delta^{ab} \varepsilon_\mu(p,\lambda), \tag{1.73}$$

$$\langle 0|J_{A\mu\|}^a(0)|\pi_n^b(q)\rangle = if_n^\pi q_\mu \delta^{ab}, \tag{1.74}$$

where $\varepsilon_\mu(p,\lambda)$ is the polarization vector of a rho meson with helicity λ. One obtains the decay constant for the vector meson,

$$F_n^\rho = \left.\frac{\partial_z \psi_n(z)}{g_5 z}\right|_{z\to 0}. \tag{1.75}$$

Similar calculations for a_1 mesons and pions yield

$$F_n^{a_1} = \left.\frac{\partial_z \psi_n^{a_1}(z)}{g_5 z}\right|_{z\to 0}, \tag{1.76}$$

$$f_n^\pi = \left.-\frac{\partial_z \phi_n^a(z)}{g_5 z}\right|_{z\to 0}. \tag{1.77}$$

The rescaling factor ζ in (1.60) can be obtained by matching the 2-point correlator of the $\bar\psi_L \psi_R$ operator obtained from AdS/QCD calculation with that of the perturbative QCD calculation, both in the large Q^2 limit.

If the x dependence of the X_0 field is turned on, the equation of motion becomes

$$\partial_z \frac{1}{z^3} \partial_z X_0(q,z) + \frac{3+q^2 z^2}{z^5} X_0(q,z) = 0, \tag{1.78}$$

where the solution can be written in terms of Bessel functions,

$$X_0(q,z) = z^2 \left(d_1 J_1(qz) + d_2 Y_1(qz)\right). \tag{1.79}$$

This solution can be matched with equation (1.60) in the limit of small q^2, fixing the coefficient $d_2 = -\pi q \zeta M/4$. Furthermore, imposing Neumann boundary condition at $z = z_0$, one can determine d_1.

The relevant part of the action can be written as

$$S_{5D} = \int \frac{d^4 q}{(2\pi)^4} \text{Tr} \left(X_0(q,z) \frac{\partial_z X_0(q,z)}{z^3} \right)_{z \to 0} \tag{1.80}$$

Differentiating over the source, M, twice, one obtains the 2-point correlator,

$$i \int d^4 x e^{iqx} \left\langle 0 \left| T \bar{\psi}\psi(x) \bar{\psi}\psi(0) \right| 0 \right\rangle = \frac{\zeta^2 Q^2}{2} \ln(Q^2) \tag{1.81}$$

where large Q^2 limit has been taken and the contact term has been dropped. Comparing this with the perturbative QCD result, one obtains $\zeta = \sqrt{N_C}/(2\pi)$.

The two-flavor AdS/QCD model has three free parameters, z_0, m_q, σ_q. Parameter z_0 can be chosen to fit the calculated rho meson mass with experimental data. Parameters m_q and σ_q can be chosen to fit the calculated pion mass and pion decay constant with experimental data. One obtains,

$$
\begin{aligned}
z_0 &= 1/(322.5\,\text{MeV}) \\
m_q &= (2\pi/\sqrt{3})\,2.29\,\text{MeV} = 8.31\,\text{MeV}\,, \\
\sigma_q &= (\sqrt{3}/(2\pi))\,(328.3\,\text{MeV})^3 = (213.7\,\text{MeV})^3\,.
\end{aligned} \tag{1.82}
$$

The results are displayed in Table 1.2.

1.3.4 Electromagnetic Form Factors

Electromagnetic form factors and gravitational form factors of mesons can be obtained from 3-point correlator involving J^μ_{EM}, the electromagnetic current operator, and $T^{\mu\nu}$, the stress-energy tensor operator, respectively. In this section, we will discuss the former and postpone the discussion for the latter to the next two chapters. Electromagnetic form factors for rho mesons are first calculated in [21], and for pions in [22, 23].

TABLE 1.2: Masses and decay constants.

Observable	AdS/QCD (MeV)	Measured (MeV)
m_π	(fit)	139.6
f_π	(fit)	92.4
m_ρ	(fit)	775.5
$F_\rho^{1/2}$	329	345 ± 8
m_{a_1}	1366	1230 ± 40
$F_{a_1}^{1/2}$	489	433 ± 13

The matrix element of the current operator for spin-1 state can be extracted from the 3-point function using

$$\langle \rho_n^a(p, \lambda_2)|J_\perp^{c\mu}(0)|\rho_k^b(k, \lambda_1)\rangle = \lim_{\substack{p^2 \to m_n^{a\,2} \\ k^2 \to m_k^{c\,2}}} \frac{(p^2 - m_n^{a\,2})(k^2 - m_k^{c\,2})}{F_n^\rho F_k^\rho} \varepsilon_\alpha^*(p, \lambda_2)\varepsilon(k, \lambda_1)$$

$$\times \int d^4x \, d^4w \, e^{ipx - ikw} \langle 0|\mathcal{T}J_\perp^{\alpha a}(x)J_\perp^{\mu c}(0)J_\perp^{\beta b}(w)|0\rangle , \quad (1.83)$$

and for spin-0 state using

$$\langle \pi_n^a(p)|J_\perp^{\mu b}(0)|\pi_k^c(k)\rangle = \lim_{\substack{p^2 \to m_n^{a\,2} \\ k^2 \to m_k^{c\,2}}} \frac{p_\alpha k_\beta}{p^2 k^2} \frac{(p^2 - m_n^{a\,2})(k^2 - m_k^{c\,2})}{f_n^\pi f_k^\pi}$$

$$\times \int d^4x \, d^4w e^{ipx - ikw} \langle 0|\mathcal{T}J_{A\|}^{\alpha a}(x)J_\perp^{\mu b}(0)J_{A\|}^{\beta c}(w)|0\rangle , \quad (1.84)$$

The relevant terms of the action are

$$S_{VVV} = \frac{1}{g_5^2} \int d^5x \frac{1}{z} V^{a\mu} \partial_\mu V_\nu^b V^{c\nu} \varepsilon^{abc} , \quad (1.85)$$

and

$$S_{V\pi\pi} = \int d^5x \left(\frac{1}{2g_5^2 z} \partial^\mu \phi^a V_{\mu\nu}^b \partial^\nu \phi^c + \frac{v(z)^2}{z^3} (\partial^\mu \pi^a - \partial^\mu \phi^a) V_\mu^b \pi^c \right) \varepsilon^{abc} \quad (1.86)$$

For spin-1 state, the general form of the electromagnetic current matrix element can

be written in terms of three form factors,

$$\left\langle \rho_n^+(p_2, \lambda_2) | J_{EM}^\mu(0) | \rho_n^+(p_1, \lambda_1) \right\rangle = -\varepsilon_{2\alpha}^*(p_2, \lambda_2)\varepsilon_{1\beta}(p_1, \lambda_1) \left[\eta^{\alpha\beta}(p_1 + p_2)^\mu G_1(Q^2) \right.$$

$$\left. + \left(\eta^{\mu\alpha} q^\beta - \eta^{\mu\beta} q^\alpha \right) G_2(Q^2) - \frac{1}{2m_n^2} q^\alpha q^\beta (p_1 + p_2)^\mu G_3(Q^2) \right]. \quad (1.87)$$

The three form factors are related to, electric G_C, magnetic G_M, and quadrupole G_Q form factors via

$$G_C = G_1 + \frac{Q^2}{6m_n^2} G_Q, \quad G_M = G_2$$

$$G_Q = G_1 - G_2 + (1 + \frac{Q^2}{4m_n^2}) G_3. \quad (1.88)$$

For spin-0 state, there is only one form factor for the current matrix element,

$$\left\langle \pi_n^+(p_2) | J_{EM}^\mu(0) | \pi_n^+(p_1) \right\rangle = F_{nn}^\pi(Q^2)(p_1 + p_2)^\mu. \quad (1.89)$$

The 3-point functions in (1.83) and (1.84) can be calculated by performing functional derivative over the sources three times to (1.85) and (1.86), respectively. The AdS/QCD model yields, for the rho meson,

$$G_1(Q^2) = F_{nn}^\rho(Q^2), \qquad G_2(Q^2) = 2F_{nn}^\rho(Q^2), \qquad G_3(Q^2) = 0, \quad (1.90)$$

where

$$F_{nn}^\rho(Q^2) = \int_0^{z_0} \frac{dz}{z} \mathcal{V}(Q^2, z)\psi_n(z)\psi_n(z), \quad (1.91)$$

and for the pion,

$$F_{nn}^\pi(Q^2) = \int_0^{z_0} dz \, \mathcal{V}(Q^2, z) \left\{ \frac{1}{z}(\partial_z \phi_n(z))^2 + \frac{g_5^2 v^2(z)}{z^3} (\phi_n(z) - \pi_n(z))^2 \right\}. \quad (1.92)$$

The pion charge form factor is shown in Figure 1.1.

When $Q^2 = 0$, the AdS/QCD results normalize correctly, to give a correct unit charge of the ρ^+ and π^+. The model also "predicts" the magnetic moment $\mu = G_M(0) = 2$ and the quadrupole moment $D = G_Q(0)/m_\rho^2 = -1/m_\rho^2$, for the rho mesons, which are just what we expect for point-like spin-1 particle.
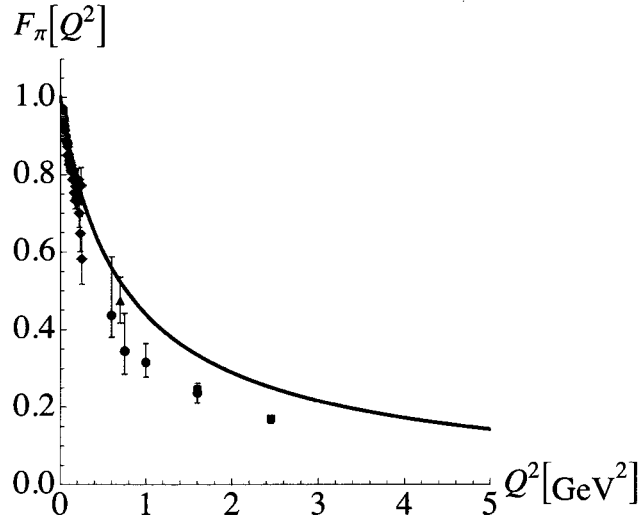
FIG. 1.1: Plot of pion charge form factor. Solid line is the AdS/QCD result. Diamonds are from [24], circles and triangle are from [25], boxes are from [26]

The charge RMS radius is defined from

$$\langle r^2 \rangle_C = -6 \frac{\partial G_C}{\partial Q^2} \bigg|_{Q^2 \to 0} . \tag{1.93}$$

with analogous expressions for the a_1 and for the pion. In the limit of low Q^2, the vector bulk-to-boundary propagator can be expanded as

$$\mathcal{V}(Q^2, z) = 1 - \frac{Q^2 z^2}{4} \left(1 - \ln \left(\frac{z^2}{z_0^2} \right) \right) . \tag{1.94}$$

This gives, $\langle r_\rho^2 \rangle_C = (0.73\,\text{fm})^2$ for the rho meson, $\langle r_{a_1}^2 \rangle_C = (0.62\,\text{fm})^2$ for the a_1 meson, and $\langle r_\pi^2 \rangle_C = (0.57\,\text{fm})^2$ for the pion. These can be compared with a lattice calculation [27] for the rho meson charge radius, $\langle r_\rho^2 \rangle_C = (0.77\,\text{fm})^2$, and with experimental data [28] for the pion charge radius, $\langle r_\pi^2 \rangle_C = (0.67\,\text{fm})^2$.

The scaling behavior of the form factors at large Q^2 can be figured out by noting that, in this limit, the vector bulk-to-boundary propagator (1.66) is essentially $(Qz)K_1(Qz)$, where the modified Bessel function falls asymptotically like e^{-Qz}. Hence, the form factor integrals in (1.91) and (1.92) are supported mainly in the low z region. Furthermore, in

the case of vector meson, near $z = 0, \psi_n(z) = \psi_n''(0)z^2/2$. Therefore,

$$F_{nn}^\rho(Q^2) \to \frac{Q\psi_n''(0)}{4} \int_0^\infty dz z^4 K_1(Qz) = \frac{4(\psi_n''(0))^2}{Q^4} = \frac{8m_n^4}{\gamma_{0,n}^2 J_1^2(\gamma_{0,n})Q^4} , \qquad (1.95)$$

where $\gamma_{0,n}$ is the n-th zero of J_0. Accordingly,

$$G_C \sim 1/Q^2 , \qquad G_M, G_Q \sim 1/Q^4 . \qquad (1.96)$$

One can calculate the ratio among the form factors in the limit of large Q^2 and obtains

$$G_C : G_M : G_Q = \left(1 - \frac{Q^2}{6m_\rho^2}\right) : 2 : -1 , \qquad (1.97)$$

which agrees with perturbative QCD result [29, 30].

For the pion form factor, defining

$$\rho(z) = \left\{ \frac{1}{z^2}(\partial_z \phi_n(z))^2 + \frac{g_5^2 v^2(z)}{z^4} (\phi_n(z) - \pi_n(z))^2 \right\} \qquad (1.98)$$

and noting that for small $z, \rho(z) = \rho(0) + \rho'(0)z + \ldots$, one obtains

$$F_{nn}^\pi(Q^2) \to \frac{2\rho(0)}{Q^2} = \frac{8\pi^2 f_n^{\pi 2}}{Q^2} . \qquad (1.99)$$

which is the an expected scaling behavior from perturbative QCD.

1.3.5 Soft-wall Model

The meson spectrum in the hard-wall AdS/QCD model arises as eigenmodes, satisfying Neumann boundary conditions on the IR boundary and vanishing sufficiently fast on the UV boundary. We have shown that for vector mesons, the mass eigenvalue is $m_n = \gamma_{0,n}/z_0$, where $\gamma_{0,n}$ is the n-th root of J_0. For large n, this becomes, $m_n \sim n$. Similar behavior is obtained for a_1 mesons and pions. However, data shows that the meson masses satisfy, $m_n^2 \sim n$.

A solution to this problem is to introduce a background dilaton field [31], $\Phi(z) = \kappa^2 z^2$, instead of cutting off the AdS metric. The dilaton field will provide some kind

of confinement effect to the mesons wave function. The five dimensional action can be written as

$$S_{5D} = \int d^5 x \, e^{-\Phi(z)} \mathcal{L} \,, \tag{1.100}$$

where $\mathcal{L}$ is the Lagrangian density appears in (1.58).

Consider the vector part of the action. The equation of motion now reads,

$$\left(\partial_z \left(\frac{e^{-\Phi}}{z} \partial_z V_\mu^a(q,z) \right) + \frac{q^2 \, e^{-\Phi}}{z} V_\mu^a \right)_\perp = 0. \tag{1.101}$$

The corresponding normalizable wave functions, denoted by $\psi_n(z)$, solve the above equation with $q^2 = \left(m_n^\rho\right)^2$. Defining $\psi_n = N_1 \xi L_n(\xi)$, where $\xi = \kappa^2 z^2$ and N_1 is a normalization constant, one obtains,

$$\xi \ddot{L}_n(\xi) + (2 - \xi)\dot{L}(\xi) + \left(\frac{m_n^2}{4\kappa^2} - 1 \right) L_n(\xi) = 0 \tag{1.102}$$

which is just the equation for the generalized Laguerre polynomial, $L_n^{(\alpha)}$, with $\alpha = 1$. The wave function becomes,

$$\psi_n(z) = \kappa^2 z^2 \sqrt{\frac{2}{n+1}} L_n^{(1)}(\kappa^2 z^2) \,, \tag{1.103}$$

where the normalization factor has been set such that $\int (dz/z) \exp(-\kappa^2 z^2)\psi_n^2 = 1$. The resulting mass eigenvalue is $(m_n^\rho)^2 = 4\kappa^2(n+1)$, for $n = 0, 1, \ldots$. Hence, the constant κ can be fixed by identifying the lowest state as the rho meson, yielding $\kappa = 388$ MeV.

The bulk-to-boundary propagator of the vector field is given by Kummer's functions [32]. However, one uses only the Kummer's function of the second kind that is not singular near $z = 0$,

$$\mathcal{V}(q^2, z) = N_2 U(a, 0; \xi) \,, \tag{1.104}$$

where $a = -q^2/4\kappa^2$. The Kummer function can be written in integral representation

$$U(a, b; \xi) = \frac{1}{\Gamma(a)} \int_0^1 dx \exp\left(-\xi \frac{x}{1-x} \right) x^{a-1}(1-x)^{-b} \,, \tag{1.105}$$

where in our case $b = 0$. In the limit, $\xi \to 0$, one obtains $U(a, b; 0) = \Gamma(1-b)/\Gamma(a-b+1)$. Hence, by demanding $\mathcal{V}(0, z) = 1$, the coefficient N_2 can be fixed to be $N_2 = a\,\Gamma(a)$.

As in the case of the hard-wall model, the bulk-to-boundary propagator can be expanded as a sum over normalizable modes. To see this, one can write the bulk-to-boundary propagator as

$$\mathcal{V}(q^2, z) = \kappa^2 z^2 \int_0^1 dx \exp\left(-\frac{\kappa^2 z^2\, x}{1-x}\right) \frac{x^a}{(1-x)^2}\,, \tag{1.106}$$

by integration by parts. The integrand contains the generating function for Laguerre polynomials

$$\frac{1}{(1-x)^2} \exp\left(-\frac{x}{1-x}\xi\right) = \sum_{n=0}^{\infty} L_n^{(1)}(\xi) x^n. \tag{1.107}$$

Performing the integrals, one obtains,

$$\mathcal{V}(q^2, z) = -4\kappa^4 z^2 \sum_{n=0}^{\infty} \frac{L_n^{(1)}(\kappa^2 z^2)}{q^2 - 4\kappa^2(n+1)} = -4\kappa^2 \sum_{n=0}^{\infty} \sqrt{\frac{n+1}{2}}\, \frac{\psi_n(z)}{q^2 - m_n^{\rho 2}}\,. \tag{1.108}$$

This result can be compared with equation (1.69) and equation (1.75) in the case of hard-wall model to obtain the decay constant of the vector mesons,

$$F_n^\rho = \frac{\kappa^2}{g_5} \sqrt{8(n+1)}\,. \tag{1.109}$$

For the lightest state, we have $F_0^\rho = (260\,\mathrm{MeV})^2$.

In the soft-wall model, the form factor (1.91) becomes,

$$F_{nn}^\rho(Q^2) = \int_0^{z_0} \frac{dz}{z} e^{-\kappa^2 z^2} \mathcal{V}(Q^2, z) \psi_n(z) \psi_n(z)\,. \tag{1.110}$$

The solution is analytic. In particular for the lightest state, F_{00}^ρ, we have [32]

$$F_{00}^\rho(Q^2) = \frac{2}{1 + Q^2/m_0^{\rho 2}} - \frac{1}{1 + Q^2/m_1^{\rho 2}}\,. \tag{1.111}$$

Hence, only the lowest two bound states contribute to the form factor.

1.3.6 Various AdS/QCD models

The bottom-up AdS/QCD model used in this dissertation is based mainly on [13] and [14], where a bifundamental scalar field is introduced to break the full symmetry down

to its vector subgroup. Other bottom-up models omit the scalar field, instead, they use modified geometry [33] and appropriate choice of boundary conditions [15] to break the full symmetry.

The AdS/QCD calculation of electromagnetic form factors is originally from [21] in the case of rho mesons, and from [22, 23] in the case of pions. The gravitational form factor calculations discussed in Chapter 2 and Chapter 3 of this dissertation is essentially taken from [34, 35]. This is also discussed in [36]. Generalization to three flavors is considered in [37], with subsequent improvement given in [38], which will be discussed in Chapter 4.

As a reference, let me mention other AdS/QCD phenomenological models. AdS/QCD relations to light-front QCD is discussed in [39, 40, 41]. A soft-wall model was proposed in [31] and they also considered higher spin mesons. A soft-wall model with a dynamical dilaton field is considered in [42]. The axial anomaly, in particular for the decay of neutral pions into two photons, is discussed in [43]. The four point correlator, specifically the calculation of the B_K parameter is analyzed in [44].

The AdS/CFT correspondence has been applied to baryons in [45], where a fermion field is introduced in the AdS space, and baryons arise as eigenmodes of the fermion fields. In [46, 47], using five dimensional action with gauge field only and Chern-Simons term added, the baryon arises as a stable soliton solution.

In [48, 49], a bottom-up holographic model for confinement/deconfinement is built. In short, they consider thermal AdS metric, which is metric (1.57) with periodicity in time direction. This corresponds to the confinement phase of QCD. In addition, they also consider the black-hole AdS metric (1.43), which corresponds to the deconfinement phase of QCD.

CHAPTER 2

Gravitational Form Factors of Vector Mesons in an AdS/QCD Model

2.1   Introduction

In this chapter we calculate gravitational form factors — form factors for the stress or energy-momentum tensor — of vector mesons using a hard-wall model of AdS/QCD.

There has been much interest in the AdS/CFT, or gauge/gravity, correspondence because it offers the possibility of relating nonperturbative quantities in theories akin to QCD in 4 dimensions to gravitationally coupled 5-dimensional theories that are treated perturbatively [8]. Many applications have already been made; see references [12, 15, 9, 13, 14, 45, 40, 31, 50, 21, 32, 51, 52, 53] and other works cited in those references. However, for objects of particular interest to hadron structure physics such as ordinary parton distribution functions, form factors, transverse momentum dependent parton distribution functions, and generalized parton distributions, there is a smaller body of work, particularly for the latter two topics.

Part of the interest in gravitational form factors comes because of their connections

to generalized parton distributions (GPDs). GPDs are an important metric of hadron structure, and can be loosely described as amplitudes for removing a parton from a hadron and replacing it with one of different momentum. Moments of the GPDs are related to gravitational form factors. In particular, one of the gravitational form factors measures the total angular momentum carried by partons, and historically the possibility to find the summed spin plus orbital angular momentum of particular constituents of hadrons is what keyed the current experimental and theoretical interest in GPDs [54, 55].

The original AdS/CFT correspondence [8] related a strongly-coupled, large N_c, 4D conformal field theory with a weakly-coupled gravity theory on 5D AdS space. In QCD, N_c is not large, nor is it a conformal field theory, as evidenced by the existence of hadrons with definite mass. Nonetheless, results obtained treating N_c as large work surprisingly well, and one can argue that QCD behaves approximately conformally over wide regions of Q^2 [40]. The AdS/CFT correspondence has been studied in both a "top-down" approach, starting from string theory [12, 9], and a "bottom-up" approach, which uses the properties of QCD to construct its 5D gravity dual theory [13, 14, 45, 40, 31]. We follow the latter approach, particularly as implemented in [13, 14]. Some of the salient results include the meson spectrum, decay constants and electromagnetic form factors for both the rho and the pi [21, 23, 22, 32, 41].

The model uses a sharp cut-off in the AdS space to simulate the breaking of conformal symmetry. The unperturbed metric and relevant slice of 5-dimensional AdS space is

$$ds^2 = \frac{1}{z^2}(\eta_{\mu\nu}dx^\mu dx^\nu - dz^2), \qquad \varepsilon < z < z_0, \tag{2.1}$$

where $\eta_{\mu\nu} = \text{diag}(1, -1, -1, -1)$. The $z = \varepsilon$ wall, with $\varepsilon \to 0$ understood, corresponds to the UV limit of QCD, and the wall located at $z = z_0 \equiv 1/\Lambda_{\text{QCD}}$ sets the scale for the breaking of conformal symmetry of QCD in the IR region. [Lower case Greek indices will run from 0 to 3, and lower case Latin indices will run over $0, 1, 2, 3, 5$.]

Within AdS/CFT, every operator $\mathcal{O}(x)$ in the 4D field theory corresponds to a 5D source field $\phi(x, z)$ in the bulk. Following the model proposed in [13, 14] two of the correspondences are

$$J^a_{(L)}{}^\mu(x) \quad \leftrightarrow \quad L^{a\mu}(x, z),$$

$$J^a_{(R)}{}^\mu(x) \quad \leftrightarrow \quad R^{a\mu}(x, z), \tag{2.2}$$

where $J^a_{(L)}{}^\mu = \bar{\psi}_L \gamma^\mu t^a \psi_L$ and $J^a_{(R)}{}^\mu = \bar{\psi}_R \gamma^\mu t^a \psi_R$ are the chiral flavor currents.

In Lagrangian formulations of general relativity, the source for the stress tensor $T_{\mu\nu}$ is the metric $g^{\mu\nu}$, whose variation is given in terms of $h^{\mu\nu}$. We will use $h_{\mu\nu}$ in the Randall-Sundrum gauge, wherein $h_{\mu\nu}$ is transverse and traceless (TT) and also satisfies $h_{\mu z} = h_{zz} = 0$. Variations of the metric tensor in a TT gauge will only give us the transverse-traceless part of the stress tensor. This will, we shall see below, to uniquely determine 4 of the 6, for spin-1 particles, form factors of the stress tensor, including the two form factors that enter the momentum and angular momentum sum rules.

The layout of this chapter is as follows. Sections 2.2, 2.3, and 6.4, obtain the form factors of the stress tensor using the AdS/CFT correspondence. Specifically, Sec. 2.2 obtains some necessary results for the purely gravitational parts of the theory, and Sec. 2.3 similarly focuses on the vector parts of the action, reviewing necessary results originally obtained in [13, 21]. Section 6.4 works out the three-point functions, and extracts from them the stress tensor matrix elements.

Section 3.4 begins by giving the general expansion of the stress tensor for spin-1 particles, as constrained by the conservation law and symmetries, and then relates five combinations of stress tensor form factors to integrals over the five vector GPDs that exist for spin-1 particles [56]. One of these relations is the spin-1 version of the X. Ji or angular momentum sum rule [54]. The relations as a whole are a set of constraints upon the spin-1 GPDs. We also determine the radius of the vector meson from the form factors that enter the momentum and angular momentum sum rules, and compare it to the electromagnetic

radius. Some conclusions are offered in Sec. 3.5.

2.2 Gravity Sector

The action on the 5-dimensional AdS space is

$$S_{5D} = \int d^5x \sqrt{g} \left\{ \mathcal{R} + 12 + \text{Tr} \left[|DX|^2 + 3|X|^2 - \frac{1}{4g_5^2} (F_{(L)}^2 + F_{(R)}^2) \right] \right\}, \quad (2.3)$$

where $F_{MN}^{(L)} = \partial_M L_N - \partial_N L_M - i[L_M, L_N]$, $L_M = L_M^a t^a$ (analogously for R_M), with $\text{Tr}(t^a t^b) = \delta^{ab}/2$ and $D^M X = \partial^M X - iL^M X + iX R^M$. Only the gravity and vector sectors of the above action are needed in this chapter, and we impose Neumann boundary conditions on the z_0 boundary.

In the purely gravitational part of the action,

$$S_G = \int d^5x \sqrt{g} \, (\mathcal{R} + 12), \quad (2.4)$$

the metric is perturbed from its AdS background according to

$$ds^2 = \frac{1}{z^2} ((\eta_{\mu\nu} + h_{\mu\nu}) dx^\mu dx^\nu - dz^2), \quad 0 < z < z_0, \quad (2.5)$$

where (so far) $h_{zz} = 0$, $h_{z\mu} = 0$ gauge choices have been used. The linearized Einstein equations are

$$
\begin{aligned}
0 &= -h_{\mu\nu,zz} + \frac{3}{z} h_{\mu\nu,z} + h_{\mu\nu,\rho}{}^\rho - 2h^\rho{}_{(\mu,\nu)\rho} \\
&\quad + \eta_{\mu\nu} (\tilde{h}_{,zz} - \frac{3}{z} \tilde{h}_{,z} - \tilde{h}_{,\rho}{}^\rho + h_{\rho\sigma,}{}^{\rho\sigma}) + \tilde{h}_{,\mu\nu} \\
0 &= \tilde{h}_{,\mu z} - h_{\mu\nu,z}{}^\nu \\
0 &= \frac{3}{z} \tilde{h}_{,z} + \tilde{h}_{,\rho}{}^\rho - h_{\rho\sigma,}{}^{\rho\sigma}
\end{aligned}
\quad (2.6)
$$

which come from the $\mu\nu$, μz, and zz sector of the Einstein equation. The trace of $h_{\mu\nu}$ is denoted by $\tilde{h}$. In transverse-traceless gauge, $h_{\mu\nu,}{}^\nu = 0$ and $h_\mu^\mu = 0$. The equation of motion becomes

$$-z^3 \partial_z \left(\frac{1}{z^3} \partial_z h_{\mu\nu} \right) + \partial^\rho \partial_\rho h_{\mu\nu} = 0. \quad (2.7)$$

We do a 4D Fourier transform, and factor the transformed solution as $h_{\mu\nu}(q,z) = h(q,z)h^0_{\mu\nu}(q)$. With $h(q,\epsilon) = 1$, then $h^0_{\mu\nu}(q)$ is the Fourier transform of the UV-boundary value of the graviton. The IR boundary condition becomes $\partial_z h(q,z_0) = 0$. The surface term from the IR boundary obtained when varying the action then vanishes. One finds

$$h(q,z) = \frac{\pi}{4}q^2 z^2 \left(\frac{Y_1(qz_0)}{J_1(qz_0)} J_2(qz) - Y_2(qz) \right). \tag{2.8}$$

For spacelike momentum transfer $q^2 = -Q^2 < 0$ the solution is conveniently rewritten as

$$\mathcal{H}(Q,z) = \frac{1}{2}Q^2 z^2 \left(\frac{K_1(Qz_0)}{I_1(Qz_0)} I_2(Qz) + K_2(Qz) \right). \tag{2.9}$$

Symmetry of the two-index tensor $T^{\mu\nu}$ implies that there are 10 independent components. Conservation of energy-momentum, $q_\mu T^{\mu\nu} = 0$, reduces this to 6 independent components. $T^{\mu\nu}$ can be decomposed into transverse-traceless part $\hat{T}^{\mu\nu}$ with 5 independent components, which leaves the transverse-not-traceless part with one independent component given by $\tilde{T}^{\mu\nu} = \frac{1}{3}(\eta^{\mu\nu} - q^\mu q^\nu/q^2)T$, where T is the trace of $T^{\mu\nu}$:

$$T^{\mu\nu} = \hat{T}^{\mu\nu} + \frac{1}{3}(\eta^{\mu\nu} - \frac{q^\mu q^\nu}{q^2})T. \tag{2.10}$$

This conserved operator couples only to a transverse source. A variation $h^0_{\mu\nu}$ which is transverse and traceless can couple only to $\hat{T}^{\mu\nu}$.

2.3 Vector Sector

Define the vector field $V = (L + R)/2$ and the axial-vector field $A = (L - R)/2$, and consider only the vector part of the action, Eq. (2.3):

$$S_V = \int d^5 x \sqrt{g}\, \mathrm{Tr}\{-\frac{1}{2g_5^2}F_V^2\}, \tag{2.11}$$

where $(F_V)_{MN} = \partial_M V_N - \partial_N V_M$ up to quadratic order in the action. The metric used in this section is non-dynamical, *i.e.*, only the unperturbed part of Eq. (2.5).

In the $V_z = 0$ gauge, the transverse part of the vector field satisfies the following equation of motion,

$$\left(\partial_z (\frac{1}{z} \partial_z V_\mu^a(q, z)) + \frac{q^2}{z} V_\mu^a \right)_\perp = 0. \tag{2.12}$$

The solution can be written as

$$V_{\perp\mu}(q, z) = V(q, z) V_\mu^0(q), \tag{2.13}$$

where $V_\mu^0(q)$ is the Fourier transform of the source of the 4D vector current operator $J_{V\mu}^a = \bar{\psi}\gamma_\mu t^a \psi$. Current conservation, $q_\mu J_V^\mu = 0$, requires that the source is transverse. Therefore only the transverse part of the UV-boundary of 5D vector field will be considered as the source of J_V^μ.

$V(q, z)$ is called the bulk-to-boundary propagator for the vector field, and has boundary conditions $V(q, \epsilon) = 1$ and $\partial_z V(q, z_0) = 0$. The bulk-to-boundary propagator is

$$V(q, z) = \frac{\pi}{2} z q \left(\frac{Y_0(q z_0)}{J_0(q z_0)} J_1(q z) - Y_1(q z) \right). \tag{2.14}$$

Evaluating the action, Eq. (2.11), on the solution leaves only the surface term

$$S_V = \int \frac{d^4 q}{(2\pi)^4} V^{0\mu}(q) V^0{}_\mu(q) \left(-\frac{\partial_z V(q, z)}{2 g_5^2 z} \right)_{z=\epsilon}. \tag{2.15}$$

The Kaluza-Klein tower of the ρ mesons can be obtained from the normalizable solutions of Eq. (2.12) with $q^2 = m_n^2$. The boundary conditions for $\psi_n(x, z)$, the n-th KK-mode ρ-meson's wave function, are $\psi_n(z = 0) = 0$ and $\partial_z \psi_n(z_0) = 0$. The solutions are

$$\psi_n = \frac{\sqrt{2}}{z_0 J_1(m_n z_0)} z J_1(m_n z), \tag{2.16}$$

and satisfy normalization conditions $\int (dz/z) \psi_n^2(z) = 1$.

Using Green's function methods to solve Eq. (2.12), one can show that the bulk-to-boundary propagator can be written in terms of a sum over the infinite tower of KK-modes of the ρ-meson as

$$V(q, z) = -g_5 \sum_n \frac{F_n \psi_n(z)}{q^2 - m_n^2}, \tag{2.17}$$

where $F_n = (1/g_5)(-\frac{1}{z'}\partial_{z'}\psi_n(z'))|_{z'=\epsilon}$. Similar results can be obtained by incorporating the Kneser-Sommerfeld expansion of Bessel functions. The constant F_n is the decay constant of the vector meson, defined by

$$< 0|J_\mu^a(0)|\rho_n^b(p) >= F_n\delta^{ab}\varepsilon_\mu(p). \tag{2.18}$$

This can be seen by calculating 2-point function of vector currents. Taking functional derivatives with respect to V^0 in the 5D action in Eq. (2.15), and changing $V^{0\mu}V^0_{\ \mu}$ to $V^{0\mu}P_{\mu\nu}^T V^{0\nu}$ using the restriction that V^0 is transverse, one finds

$$i\int d^4x\, e^{iqx}\, \langle 0|\, \mathcal{T}J_\mu^a(x)J_\nu^b(0)\, |0\rangle = \Sigma(q^2)P_{\mu\nu}^T\delta^{ab}, \tag{2.19}$$

where $P_{\mu\nu}^T = (\eta_{\mu\nu} - q_\mu q_\nu/q^2)$ is the transverse projector, and

$$\Sigma(q^2) = -\frac{\partial_z V(q,z)}{g_5^2 z}\bigg|_{z=\epsilon} = \frac{1}{g_5^2}\sum_n \frac{(\psi'_n(\epsilon)/\epsilon)^2}{q^2 - m_n^2 + i\varepsilon}. \tag{2.20}$$

Using Eq. (2.18), the left hand side of Eq. (2.19) can be written as

$$i\int d^4x\, e^{iqx}\, \langle 0|\, \mathcal{T}J_\mu^a(x)J_\nu^b(0)\, |0\rangle = \sum_n \frac{F_n^2\delta^{ab}}{q^2 - m_n^2 + i\varepsilon}P_{\mu\nu}^T, \tag{2.21}$$

which confirms the interpretation of F_n in Eq. (2.17) as the decay constants of the ρ-meson tower.

2.4   Gravitational Form Factors of Vector Meson

Stress tensor matrix elements of spin-1 particles defined by $\langle \rho_n^a(p_1)|T^{\mu\nu}(q)|\rho_n^b(p_2)\rangle$ can be extracted from 3-point function

$$\langle 0|\mathcal{T}\big(J_a^{\ \alpha}(x)T^{\mu\nu}(y)J_b^{\ \beta}(w)\big)|0\rangle. \tag{2.22}$$

The Fourier transform of the above 3-point function can be expressed as

$$\langle J^{a\alpha}(-p_2)T^{\mu\nu}(q)J^{b\beta}(p_1)\rangle = \int e^{i(p_1 x - qy - p_2 w)}\langle 0|\mathcal{T}\big(J_a^{\ \alpha}(x)T^{\mu\nu}(y)J_b^{\ \beta}(w)\big)|0\rangle \tag{2.23}$$

In order to pick up the correct term for the elastic stress tensor matrix elements, we apply the completeness relation

$$\sum_n \frac{d^3p}{(2\pi)^3 2p^0} |\rho_n^a(p)\rangle \langle \rho_n^a(p)| = 1 \qquad (2.24)$$

twice, then multiply by

$$\varepsilon_\alpha^*(p_2, \lambda_2)\varepsilon_\beta(p_1, \lambda_1) \left(p_1^2 - m_n^2\right) \left(p_2^2 - m_n^2\right) \frac{1}{F_n^2}, \qquad (2.25)$$

and take the limit $p_1^2 \to m_n^2$ and $p_2^2 \to m_n^2$.

Consider the following part of the full action, Eq. (2.3),

$$S_V = -\frac{1}{4g_5^2} \int d^5x \sqrt{g}\, g^{LM} g^{PN} F_{MN}^a F_{LP}^a. \qquad (2.26)$$

Only hVV terms contribute to the 3-point functions,

$$\langle 0|\mathcal{T} J^\alpha(x)\hat{T}^{\mu\nu}(y)J^\beta(w)|0\rangle = \frac{-2\,\delta^3 S}{\delta V_\alpha^0(x)\delta h_{\mu\nu}^0(y)\delta V_\beta^0(w)}, \qquad (2.27)$$

where the functional derivative is evaluated at $h^0 = V^0 = 0$.

The relevant terms in the action that contribute to the 3-point function can be written as

$$S_V \stackrel{\rightarrow}{=} \frac{1}{2g_5^2} \int \frac{d^5x}{z} \left(\eta^{\rho\gamma}\eta^{\sigma\delta} h_{\gamma\delta} \left[-F_{\sigma z}F_{\rho z} + \eta^{\alpha\beta} F_{\sigma\alpha} F_{\rho\beta}\right]\right), \qquad (2.28)$$

The energy-momentum tensor from Eq. (3.21) must be conserved and traceless. Therefore one may apply the transverse-traceless projector

$$\eta^{\rho\gamma}\eta^{\sigma\delta} h_{\gamma\delta} \to h_{\gamma\delta} \left[\left[\eta^{\rho\gamma} - \frac{q^\rho q^\gamma}{q^2}\right]\left[\eta^{\sigma\delta} - \frac{q^\sigma q^\delta}{q^2}\right] - \frac{1}{3}\left[\eta^{\rho\sigma} - \frac{q^\rho q^\sigma}{q^2}\right]\left[\eta^{\gamma\delta} - \frac{q^\gamma q^\delta}{q^2}\right]\right].(2.29)$$

Taking the functional derivatives and then extracting the gravitational form factor from the 3-point function, one obtains

$$\langle \rho_n^a(p_2, \lambda_2)|\hat{T}^{\mu\nu}(q)|\rho_n^b(p_1, \lambda_1)\rangle = (2\pi)^4 \delta^{(4)}(q + p_1 - p_2)\, \delta^{ab}\, \varepsilon_{2\alpha}^* \varepsilon_{1\beta}$$

$$\times \left[-A(q^2)\left(4q^{[\alpha}\eta^{\beta](\mu} p^{\nu)} + 2\eta^{\alpha\beta} p^\mu p^\nu\right) - \frac{1}{2}\hat{C}(q^2)\eta^{\alpha\beta}\left(q^2\eta^{\mu\nu} - q^\mu q^\nu\right) \qquad (2.30)\right.$$

$$\left. + D(q^2)\left(q^2\eta^{\alpha(\mu}\eta^{\nu)\beta} - 2q^{(\mu}\eta^{\nu)(\alpha}q^{\beta)} + \eta^{\mu\nu}q^\alpha q^\beta\right) - \hat{F}(q^2)\frac{q^\alpha q^\beta}{m_n^2}\left(q^2\eta^{\mu\nu} - q^\mu q^\nu\right)\right],$$

where $p = (p_1 + p_2)/2$, $q = p_2 - p_1$, $a^{[\alpha}b^{\beta]} = (a^\alpha b^\beta - a^\beta b^\alpha)/2$, and $a^{(\alpha}b^{\beta)} = (a^\alpha b^\beta + a^\beta b^\alpha)/2$. The invariant functions are given by

$$
\begin{aligned}
A(q^2) &= Z_2, \\
\hat{C}(q^2) &= \frac{1}{q^2}\left(\frac{4}{3}Z_1 + \left(q^2 - \frac{8m_n^2}{3}\right)Z_2\right), \\
D(q^2) &= \frac{2}{q^2}Z_1 + \left(1 - \frac{2m_n^2}{q^2}\right)Z_2, \\
\hat{F}(q^2) &= \frac{4m_n^2}{3q^4}\left(Z_1 - m_n^2 Z_2\right),
\end{aligned}
\tag{2.31}
$$

with

$$
\begin{aligned}
Z_1 &= \int_0^{z_0} \frac{dz}{z}\mathcal{H}(Q,z)\partial_z\psi_n\partial_z\psi_n, \\
Z_2 &= \int_0^{z_0} \frac{dz}{z}\mathcal{H}(Q,z)\psi_n\psi_n,
\end{aligned}
\tag{2.32}
$$

for spacelike momentum transfer.

The matrix element of $\hat{T}^{\mu\nu}$ in Eq. (2.30) is indeed traceless. It is not traceless term by term, but rather is written in a form that allows easy contact with the general expression for spin-1 matrix elements of the stress tensor, to be given shortly.

The difference between $\hat{T}^{\mu\nu}$, the traceless part of the stress tensor, and the full stress tensor is a term proportional to $(\eta^{\mu\nu} - q^\mu q^\nu/q^2)$, shown in Eq. (2.10). Adding such a term can only affect the terms $\hat{C}(q^2)$ and $\hat{F}(q^2)$ in Eq. (2.30). The form factors $A(q^2)$ and $D(q^2)$ will not change.

2.5 Sum rules for the GPDs

2.5.1 Stress tensor

The stress tensor is a symmetric and transverse two-index object, and is even under parity and time reversal. As such has six independent components, which can be composed as a spin-2 operator plus a spin-0 operator. Its matrix elements with spin-1

particles may in general be expanded in terms of six Lorentz structures multiplying six scalar functions,

$$
\begin{aligned}
\langle p_2, \lambda_2 | T^{\mu\nu} | p_1, \lambda_1 \rangle = \varepsilon_{2\alpha}^* \varepsilon_{1\beta} \Big\{ &- 2A(q^2) \eta^{\alpha\beta} p^\mu p^\nu - 4\big(A(q^2) + B(q^2)\big) q^{[\alpha} \eta^{\beta](\mu} p^{\nu)} \\
&+ \frac{1}{2} C(q^2) \eta^{\alpha\beta} \big(q^\mu q^\nu - q^2 \eta^{\mu\nu}\big) + D(q^2) \big[q^\alpha q^\beta \eta^{\mu\nu} - 2q^{(\alpha} \eta^{\beta)(\mu} q^{\nu)} + q^2 \eta^{\alpha(\mu} \eta^{\nu)\beta} \big] \\
&+ E(q^2) \frac{q^\alpha q^\beta}{m_n^2} p^\mu p^\nu + F(q^2) \frac{q^\alpha q^\beta}{m_n^2} \big(q^\mu q^\nu - q^2 \eta^{\mu\nu}\big) \Big\}.
\end{aligned}
\tag{2.33}
$$

The second listed component has coefficient $(A + B)$ to notationally match the corresponding expansion for spin-1/2 particles. Four of the scalar functions were given from the gauge-gravity correspondence in the last section, and one also learns

$$
B(q^2) = E(q^2) = 0.
\tag{2.34}
$$

This is consistent with the proof given in [57] that the anomalous gravitomagnetic moment $B(0)$ vanishes for any composite system, although here we find B vanishes for all q^2.

2.5.2 Vector GPDs for spin-1 particles

For a spin-1 particle, there are five vector GPDs, defined by [56]

$$
\begin{aligned}
\int \frac{p^+ dy^-}{2\pi} e^{ixp^+ y^-} \quad &\langle p_2, \lambda_2 | \bar{\psi}_q(-\frac{y}{2}) \gamma^+ \psi_q(\frac{y}{2}) | p_1, \lambda_1 \rangle_{y^+=0, y_\perp=0} \\
= &-2(\varepsilon_2^* \cdot \varepsilon_1) p^+ H_1 - \left(\varepsilon_1^+ \varepsilon_2^* \cdot q - \varepsilon_2^{+*} \varepsilon_1 \cdot q\right) H_2 + q \cdot \varepsilon_1 \, q \cdot \varepsilon_2^* \frac{p^+}{m_n^2} H_3 \\
&- \left(\varepsilon_1^+ \varepsilon_2^* \cdot q + \varepsilon_2^{+*} \varepsilon_1 \cdot q\right) H_4 + \left(\frac{m_n^2}{(p^+)^2} \varepsilon_1^+ \varepsilon_2^{+*} + \frac{1}{3}(\varepsilon_2^* \cdot \varepsilon_1)\right) 2p^+ H_5.
\end{aligned}
\tag{2.35}
$$

Each of the GPDs has arguments, $H_i = H_i(x, \xi, t)$, where $q^+ = -2\xi p^+$ and $t = q^2$, and they are related to form factors for spin-1 particles by

$$
\int_{-1}^{1} dx \, H_i(x, \xi, t) = G_i(t), \qquad\qquad i = 1, 2, 3,
$$

$$
\int_{-1}^{1} dx \, H_i(x, \xi, t) = 0, \qquad\qquad i = 4, 5.
\tag{2.36}
$$

The form factors are defined by the matrix elements of the vector current,

$$
\begin{aligned}
\langle p_2, \lambda_2 | \, \bar{\psi}(0)\gamma^\mu\psi(0) \, | p_1, \lambda_1 \rangle \;=\; & -(\varepsilon_2^* \cdot \varepsilon_1)2p^\mu G_1(t) - \left(\varepsilon_1^\mu \varepsilon_2^* \cdot q - \varepsilon_2^{\mu*}\varepsilon_1 \cdot q\right) G_2(t) \\
& + q \cdot \varepsilon_1 \, q \cdot \varepsilon_2^* \frac{p^\mu}{m_n^2} G_3(t) \,.
\end{aligned} \tag{2.37}
$$

The G_i are in turn related to the charge, magnetic, and quadrupole form factors by ($\eta = -t/(4m_n^2)$) [58],

$$
\begin{aligned}
G_1 \;&=\; G_C - \frac{2}{3}\eta G_Q, \\
G_2 \;&=\; G_M, \\
(1+\eta)G_3 \;&=\; -G_C + G_M + \left(1 + \frac{2}{3}\eta\right) G_Q,
\end{aligned} \tag{2.38}
$$

normalized by $G_C(0) = 1$, $G_M(0) = \mu_d$ (magnetic moment in units $(2m_n)^{-1}$), and $G_Q(0) = Q_d$ (quadrupole moment in units m_n^{-2}).

2.5.3 Sum rules

For spin-1/2 constituents,

$$
T^{++}(y) = \frac{i}{2}\bar{\psi}_q(y)\gamma^+ \overleftrightarrow{\partial}^+ \psi_q(x) \tag{2.39}
$$

or,

$$
T^{++}(0) = (p^+)^2 \int x dx \int \frac{dy^-}{2\pi} e^{ixp^+y^-} \left[\bar{\psi}_q(-\frac{y}{2})\gamma^+\psi_q(\frac{y}{2}) \right]_{y^+=0, y_\perp=0}, \tag{2.40}
$$

so that there is a direct relation between the scalar functions in the stress tensor matrix elements and integrals over the GPDs. These read,

$$\int_{-1}^{1} xdx\, H_1(x,\xi,t) = A(t) - \xi^2 C(t) + \frac{t}{6m_n^2}D(t),$$

$$\int_{-1}^{1} xdx\, H_2(x,\xi,t) = 2\left(A(t) + B(t)\right),$$

$$\int_{-1}^{1} xdx\, H_3(x,\xi,t) = E(t) + 4\xi^2 F(t),$$

$$\int_{-1}^{1} xdx\, H_4(x,\xi,t) = -2\xi D(t),$$

$$\int_{-1}^{1} xdx\, H_5(x,\xi,t) = +\frac{t}{2m_n^2}D(t). \tag{2.41}$$

(By time reversal invariance, H_4 is odd in ξ while the other vector GPDs are even in ξ [56, 55].)
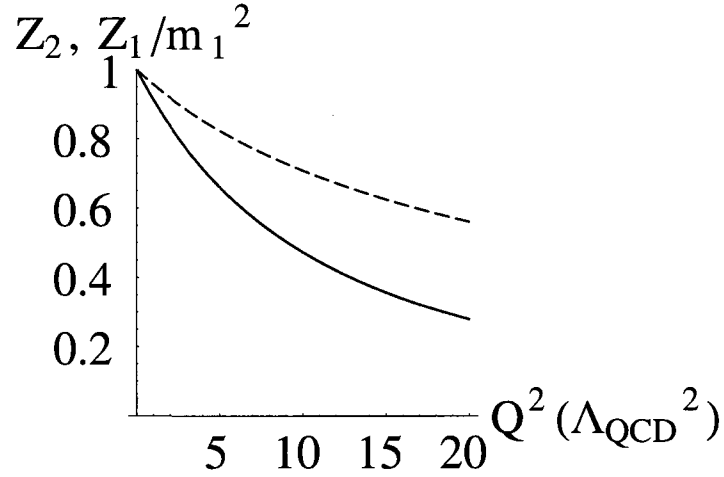
FIG. 2.1: Plot of Z_2 (solid blue curve) and Z_1/M^2 (dashed red curve), with momentum transfer in units of $\Lambda_{QCD} = 1/z_0$.

The relations between the stress tensor and the momentum and angular mometum

operators lead to the sum rules (for any spin) [54],

$$2p^0 p^\mu \delta_{\lambda_1 \lambda_2} = \langle p, \lambda_2| T^{0\mu} |p, \lambda_1 \rangle \tag{2.42}$$

$$2p^0 \lambda_1 \delta_{\lambda_1 \lambda_2} = i\left\{ \frac{\partial}{\partial q^x} \langle p_2, \lambda_2| T^{02} |p_1, \lambda_1 \rangle - \frac{\partial}{\partial q^y} \langle p_2, \lambda_2| T^{01} |p_1, \lambda_1 \rangle \right\}_{q=0},$$

where the latter is written for $\vec{p}$ in the z-direction. Applied to spin-1 particles, this gives the normalizations

$$A(0) = 1,$$

$$A(0) + B(0) = (J_z)_{\text{max}} = 1. \tag{2.43}$$

When connected to the GPDs, the first of these is just the momentum sum rule,

$$\int_{-1}^1 x dx\, H_1(x, 0, 0) = 1, \tag{2.44}$$

and the second gives the spin-1 version of the X. Ji sum rule [54]

$$\int_{-1}^1 x dx\, H_2(x, 0, 0) = 2(J_z)_{\text{max}} = 2. \tag{2.45}$$

(Recall that $0 \leq \xi \leq \sqrt{-t/(4M^2 - t)}$.)

Away from $t = 0$, the gauge-gravity correspondence has led to a set of constraints, of which we will explicitly quote,

$$\int_{-1}^1 x dx \left(H_1(x, 0, t) - \frac{1}{3} H_5(x, 0, t) \right) = Z_2(t),$$

$$\int_{-1}^1 x dx\, H_2(x, 0, t) = 2Z_2(t), \tag{2.46}$$

where the $Z_i(t)$ are explicitly known, and are shown graphically in Fig. 2.1.

2.5.4 Radii

The RMS radius obtained from the gravitational form factor $A(q^2)$ is defined from

$$\langle r^2 \rangle_{\text{grav}} = -6 \left. \frac{\partial A}{\partial Q^2} \right|_{Q^2=0}. \tag{2.47}$$

For small Q^2 we expand

$$\mathcal{H}(Q, z) = 1 - \frac{Q^2 z^2}{4}\left(1 - \frac{z^2}{2z_0^2}\right) + \mathcal{O}(Q^4 z^4), \tag{2.48}$$

and for the lightest vector meson obtain

$$\left\langle r^2 \right\rangle_{\mathrm{grav}} = \frac{3.24}{m_1^2} = 0.21 \text{ fm}^2, \tag{2.49}$$

where we identified $m_1 = m_\rho$.

This is quite small. The charge radius of the rho-meson obtained from AdS/CFT in [21] (and verified by us) is $\langle r^2 \rangle_C = 0.53$ fm^2. Similar charge radius results are obtained by a Dyson-Schwinger equation study [59] and from lattice gauge theory [60]. The result indicates that while the charge is spread over a certain volume, the energy that contributes to the mass of the particle is concentrated in a smaller kernel.

2.5.5 High Q^2 behavior

Asymptotically the non-zero form factors obtained from AdS/QCD fall like $1/Q^4$ for A, C, and D and like $1/Q^6$ for F.

To see this [23], note that at high Qz, the function $\mathcal{H}$ is essentially $\frac{1}{2}Q^2 z^2 K_2(Qz)$, and K_2 falls asymptotically like e^{-Qz}. Hence the integrals for $Z_{1,2}(q^2)$, given in Eq. (2.32), are dominated by low z. Also note that the wave function ψ_n, shown in Eq. (2.16), is proportional to z^2 as $z \to 0$. Hence, for high Q^2,

$$
\begin{aligned}
A(q^2) &= Z_2(q^2) = \frac{Q^2}{8}\int_0^\infty dz\, z^5 K_2(Qz)\, |\psi_n''(0)|^2 \\
&= \frac{12|\psi_n''(0)|^2}{Q^4} = \frac{24 m_n^4}{\gamma_{0,n}^2 J_1^2(\gamma_{0,n}) Q^4},
\end{aligned}
\tag{2.50}
$$

where $\gamma_{0,n}$ is the nth zero of $J_0(z)$. One can similarly show that $Z_1 \sim 1/Q^2$, and the results for C, D, and F follow.

The perturbative QCD (pQCD) predictions for the gravitational form factors are not, to our knowledge, available in the literature, but can be shown to be

$$A, B, C, D \sim 1/Q^4$$

$$E, F \sim 1/Q^6. \tag{2.51}$$

The AdS/CFT results are in precise accord with this.

A complete explication of the pQCD results for the stress tensor form factors would require extensive space and is beyond the scope of the comments in this subsection. However, as a reminder, for electromagnetic form factors of vector mesons, the pQCD predicted scaling behavior is [61]

$$G_C \sim 1/Q^2,$$

$$G_M, G_Q \sim 1/Q^4, \tag{2.52}$$

with an additional result from hadron helicity conservation that $G_C \sim (Q^2/6m_n^2)G_Q$ [61]. One may examine [21] and find that these scaling relations also follow from the AdS/CFT correspondence.

A more detailed prediction follows if the $0 \to 0$ helicity amplitude, in the light front frame, is highly dominant [29, 30]. This is

$$G_C : G_M : G_Q = \left(1 - \frac{Q^2}{6M^2}\right) : 2 : -1, \tag{2.53}$$

a result that also obtains in AdS/CFT [21]. (One may further wish to examine some comments about this relation in [62].)

It was first pointed out in [63] that AdS/CFT could give scaling results that are in accord with pQCD. It is interesting that AdS/CFT can obtain scaling results identical to dimensional analysis results, which depend on the number of quarks in a a bound state [64], when there are no quarks explicitly present in the AdS/CFT correspondence.

Reference [63] also pointed out, however, that the powers of the perturbative QCD coupling were not the same in the two predictions, which we also see here, as the perturbative QCD coupling is not seen in the AdS/CFT results.

2.6 Conclusions

We have worked out the gravitational form factors of the vector mesons using the AdS/CFT correspondence, and have given the sum rules connecting the gravitational form factors, which can also be called stress tensor or energy-momentum tensor form factors, to the vector meson GPDs.

A striking numerical result is the smallness of the vector meson radius as obtained from $A(q^2)$, the gravitational form factor that enters the momentum sum rule. This suggests that the energy that makes up the mass of the meson is well concentrated, with the charge measured by the electromagnetic form factors spreading more broadly.

CHAPTER 3

Gravitational Form Factors in the Axial Sector from an AdS/QCD Model

3.1 Introduction

In this chapter we calculate gravitational form factors, which are form factors of the stress or energy-momentum tensor, in the axial sector using a hard-wall model of AdS/QCD.

The gauge/gravity or AdS/CFT correspondence is studied because it offers the possibility of relating nonperturbative quantities in theories akin to QCD in 4 dimensions to weakly coupled 5-dimensional gravitational theories [8, 65]. Some applications that particularly involve mesons are found in [63, 12, 15, 9, 13, 14, 45, 40, 31, 50, 21, 32, 66, 51, 52, 53] and other works cited therein. The mesons studied are mainly vector and scalar mesons and topics studied include masses, decay constants, coupling constants, and electromagnetic form factors. Less studied to date are parton distributions, be they ordinary ones, or transverse momentum dependent ones, or generalized parton distributions (GPDs).

The present authors [34] have studied gravitational form factors and the connection to GPDs for vector mesons, obtaining sum rules for the GPDs and finding that the vector meson radius appeared notably smaller when measured from a gravitational form factor than from the electromagnetic form factor. We wish to obtain the corresponding results for the pion, a particle for which it may be easier to obtain experimental information about the GPD [67] and for which there is already information on the electromagnetic form factor [26].

Technically, studying the pion is more involved than studying the vector mesons because there are additional terms in the action involving the chiral fields. The ground has been broken by workers who have studied the pion electromagnetic form factor [41, 22, 23]. Our work is similar in its basic approach to the latter two references, but we have attempted to make the present chapter reasonably self-contained. Also, as we are studying the axial sector to learn about the pion, it requires only a small extra effort to also study the axial vector mesons a_1, and we quote results for these in this chapter. We have limited ourselves to the chiral limit, where one can obtain analytic results for many of the quantities of interest.

In general, in AdS/CFT there is a correspondence between 4-dimensional operators $\mathcal{O}(x)$ and fields in the 5-dimensional bulk $\phi(x, z)$, where z is the fifth coordinate. The 4D sources used in the 4D generating function Z_{4D} we will call $\phi^0(x)$, and

$$Z_{4D}[\phi^0] = \left\langle \exp\left(i \int d^4x \, \mathcal{O}(x)\phi^0(x)\right) \right\rangle. \tag{3.1}$$

The correspondence may be written as

$$Z_{4D}[\phi^0] = e^{iS_{5D}[\phi_{cl}]}, \tag{3.2}$$

where on the right, $S[\phi_{cl}]$ is the classical action evaluated for classical solutions ϕ_{cl} to the field equations with boundary condition

$$\lim_{z \to 0} \phi_{cl}(x, z) = z^\Delta \phi^0(x). \tag{3.3}$$

The constant Δ depends on the nature of the operator $\mathcal{O}$, and is zero in simple cases [68].

The original correspondence [8] related a strongly-coupled, large N_c, 4D conformal field theory to a weakly-coupled gravity theory on 5D AdS space. In QCD, N_c is not large, nor is the theory conformal, as evidenced by the existence of hadrons with definite mass. Nonetheless, results obtained treating N_c as large work surprisingly well, and one can argue that QCD behaves approximately conformally over wide regions of Q^2 [40]. We simulate the breaking of conformal symmetry, following the so-called "bottom-up" approach as implemented in [13, 14], by introducing a sharp cutoff in AdS space at $z = z_0$. The unperturbed AdS space metric is

$$ds^2 = g_{MN}dx^M dx^N = \frac{1}{z^2}\eta_{MN}dx^M dx^N, \quad \varepsilon < z < z_0, \tag{3.4}$$

where $\eta_{MN} = \text{diag}(1, -1, -1, -1, -1)$. The $z = \varepsilon$ wall, with $\varepsilon \to 0$ understood, corresponds to the UV limit of QCD, and the wall located at $z = z_0 \equiv 1/\Lambda_{\text{QCD}}$ sets the scale for the breaking of conformal symmetry of QCD in the IR region. [Lower case Greek indices will run from 0 to 3, and upper case Latin indices will run over $0, 1, 2, 3, 5$.]

The $\mathcal{O}$ to ϕ operator correspondences of particular interest here are [13, 14, 68]

$$J_5^{a\mu}(x) \quad \leftrightarrow \quad A^{a\mu}(x, z),$$

$$T_{\mu\nu}(x) \quad \leftrightarrow \quad h_{\mu\nu}(x, z), \tag{3.5}$$

where $J_5^{a\mu} = \bar{\psi}\gamma^\mu\gamma_5 t^a\psi$ is an axial current with flavor index a, $A^{a\mu}$ is an axial field, $T_{\mu\nu}$ is the stress tensor, and $h_{\mu\nu}$ represents variations of the metric tensor,

$$g_{\mu\nu}(x, z) = \frac{1}{z^2}\left(\eta_{\mu\nu} + h_{\mu\nu}(x, z)\right) \tag{3.6}$$

We will use $h_{\mu\nu}$ in the Randall-Sundrum gauge [69], wherein $h_{\mu\nu}$ is transverse and traceless (TT) and also satisfies $h_{\mu z} = h_{zz} = 0$. Variations of the metric tensor in a TT gauge will only give us the transverse-traceless part of the stress tensor. This will determine uniquely one of the two gravitational form factors of the pion, the one that

enters the momentum sum rule, and correspondingly 4 of the 6 gravitational form factors for spin-1 particles, including the two that enter the momentum and angular momentum sum rules.

Relevant details regarding the pion and axial-vector mesons, including the wave functions and the two-point functions, are worked out in Sec. 3.2, and Sec. 6.4 works out the three-point functions, and extracts from them the stress tensor matrix elements. Sum rules and stress tensor form factor radii are given in Sec. 3.4 and some conclusions are offered in Sec. 3.5.

3.2 Pion and Axial-Vector Meson

3.2.1 AdS/QCD Model

The action on the 5-dimensional AdS space is [13]

$$S_{5D} = \int d^5x \sqrt{g} \left\{ \mathcal{R} + 12 + \mathrm{Tr} \left[|DX|^2 + 3|X|^2 - \frac{1}{4g_5^2}(F_{(L)}^2 + F_{(R)}^2) \right] \right\}. \quad (3.7)$$

This action contains the X field, which corresponds to 4D operator $\bar{q}_R q_L$ and, through $F_{(L)}^{MN} = \partial^M L^N - \partial^N L^M - i[L^M, L^N]$ (analogously for $F_{(R)}^{MN}$), also contains the $L^a{}_\mu$ and $R^a{}_\mu$ fields, which correspond to operators $J_{(L)\mu}^a = \bar{q}_L \gamma_\mu t^a q_L$ and $J_{(R)\mu}^a = \bar{q}_R \gamma_\mu t^a q_R$ respectively. We define $L_M(x,z) = L_M^a(x,z)t^a$ and $R_M(x,z) = R_M^a(x,z)t^a$, where the group generators satisfy $\mathrm{Tr}(t^a t^b) = \delta^{ab}/2$. The covariant derivative of the X field is given by $D^M X = \partial^M X - iL^M X + iX R^M$. Moreover, the X field can be written in exponential form as $X(x,z) = X_0(z) \exp(2it^a\pi^a)$. Solving the equation of motion of $X_0(z)$, one obtains $X_0 = \frac{1}{2}\mathbb{I}v(z)$, where $v(z) = m_q z + \sigma z^3$. Using the AdS/CFT prescription and the fact that $\bar{q}_R q_L$ appears in the mass term of QCD Lagrangian, parameter m_q can be identified as the quark mass and parameter σ as the quark condensate $\langle \bar{q}q \rangle$. In this chapter, we will discuss only the chiral limit of the AdS/QCD model, i.e $m_\pi = 0$ case, or equivalently $m_q = 0$.

The axial-vector and pseudoscalar sector of the action up to second order is given by [13]

$$S_A = \int d^5x \sqrt{g} \left[\frac{v(z)^2 g^{MN}}{2} [\partial_M \pi^a - A_M^a][\partial_N \pi^a - A_N^a] - \frac{g^{KL} g^{MN}}{4g_5^2} F^a{}_{KM} F^a_{LN} \right], \quad (3.8)$$

where $F_{KM}^a = \partial_K A_M^a - \partial_M A_K^a$, with $A_M = (L_M - R_M)/2$.

3.2.2 Equations of Motion

Using the unperturbed 5-dimensional AdS space metric, and taking the variation over A_M^a of equation (3.8), one obtains the equations of motion, which are expressed in 4D momentum space as

$$\partial_z \left(\frac{1}{z} \partial_z A_{\nu\perp}^a \right) + \frac{q^2}{z} A_{\nu\perp}^a - \frac{g_5^2 v^2}{z^3} A_{\nu\perp}^a = 0, \quad (3.9)$$

$$\partial_z \left(\frac{1}{z} \partial_z \phi^a \right) + \frac{g_5^2 v^2}{z^3} (\pi^a - \phi^a) = 0, \quad (3.10)$$

$$-q^2 \partial_z \phi^a + \frac{g_5^2 v^2}{z^2} \partial_z \pi^a = 0, \quad (3.11)$$

where the gauge choice $A_z = 0$ has been imposed. The ϕ field comes from the longitudinal part of $A_\mu^a = A_{\mu\perp}^a + \partial_\mu \phi^a$.

The fields above can be written conveniently in terms of bulk-to-boundary propagators as follows

$$A_\mu^a(q, z) = A_\mu^{a0}(q)_\perp \mathcal{A}(q, z) + A_\mu^{a0}(q)_\parallel \phi(q, z),$$

$$\pi^a(q, z) = \frac{iq^\mu}{q^2} A_\mu^{a0}(q)_\parallel \pi(q, z),$$

with $A_\mu^{a0}(q)_\perp$ and $A_\mu^{a0}(q)_\parallel$ are the Fourier transform of the source functions of the 4D axial current operators $J_{A,\mu}^a(x)_\perp$ and $J_{A,\mu}^a(x)_\parallel$ respectively.

The nth KK-mode axial-vector meson's wave function, denoted by $\psi_{A,n}(z)$, is the solution of equation (3.9) with $q^2 = m_{A,n}^2$, and with boundary conditions $\psi(0) = 0$ and $\partial_z \psi(z_0) = 0$. The normalization of $\psi_{A,n}$ is identical to that of the ρ-meson's wave

function, and is given by $\int (dz/z)\psi_{A,n}(z)^2 = 1$ [13]. On the other hand, the pion's wave function, denoted by $\phi(z)$ or $\pi(z)$, is the solution of the coupled differential equations, *i.e.*, equation (3.10) and (3.11), with $q^2 = 0$ in the limit of massless pion. Furthermore, in this limit, the boundary conditions for the pion wave functions are $\phi(0) = 0, \pi(0) = -1$ and $\partial_z\phi(z_0) = 0$. [A careful analysis is given in ref. [13] for m_π small. There, the UV boundary conditions for the scalar wave functions are $\phi(0) = 0$ and $\pi(0) = 0$. However, the function $\pi(z)$ away from $z = 0$ approaches -1 rather quickly. For $m_\pi \to 0$, the function $\pi(z)$ equals -1 in essentially the entire slice of 5D AdS space, $0 < z < z_0$.]

Using Eq. (3.11) and the UV boundary conditions, one finds $\pi(z) = -1$ for all z. Therefore equation (3.10) can be rewritten in terms of $\Psi(z) = \phi(z) - \pi(z)$ as

$$\partial_z\left(\frac{1}{z}\partial_z\Psi\right) - \frac{g_5^2 v^2}{z^3}\Psi = 0. \tag{3.12}$$

The solution is given by [23]

$$\Psi(z) = z\Gamma[2/3]\left(\frac{\alpha}{2}\right)^{\frac{1}{3}}\left(I_{-\frac{1}{3}}(\alpha z^3) - I_{\frac{1}{3}}(\alpha z^3)\frac{I_{\frac{2}{3}}(\alpha z_0^3)}{I_{-\frac{2}{3}}(\alpha z_0^3)}\right), \tag{3.13}$$

where $\alpha = g_5\sigma/3$, with $g_5 = 2\pi$ as shown in ref [13]. Note that $\Psi(z)$ is identical to $\mathcal{A}(0, z)$. Parameter $z_0 = 1/\Lambda_{QCD}$ is determined by the experimental value of ρ-meson's mass $m_\rho = 775.5$ MeV [70], which corresponds to $z_0 = 1/(322\text{ MeV})$ [13].

For the a_1's wave functions, one has to rely on numerical methods. However, other aspects of the axial-vector mesons are analogous to the vector mesons. For instance, the bulk-to-boundary propagator of a_1 can be written in terms of $\psi_{A,n}$ as

$$\mathcal{A}(q, z) = \sum_n \frac{(\frac{1}{\varepsilon}\partial_{z'}\psi_{A,n}(\varepsilon))\psi_{A,n}(z)}{m_{A,n}^2 - q^2}, \tag{3.14}$$

c.f equation (17) of ref. [34] and ref. [13, 21]. The bulk-to-boundary propagator $\mathcal{A}(q, z)$ satisfies $\mathcal{A}(q, \varepsilon) = 1$ and $\partial_z\mathcal{A}(q, z_0) = 1$.

3.2.3 Two-Point Functions

The completeness relation is given by

$$\sum_n \int \frac{d^3q}{(2\pi)^3 2q^0} |n(q)\rangle \langle n(q)| = 1 \,. \tag{3.15}$$

The complete set of states includes $|A_n^a(q,\lambda)\rangle$, the nth axial-vector state, as well as $|\pi^a(q)\rangle$, the pion state.

By applying the completeness relation into 2-point functions $\langle 0|\mathcal{T} J_A^\mu(x)_\perp J_A^\nu(0)_\perp|0\rangle$ and $\langle 0|\mathcal{T} J_A^\mu(x)_{\shortparallel} J_A^\nu(0)_{\shortparallel}|0\rangle$, then multiplying $q^2 - m_n^2$ and taking the limit $q^2 \to m_n^2$, one can extract the following quantities from the AdS/QCD correspondence [13]

$$F_{A,n} = \left. \frac{\partial_z \psi_{A,n}(z)}{g_5 z} \right|_{z=\epsilon}, \tag{3.16}$$

$$f_\pi^2 = -\left. \frac{\partial_z \Psi(z)}{g_5^2 z} \right|_{z=\epsilon}, \tag{3.17}$$

where $F_{A,n}$ is the decay constant of the nth mode of the a_1, and f_π is that of the pion. The latter is obtained in the chiral limit $q^2 \to m_\pi^2 = 0$. The decay constants are defined by

$$\langle 0|J_{A,\mu}^a(0)_\perp|A_n^b(p,\lambda)\rangle = F_{A,n}\varepsilon_\mu(p,\lambda)\delta^{ab}, \tag{3.18}$$

$$\langle 0|J_{A,\mu}^a(0)_{\shortparallel}|\pi^b(p)\rangle = f_\pi p_\mu \delta^{ab}. \tag{3.19}$$

Equation (3.17) and (3.13) relate the input parameter σ to the pion decay constant

$$f_\pi^2 = \frac{3}{4\pi^2} \frac{\Gamma(2/3)}{\Gamma(1/3)} \left(2\alpha^2\right)^{\frac{1}{3}} \frac{I_{\frac{2}{3}}(\alpha z_0^3)}{I_{-\frac{2}{3}}(\alpha z_0^3)}. \tag{3.20}$$

Using the experimental value $f_\pi = 92.4$ MeV, we find $\alpha = 2.28 \Lambda_{QCD}^3$, therefore $\sigma = (332 \text{ MeV})^3$. Consequently, other observables can be determined, $m_{A,1} = 1376$ MeV and $F_{A,1}^{1/2} = 493$ MeV. They are in a good agreement with the experimental values $m_{A,1} = 1230$ MeV and $F_{A,1}^{1/2} = 433$ MeV.

3.3 Gravitational Form Factors

The three-point function that includes the stress tensor follows from

$$\langle 0|\mathcal{T}J_5^{a\alpha}(x)\hat{T}_{\mu\nu}(y)J_5^{b\beta}(w)|0\rangle = -\frac{2\,\delta^3 S}{\delta A_\alpha^{a0}(x)\delta h^{\mu\nu 0}(y)\delta A_\beta^{b0}(w)}, \qquad (3.21)$$

and the relevant part of the action (3.7) that contributes to the 3-point function is linear in $h^{\mu\nu}$ and quadratic in the non-gravitational fields,

$$\begin{aligned}
S_A^{(3)} &= \int d^5x\left[-\frac{v(z)^2 h^{\rho\sigma}}{2z^3}(\partial_\rho\pi^a - A_\rho^a)(\partial_\sigma\pi^a - A_\sigma^a)\right.\\
&\quad\left.+\frac{1}{2g_5^2 z}h^{\rho\sigma}\left[-F_{\sigma z}F_{\rho z} + \eta^{\alpha\beta}F_{\sigma\alpha}F_{\rho\beta}\right]\right],
\end{aligned} \qquad (3.22)$$

where $h^{\rho\sigma}$ is the metric perturbation defined analogously to equation (3.6), viz., $g^{\rho\sigma} = z^2(\eta^{\rho\sigma} - h^{\rho\sigma})$.

To isolate the pion-to-pion elastic stress tensor matrix elements from the Fourier transformed 3-point functions $\langle J^\alpha(-p_2)T^{\mu\nu}(q)J^\beta(p_1)\rangle$, we apply the completeness relation (3.15) twice, then multiply by

$$p_1^\alpha p_2^\beta \frac{1}{f_\pi^2}, \qquad (3.23)$$

and take the limit $p_1^2 \rightarrow m_\pi^2 = 0$ and $p_2^2 \rightarrow m_\pi^2 = 0$.

We obtain the transverse-traceless part of the stress tensor matrix elements, for $\hat{T}^{\mu\nu}(0)$ at the origin in coordinate space,

$$\langle\pi^a(p_2)|\,\hat{T}^{\mu\nu}(0)\,|\pi^b(p_1)\rangle = 2\delta^{ab}A_\pi(Q^2)\left[p^\mu p^\nu + \frac{1}{12}\left(q^2\eta^{\mu\nu} - q^\mu q^\nu\right)\right], \qquad (3.24)$$

where $p = (p_1 + p_2)/2$ and $q = p_2 - p_1$. The gravitational form factor A_π is given by

$$A_\pi(Q^2) = \int dz\,\mathcal{H}(Q,z)\left(\frac{(\partial_z\Psi(z))^2}{g_5^2 f_\pi^2 z} + \frac{v(z)^2\Psi(z)^2}{f_\pi^2 z^3}\right). \qquad (3.25)$$

Note that, except for the $\mathcal{H}$, this form factor is similar to the electromagnetic form factor given in [22, 23] although they come from different terms of the action (3.7). $\mathcal{H}(Q, z)$ is the bulk-to-boundary propagator of the graviton for spacelike momentum transfer $q^2 = $

$-Q^2 < 0$. It is defined by $h_{\mu\nu}(q, z) = \mathcal{H}(Q, z)h_{\mu\nu}^0(q)$, where $h_{\mu\nu}(q, z)$ is the Fourier transform of the metric perturbation $h_{\mu\nu}(x, z)$. In transverse-traceless gauge, $q^\mu h_{\mu\nu} = 0$ and $h_\mu^\mu = 0$, the linearized Einstein equation becomes

$$z^3 \partial_z \left(\frac{1}{z^3} \partial_z h_{\mu\nu} \right) + q^2 h_{\mu\nu} = 0, \tag{3.26}$$

with boundary conditions $h(q, \varepsilon) = 1$ and $\partial_z h(q, z_0) = 0$. The solution is given by [34]

$$\mathcal{H}(Q, z) = \frac{1}{2}Q^2 z^2 \left(\frac{K_1(Qz_0)}{I_1(Qz_0)} I_2(Qz) + K_2(Qz) \right). \tag{3.27}$$

Since $\mathcal{H}(0, z) = 1$, one can check that $A_\pi(0) = 1$, which is a correct normalization for A_π.

Our procedure obtains the transverse-traceless part of the stress tensor; the full stress tensor can have a trace, which means there could be a term $\frac{1}{3}(\eta^{\mu\nu} - q^\mu q^\nu / q^2)T$, where T is the trace of $T^{\mu\nu}$. In general, there are two gravitational form factors for spin-0 particles. The expression for the pion matrix elements written in terms of the two independent form factors is

$$\langle \pi^a(p_2)|T^{\mu\nu}(0)|\pi^b(p_1)\rangle = \delta^{ab} \left[2A_\pi(Q^2)p^\mu p^\nu + \frac{1}{2}C_\pi(Q^2)\left(q^2 \eta^{\mu\nu} - q^\mu q^\nu\right) \right]; \tag{3.28}$$

we have calculated $A_\pi(Q^2)$, but $C_\pi(Q^2) = A_\pi(Q^2)/3 + \widetilde{C}_\pi(Q^2)$ where $\widetilde{C}$ is not determined here.

For a_1, the corresponding matrix element is identical to the ρ-meson's [34]. The only difference is that the ρ-meson's wave function ψ_n is replaced by $\psi_{A,n}$, the a_1's wave function. The A form factor is now given by

$$A_{a_1}(Q^2) = \int \frac{dz}{z} \mathcal{H}(Q, z)\psi_{A,n}\psi_{A,n}. \tag{3.29}$$

The other form factors mirror the ρ-meson's form factors expression.

Both $A_\pi(Q^2)$ and $A_{a_1}(Q^2)$ are shown in Fig. 3.1.

3.4 Consequences

3.4.1 Radii

In the limit $Qz_0 \ll 1$, one can expand $\mathcal{H}(Q^2, z)$ and obtain the radius

$$\left\langle r_\pi^2 \right\rangle_{\text{grav}} \equiv -6\frac{dA_\pi}{dQ^2}\bigg|_{Q^2=0}$$

$$= \frac{6}{4} \int dz\, z^3 \left(1 - \frac{z^2}{2z_0^2}\right) \rho(z), \tag{3.30}$$

where

$$\rho(z) = \left(\frac{(\partial_z \Psi(z))^2}{g_5^2 f_\pi^2 z^2} + \frac{v(z)^2 \Psi(z)^2}{f_\pi^2 z^4}\right). \tag{3.31}$$

Gravitational Form Factors
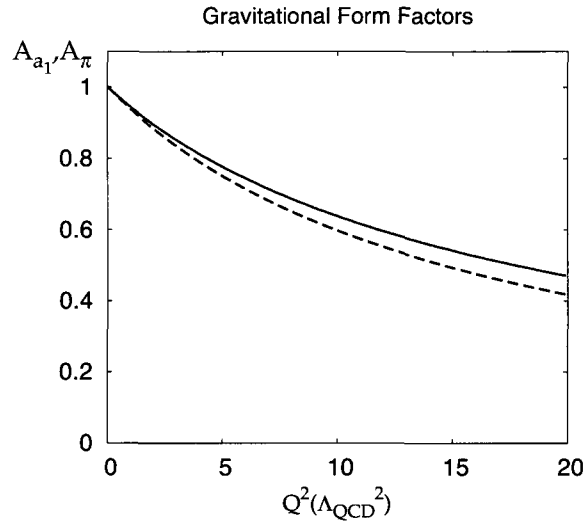
FIG. 3.1: Plot of A with momentum transfer squared in units of $\Lambda_{\text{QCD}} = 1/z_0$. The red solid line is A_π and the blue dashed line is A_{a_1}

We find

$$\left\langle r_\pi^2 \right\rangle_{\text{grav}} = 0.13\,(\text{fm})^2 = (0.36\,\text{fm})^2. \tag{3.32}$$

M. Polyakov, in a different model [71], also found a small gravitational radius for the pion, $\left\langle r_\pi^2 \right\rangle_{\text{grav}} = (0.42\,\text{fm})^2$. The gravitational RMS radius is significantly smaller than the electromagnetic radius $\left\langle r_\pi^2 \right\rangle_C = 0.33\,(\text{fm})^2 = (0.57\,\text{fm})^2$, obtained from the AdS/QCD

model in chiral limit [23]. Compared to the experimental result $\langle r_\pi^2 \rangle_C = (0.67\,\text{fm})^2$ [70], the difference is even more apparent. This shows, as in the ρ-meson case, that the energy distribution of the pion is concentrated in a smaller volume than the charge distribution.

For a_1, the corresponding radius is

$$
\begin{aligned}
\langle r_{a_1}^2 \rangle_{\text{grav}} &= \frac{6}{4} \int dz\, z \left(1 - \frac{z^2}{2z_0^2} \right) \psi_{A,1}^2 \\
&= 0.15\,(\text{fm})^2 = (0.39\,\text{fm})^2.
\end{aligned}
\tag{3.33}
$$

As expected, it is smaller than the charge radius $\langle r_{a_1}^2 \rangle_C = 0.39\,(\text{fm})^2 = (0.62\,\text{fm})^2$ calculated from the AdS/QCD model.

3.4.2 High Q^2 limit

For high Q^2, the form factor A_π scales as $1/Q^2$. The precise expression is given by

$$
A_\pi(Q^2) = \frac{4\rho(0)}{Q^2} = \frac{16\pi^2 f_\pi^2}{Q^2},
\tag{3.34}
$$

which follows from the fact that at high Q^2, the second term of the function $H(Q, z)$ in equation (3.27) dominates. This term behaves like e^{-Qz}. Therefore, one can allow $z_0 \to \infty$ in equation (3.25), and replace $\rho(z)$ by its value at the origin, $\rho(0)$, and then do the integral analytically.

One can verify, most easily in the Breit frame, that this scaling agrees with the perturbative QCD prediction. It can be shown that [61]

$$
\langle p_2 | \eta_{\mu\nu} T^{\mu\nu} | p_1 \rangle \sim Q^0, \quad \langle p_2 | e_{\mu\nu}(q, 0) T^{\mu\nu} | p_1 \rangle \sim Q^0;
\tag{3.35}
$$

$e_{\mu\nu}(q, 0)$ gives the helicity-0 component of the spin-2 part of the stress tensor, with

$$
e_{\mu\nu}(q, 0) = \frac{1}{\sqrt{6}} \Big(2\zeta_\mu(q, 0)\zeta_\nu(q, 0) - \zeta_\mu(q, +)\zeta_\nu(q, -) - \zeta_\mu(q, -)\zeta_\nu(q, +) \Big).
\tag{3.36}
$$

Here, $\zeta(q, \lambda)$ is the polarization vector of a spin-1 particle of momentum q. Equation (3.35) is equivalent to

$$
A_\pi, C_\pi \sim 1/Q^2.
\tag{3.37}
$$

For a_1, the high Q^2 behavior of the form factor A_{a_1} is

$$A_{a_1}(Q^2) = \frac{12|\psi_{A,n}''|^2}{Q^4}.$$ (3.38)

Similarly $C_{a_1}, D_{a_1} \sim 1/Q^4$, while $F_{a_1} \sim 1/Q^6$, which mirror the scaling results for ρ-mesons, with the notation given in [34].

3.4.3 Sum Rules for the GPD

Deeply virtual Compton scattering process involves a target absorbing a virtual photon and subsequently radiating a real photon. The virtual Compton scattering amplitude can be written in terms of integral involving the generalized parton distributions (GPD) $H(x, \xi, Q^2)$ [55]. In a model with quarks, x is the light-cone momentum fraction of the struck quark constituent relative to the total momentum of the target hadron.

For spin-0 hadrons, there is only one GPD, defined by

$$\int \frac{p^+ dy^-}{4\pi} e^{ixp^+y^-/2} \left\langle p_2|\bar{\psi}_q(-\frac{y}{2})\gamma^+\psi_q(\frac{y}{2})|p_1 \right\rangle_{y^+=y_\perp=0} = 2p^+ H(x, \xi, Q^2),$$ (3.39)

where $q^+ = q^0 + q^3 = -2\xi p^+$.

There are sum rules connecting this GPD to the gravitational as well as to the electromagnetic form factors. The well known sum rule is for the first moment of the GPD [54]

$$\int_{-1}^{1} dx\, H(x, \xi, Q^2) = F(Q^2),$$ (3.40)

where $F(q^2)$ is the electromagnetic form factor defined by

$$\left\langle \pi(p_2)|\bar{\psi}_q(0)\gamma^\mu\psi_q(0)|\pi(p_1) \right\rangle = 2p^\mu F(Q^2).$$ (3.41)

A further sum rule exists because the stress tensor element T^{++} can be related to the second moment in x of the operator whose matrix element defines the GPDs. For the pion, the result was given in [67] and reads,

$$\int_{-1}^{1} dx\, x\, H(x, \xi, Q^2) = A_\pi(Q^2) - \xi^2 C_\pi(Q^2).$$ (3.42)

Ref. [67] also uses a chiral Lagrangian to show that $A_\pi(0) = 1$ (the momentum sum rule) and $C_\pi(0) = 1/4$. One can set $\xi = 0$ in the above equation so that only the first term, which is known from the AdS/QCD model, in the right-hand side survives. There are also first-moment sum rules for the axial vector meson GPDs, which precisely parallel the ones given for the ρ-mesons in [34]

3.5 Conclusions

We have worked out the gravitational form factors of pions and of axial-vector mesons using the AdS/CFT correspondence, and have given the sum rules connecting the gravitational form factors, which can also be called stress tensor or energy-momentum tensor form factors, to the axial sector GPDs.

A striking numerical result is the smallness of the pion radius and of the axial-vector meson radius as obtained from $A(q^2)$, the gravitational form factor that enters the momentum sum rule. This parallels the results for the ordinary vector mesons [34]. It suggests that the energy that makes up the mass of the meson is well concentrated, with the charge measured by the electromagnetic form factors spreading more broadly.

CHAPTER 4

Strange Mesons and Kaon to Pion Transition Form Factors

4.1 Introduction

In this chapter, we consider the extension of the anti-de Sitter space/quantum chromodynamics model (AdS/QCD) to allow broken flavor symmetry, and apply the model to the kaon system and particularly to the $K_{\ell 3}$ form factors.

The connection between 5D gravitational theories on an anti-de Sitter space and 4D conformal field theories began as a correspondence between a type IIB string theory and an $\mathcal{N} = 4$ super Yang-Mills theory in the large N_C limit [8, 17, 65]. This has inspired an analytic model referred to as AdS/QCD connecting 5D theories living on an anti-de Sitter space to 4D QCD [13, 14]. Interesting results have been obtained for masses, couplings, and electromagnetic and gravitational form factors for vector, axial vector and pseudoscalar mesons. For a selection of these results, see [63, 72, 39, 45, 40, 36, 21, 32, 23, 73, 22, 74, 66, 34, 35, 75, 76].

The $K_{\ell 3}$ form factors describe the decays $K \to \pi \ell \nu$ and are currently most known

for the role they play in high-precision extractions of the Cabibbo-Kobayashi-Maskawa (CKM) matrix element V_{us}. The form factors themselves are the K to π transition matrix elements of the strangeness changing vector current. There are two $K_{\ell 3}$ form factors, bespeaking the fact that the strangeness changing current is not conserved, and has a longitudinal as well as a transverse part. Experiments measure the product of the form factors and $|V_{us}|$. Hence the extraction of $|V_{us}|$ from the $K_{\ell 3}$-decay measurements depends on having a reliable calculation of the form factor normalization. So far, these calculations have been from chiral perturbation theory [77, 78, 79, 80] or from lattice gauge theory [81, 82, 83, 84, 85]. Here we will present a first calculation of these form factors from AdS/QCD. We will also solidify and extend our ability to calculate quantities in the flavor-broken versions of AdS/QCD.

Our form factor normalizations can be compared to those obtained from other calculational methods, our slopes can be compared to data as well as to other calculations, and since we calculate using an analytic method, we can also obtain a curvature that can be compared to experimental data. All comparisons of results to other methods and to data show good agreement, as will be detailed below.

We work with general mass pseudoscalar mesons. Previous results known to us worked in the chiral limit or calculated some quantities using expansions valid at small mass. In particular, while we can neatly derive the Gell-Mann-Oakes-Renner (GOR) [86] relation in the chiral limit, we do not use it to obtain any of our results and can test to see how accurate it is at given quark mass.

Section 4.2 reviews AdS/QCD with notation pertinent to several quarks of differing masses. Section 6.3 gives results obtained from two-point functions, including bulk-to-boundary propagators, masses, and decay constants, focusing on differences from the flavor symmetric case, in particular considering scalar mesons along with vector, axial vector, and pseudoscalar mesons. Section 4.4 contains algebraic results for the form factors, with the numerical results given in Sec. 4.5. Closing remarks are offered in Sec. 4.6.

4.2 The AdS/QCD model

We will use the following metric for the 5 dimensional Anti-de Sitter space

$$ds^2 = \frac{1}{z^2}\left(\eta_{\mu\nu}dx^\mu dx^\nu - dz^2\right), \qquad \varepsilon < z < z_0, \tag{4.1}$$

where the metric of the 4 dimensional flat space is $\eta_{\mu\nu}$ =diag$(1, -1, -1, -1)$. The cut-off at $z = \varepsilon$ (with $\varepsilon \to 0$ implied) corresponds to UV cut-off in QCD, while the hard-wall cut-off at z_0 corresponds to IR cut-off, Λ_{QCD}, to simulate confinement.

According to the AdS/CFT correspondence, for every operator in 4 dimensional theory there is a corresponding field in the AdS$_5$ space. Operators of our interest are current operators $J^a_{L\mu} = \bar\psi_{qL}\gamma_\mu t^a \psi_{qL}$, $J^a_{R\mu} = \bar\psi_{qR}\gamma_\mu t^a \psi_{qR}$ and quark bilinear $\bar\psi_{qL}\psi_{qR}$. In the AdS$_5$ space, these operators correspond to gauge fields $L^a_\mu(x, z)$, $R^a_\mu(x, z)$, and a scalar field $X(x, z)$ respectively. Following [13], we will consider a 5D action with SU(3)$_L\otimes$ SU(3)$_R$ symmetry as follows

$$S = \int d^5x \sqrt{g}\, \mathrm{Tr}\Big\{ |DX|^2 + 3\,|X|^2 - \frac{1}{4g_5^2}\left(F_{(L)}^2 + F_{(R)}^2\right)\Big\}. \tag{4.2}$$

The field strength is defined by $F^{(L)}_{MN} = \partial_M L_N - \partial_N L_M - i[L_M, L_N]$ and analogously for $F^{(R)}_{MN}$. The scalar field X and gauge fields interact through the covariant derivative $D_M X = \partial_M X - iL_M X + iX R_M$ in such a way that the action is chiral invariant. We also use the vector and the axial-vector field defined from $L = V + A$ and $R = V - A$.

The theory begins as one that has SU(3)$_L\otimes$ SU(3)$_R$ symmetry, and one would like to maintain as much of the symmetry as possible even when going to massive quarks and in particular to flavor non-symmetric quark masses. In a chirally symmetric world, the action is invariant as the X field transforms via

$$X \to X' = U_L X U_R^\dagger. \tag{4.3}$$

One can expand X as

$$X(x, z) = e^{i\pi^a(x,z)t^a} X_0(z) e^{i\pi^a(x,z)t^a} \tag{4.4}$$

whereupon an axial transformation (which has $U_L^\dagger = U_R$) induces to leading order a shift in the pion field, $\pi'^a = \pi^a - \theta^a$, where θ^a is a parameter in the transformation $U_L = e^{-i\theta^a t^a}$ and is consistent with π^a being a pseudoscalar field. With flavor symmetry, X_0 is a multiple of the unit matrix and commuting, so one can easily write $X = e^{2i\pi^a t^a} X_0$, as has often been done. However, in the flavor non-symmetric case, this would make π^a appear to be associated with left-handed transformations rather than with axial transformations, and gives it unexpected parity properties and mixing with vector as well as with axial vector fields. For example, one obtains a quadratic term in the Lagrangian proportional to $\eta^{MN} \text{Tr}\,[X_0, \partial_M \pi^b t^b][X_0, V_N]$, which will violate 4D parity when X_0 is not proportional to the unit matrix. (With the split exponential, one gets cancellations rather than just commutators.)

Shock and Wu [37] have early on considered three-flavor extensions of AdS/QCD, although keeping $X = e^{2i\pi^a t^a} X_0$. They did not study the more dynamical quantities like form factors, but did obtain many good results for masses and decay constants. However, as they themselves point out, they did not obtain good results for the ground state pseudoscalar kaons with the same parameters that gave good results for the more excited strange mesons. With the exponential split, as we think it should be, one obtains good results for pseudoscalar as well as strange axial and vector (and even scalar) meson states.

Katz and Schwartz [87] also considered flavor-broken AdS/QCD, although their main focus was on the U(1) problem and also did not study form factors. They also kept $X = e^{2i\pi^a t^a} X_0$, but only explicitly studied the part of the action that mixes the axial vectors with the pseudoscalars, where problems do not appear. We might remark already that they used the GOR relation to get the strange quark mass. The GOR relation becomes less valid as the quark mass increases, and using a different method to fix the strange quark mass, we find a larger value than they quote.

Hambye *et al.* [44] also studied three-flavor AdS/QCD, focusing on quantities that are calculated from four-point functions such as the purely hadronic $K_{\pi 2}$ decays or the

B_K parameter needed to calculate K^0-$\bar{K}^0$ mixing. They work in a limit where all quarks are massless, and so have $X_0 = X = 0$. Hence their subjects and their approximations do not greatly overlap with the present work, although we plan to consider quantities obtained from four-point functions in future work.

Turning off all fields except $X_0(z)$ and solving the equation of motion, one obtains

$$2X_{0ij} = v_{ij}(z) = \zeta M_{ij} z + \frac{1}{\zeta} \Sigma_{ij} z^3 \,, \tag{4.5}$$

where ζ is a rescaling parameter [18, 19] discussed below. From the AdS/CFT correspondence M_{ij} can be identified as quark mass matrix which responsible for the explicit breaking of the chiral symmetry of QCD and Σ_{ij} as the quark condensate $\langle \bar{q}_i q_j \rangle$ which spontaneously break the chiral symmetry of QCD to SU(3)$_V$. Assuming u and d symmetry, we have

$$M = \begin{pmatrix} m_q & 0 & 0 \\ 0 & m_q & 0 \\ 0 & 0 & m_s \end{pmatrix} \,, \qquad \Sigma = \begin{pmatrix} \sigma_q & 0 & 0 \\ 0 & \sigma_q & 0 \\ 0 & 0 & \sigma_s \end{pmatrix} \,. \tag{4.6}$$

In general $\sigma_s \neq \sigma_q$. However, we will also consider the limiting case when $\sigma_s = \sigma_q$, as an analytic solution for the vector field can be obtained.

Regarding the quark masses and the quark condensate parameter σ, we adopt a normalization parameter as advocated in [18, 19], wherein quark masses are multiplied by a factor $\zeta = \sqrt{N_C}/2\pi$ [20] compared to earlier conventions and σ is divided by the same factor. One can, of course, view the quark masses and σ in AdS/QCD as parameters of this particular model, and many important quantities, including the GOR relation and most of the results in this chapter, are unchanged by this rescaling. However, the rescaled parameters allow a precise connection to the two-point correlation function of the quark condensate at small distances, which is known from perturbative QCD, and also leads to a better agreement with mass parameters at the hadronic scale and with the quark condensate as obtained from methods disconnected from AdS/QCD. Quark masses obtained

from AdS/QCD had generally been strikingly low and the quark condensate strikingly high, but following [18, 19] one can argue that the disagreement was a matter of having incommensurate definitions.

4.3 Two-point function

Up to second order in fields, the action can be written as

$$
S = \int d^5x \left\{ \sum_a \frac{-1}{4g_5^2 z} (\partial_M V_N^a - \partial_N V_M^a)^2 + \frac{M_V^{a\,2}(z)}{2z^3} V_M^{a\,2} \right.
$$
$$
\left. \frac{-1}{4g_5^2 z} (\partial_M A_N^a - \partial_N A_M^a)^2 + \frac{M_A^{a\,2}(z)}{2z^3} (\partial_M \pi^a - A_M^a)^2 \right\}, \tag{4.7}
$$

where contraction over η_{ML} is implicit. The mass combinations come from

$$
\begin{aligned}
\frac{1}{2} M_V^{a\,2} \delta^{ab} &= -\text{Tr}\left[t^a, X_0\right]\left[t^b, X_0\right], \\
\frac{1}{2} M_A^{a\,2} \delta^{ab} &= \text{Tr}\left\{t^a, X_0\right\}\left\{t^b, X_0\right\},
\end{aligned} \tag{4.8}
$$

or,

$$
M_V^{a\,2} = \begin{cases} 0 & a = 1, 2, 3 \\ \frac{1}{4}(v_s - v_q)^2 & a = 4, 5, 6, 7 \\ 0 & a = 8, \end{cases}
$$

$$
M_A^{a\,2} = \begin{cases} v_q^2 & a = 1, 2, 3 \\ \frac{1}{4}(v_q + v_s)^2 & a = 4, 5, 6, 7 \\ \frac{1}{3}(v_q^2 + 2v_s^2) & a = 8, \end{cases}
$$

$$\tag{4.9}$$

where

$$
\begin{aligned}
v_q(z) &= \zeta m_q z + \frac{\sigma_q}{\zeta} z^3, \\
v_s(z) &= \zeta m_s z + \frac{\sigma_s}{\zeta} z^3.
\end{aligned} \tag{4.10}
$$

For later convenience we define

$$\alpha^a(z) = \frac{g_5^2 M_V^{a\,2}}{z^2}, \quad \beta^a(z) = \frac{g_5^2 M_A^{a\,2}}{z^2}. \tag{4.11}$$

As shown in Eq. (4.5), the vacuum solution contains both explicit and spontaneous symmetry breaking parameters, M_{ij} and Σ_{ij} respectively. The parameters m_q and m_s in the 5D theory are usually considered to be explicit symmetry breaking, and give quark mass terms in the 4D theory that are also explicit symmetry breaking. The condensate parameters may be considered spontaneous symmetry breaking, but in the absence of the quark mass parameters (*i.e.*, in the chiral limit where the m_q and m_s go to zero), one expects that the condensate parameters are all the same. Hence one may argue that the differences in the condensate parameters do arise from explicit symmetry breaking. Since the M_V^a functions depend only on differences $v_s - v_q$, one can say that they would be zero if there were only spontaneous symmetry breaking. In this limit, the masses of the vector mesons in the same octet are degenerate.

The axial sector of action (4.7) is invariant under gauge transformation,

$$A_M^a \rightarrow A_M^a - \partial_M \lambda^a,$$

$$\pi^a \rightarrow \pi^a - \lambda^a. \tag{4.12}$$

Hence, we are free to set $A_z^a = 0$. For the vector sector, the mass term destroys the gauge freedom for $a = 4, 5, 6, 7$. Hence, we can set $V_z^a = 0$ only for $a = 0, 1, 2, 3, 8$. We will show that the non-vanishing V_z is related to the non-vanishing longitudinal part of the vector field.

4.3.1 Vector sector

The vector field satisfies the following equation of motion

$$\eta^{ML} \partial_M \left(\frac{1}{z} \left(\partial_L V_N^a - \partial_N V_L^a \right) \right) + \frac{\alpha^a(z)}{z} V_N^a = 0. \tag{4.13}$$

For the transverse part, $\partial^\mu V_{\mu\perp}^a(x, z) = 0$, one obtains

$$\left(\partial_z \frac{1}{z}\partial_z + \frac{q^2 - \alpha^a}{z}\right) V_{\mu\perp}^a(q, z) = 0, \tag{4.14}$$

where q is the Fourier variable conjugate to the 4 dimensional coordinates, x.

We shall write the vector field in terms of its boundary value at UV multiplying a profile function, or bulk-to-boundary propagator, $V_{\mu\perp}^a(q, z) = V_{\mu\perp}^{0a}(q)\mathcal{V}^a(q^2, z)$, and set $\mathcal{V}^a(q^2, \varepsilon) = 1$ (Note that there is no summation over the group index a of the profile function). The boundary value $V_\mu^{0\,a}(q)$ acts as the Fourier transform of the source of the 4D conserved vector current operator. At the IR boundary, we choose Neumann boundary condition $\partial_z \mathcal{V}^a(q, z_0) = 0$. In the $\Sigma_{ij} = \sigma\delta_{ij}$ limit, the solution can be written in terms of Bessel function

$$\mathcal{V}^a(q^2, z) = \frac{\pi}{2}\tilde{q}z\left(\frac{Y_0(\tilde{q}z_0)}{J_0(\tilde{q}z_0)}J_1(\tilde{q}z) - Y_1(\tilde{q}z)\right), \tag{4.15}$$

for $q^2 > \alpha^a$, and

$$\mathcal{V}^a(q^2, z) = \tilde{Q}z\left(\frac{K_0(\tilde{Q}z_0)}{I_0(\tilde{q}z_0)}I_1(\tilde{Q}z) + K_1(\tilde{Q}z)\right), \tag{4.16}$$

for $q^2 < \alpha^a$, where $\tilde{q} = \sqrt{q^2 - \alpha^a}$ and $\tilde{Q} = \sqrt{\alpha^a - q^2}$. Near the UV boundary, the profile function can be written as

$$\mathcal{V}(q^2, z) = 1 + \frac{\tilde{q}^2 z^2}{4}\ln\left(\tilde{q}^2 z^2\right) + \dots. \tag{4.17}$$

The longitudinal part of the vector field, $V_{\mu\|}^a = \partial_\mu \xi^a$ and V_z are coupled as follows

$$-q^2\partial_z\tilde{\phi}^a(q^2, z) + \alpha^a\partial_z\tilde{\pi}^a(q^2, z) = 0, \tag{4.18}$$

$$\partial_z\left(\frac{1}{z}\partial_z\tilde{\phi}^a(q^2, z)\right) - \frac{\alpha^a}{z}\left(\tilde{\phi}^a(q^2, z) - \tilde{\pi}^a(q^2, z)\right) = 0, \tag{4.19}$$

where we define $V_z^a = -\partial_z\tilde{\pi}^a$ and $\xi^a = \tilde{\phi}^a - \tilde{\pi}^a$. The constancy of $\alpha^a(z)$ when $\Sigma_{ij} = \sigma\delta_{ij}$ simplifies above equations into

$$\left(\partial_z\frac{1}{z}\partial_z + \frac{q^2 - \alpha^a}{z}\right)\xi^a(q^2, z) = 0. \tag{4.20}$$

This is precisely the equation for the transverse part of the vector field. Fixing boundary conditions as $\tilde{\phi}^a(q, \varepsilon) = 0$ and $\tilde{\pi}^a(q, \varepsilon) = -1$ on the UV brane and Neumann boundary conditions on the IR brane, one concludes that in the limit where $\sigma_s = \sigma_q = \sigma$ the profile function for the longitudinal and the transverse part of the vector field are identical, $\xi^a(q^2, z) = \mathcal{V}^a(q^2, z)$, with a solution given by Eq. (4.15). In general, this is not the case, and both ξ^a and $\mathcal{V}^a$ can be solved numerically. For $a = 1, 2, 3, 8$, longitudinal vector fields are unphysical in the sense that they can be eliminated by fixing the gauge, $V_z^a = 0$.

Two-point functions can be calculated from the AdS/QCD correspondence by evaluating the action (4.7) with the classical solution and taking the functional derivative over V_μ^0 twice. One obtains

$$i \int_x e^{iqx} \left\langle 0 \left| \mathcal{T} J_\perp^{\mu a}(x) J_\perp^{\nu b}(0) \right| 0 \right\rangle = -P_T^{\mu\nu} \delta^{ab} \frac{\partial_z \mathcal{V}^a(q^2, \varepsilon)}{g_5^2 \varepsilon} ,$$
$$i \int_x e^{iqx} \left\langle 0 \left| \mathcal{T} J_\parallel^{\mu a}(x) J_\parallel^{\nu b}(0) \right| 0 \right\rangle = -P_L^{\mu\nu} \delta^{ab} \frac{\partial_z \tilde{\phi}^a(q^2, \varepsilon)}{g_5^2 \varepsilon} , \qquad (4.21)$$

where $P_T^{\mu\nu} = (\eta^{\mu\nu} - q^\mu q^\nu/q^2)$ and $P_L^{\mu\nu} = q^\mu q^\nu/q^2$ are the transverse and longitudinal projector respectively. Comparing this result with the quark bubble diagram of QCD, one can fix parameter g_5 of the model [13]

$$g_5^2 = \frac{12\pi^2}{N_c} . \qquad (4.22)$$

Hadrons correspond to normalizable modes of the 5D fields. These modes should vanish sufficiently fast near the UV brane such that the action is finite and at IR brane satisfy Neumann boundary condition. The eigenvalue, $q^2 = M_n^2$, is the squared mass of the n-th Kaluza Klein mode. We expect vector mesons to be normalizable modes of equation (4.14) and scalar mesons to be normalizable modes of Eqs. (4.18) and (4.19). In the $\Sigma_{ij} = \sigma \delta_{ij}$ limit, the scalar meson has identical mass with the corresponding vector meson. However, for $a = 1, 2, 3, 8$, longitudinal modes are unphysical. Hence, the lightest scalar meson obtained from the longitudinal mode of the vector field is a strange meson, K_0^*. Regarding scalar mesons in AdS/QCD, see also Ref. [18].

As a remark, we may note that one could include a scalar field explicitly by defining X, similarly to [18], as

$$X = e^{i\pi^a t^a} \left(X_0 + S\right) e^{i\pi^a t^a} \tag{4.23}$$

with $S = S^a t^a$ (ignoring the scalar singlet). In this case, after some manipulation, the quadratic terms in the action involving V_M^a and S^b for $a, b = 4, 5, 6, 7$ become

$$S = \int d^5x \left\{ \sum_a \frac{-1}{4g_5^2 z}(\partial_M V_N^a - \partial_N V_M^a)^2 + \frac{M_V^{a\,2}(z)}{2z^3} \left(V_M^a + \frac{2}{\sqrt{3}}f^{ab8}\partial_M \left(\frac{S^b}{M_V^a}\right)\right)^2 \right.$$
$$\left. + \frac{S^a S^a}{2z^5}\left[3 - z^5\frac{\eta^{MN}}{M_V^a}\partial_M \left(\frac{1}{z^3}\partial_N M_V^a\right)\right] \right\} \tag{4.24}$$

where one can show that the square bracket on the last line is zero. Redefining the the vector field,

$$V_M^a \rightarrow V_M^a + \frac{2}{\sqrt{3}}f^{ab8}\partial_M \left(\frac{S^b}{M_V^a}\right), \tag{4.25}$$

one obtains a massive vector field and eliminates the scalar field, and the action becomes like the one we use here.

When the condensate parameters are all the same, wave functions for the vector mesons are given by

$$\psi_n^a(z) = \frac{\sqrt{2}z J_1(z\sqrt{M_n^{a\,2} - \alpha^a})}{z_0 J_1(z_0\sqrt{M_n^{a\,2} - \alpha^a})}, \tag{4.26}$$

with normalization condition, $\int (dz/z)\psi_n^{a\,2} = 1$. In particular, we obtain an infinite tower of KK rho mesons for $a = 1, 2, 3$, the corresponding tower of K^* mesons for $a = 4, 5, 6, 7$, and ω^0 mesons for $a = 8$. The Neumann boundary condition on the IR gives $J_0(M_n^\rho z_0) = 0$. Identifying the lightest mode as the rho meson, we can fix z_0 parameter of the model.

Figure 4.1 shows wave functions of the three lightest vector mesons. By our choice of boundary conditions hadrons wave functions localized closer to IR brane than to UV brane.

The presence of $J_0(\tilde{q}z_0)$ on the denominator in Eq.(4.15) indicates the existence of poles for timelike q. More precisely, the profile function can be written as a sum over
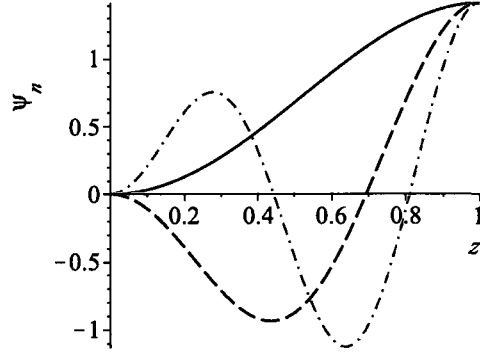
FIG. 4.1: Plot of ψ_1 (solid red curve), ψ_2 (dashed blue curve), and ψ_3 (dash-dot green curve), with z in units of z_0.

mesons poles

$$\mathcal{V}^a(q^2, z) = \sum_n \frac{-g_5 F_n^a \psi_n^a(z)}{q^2 - M_n^{a2}} , \tag{4.27}$$

where $F_n^a = |\partial_z \psi_n(\varepsilon)/(g_5\varepsilon)|$. From Eq.(4.21), F_n^a can be identified as the decay constant of the n-th KK vector meson,

$$\left\langle 0 \left| J_{\mu\perp}^a(0) \right| V_n^b(q, \lambda) \right\rangle = F_n^a \varepsilon_\mu(q, \lambda) \delta^{ab}. \tag{4.28}$$

One can substitute the above expansion of the profile function into (4.21) and obtain self energy function as a sum over narrow mesons poles. A well known signature of large N_c QCD, which is intrinsic to the AdS/QCD correspondence.

4.3.2 Axial sector

Many of our derivations for the axial sector resemble corresponding derivations for the vector sector. For example, the equation satisfied by the transverse part of the axial-vector field is analogous to Eq. (4.14), with α^a replaced by $\beta^a(z)$.

The profile functions of the longitudinal part of the axial-vector field and the π field

satisfy the following equations

$$-q^2 \partial_z \phi^a(q^2, z) + \beta^a(z) \partial_z \pi^a(q^2, z) = 0 \,, \tag{4.29}$$

$$\partial_z \left(\frac{1}{z} \partial_z \phi^a(q^2, z) \right) - \frac{\beta^a(z)}{z} \left(\phi^a(q^2, z) - \pi^a(q^2, z) \right) = 0 \,, \tag{4.30}$$

where longitudinal part of the axial-vector field denoted by $A^a_{\mu\|}(x, z) = \partial_\mu \phi^a(x, z)$. The boundary conditions are $\phi^a(q^2, \varepsilon) = 0, \pi^a(q^2, \varepsilon) = -1$, and $\partial_z \phi^a(q^2, z_0) = \partial_z \pi^a(q^2, z_0) = 0$. Note that these equations as well as boundary conditions are analogous to the longitudinal part of the vector field.

In order to solve the coupled equations, one can combine Eq. (4.29) and (4.30) into a second order differential equation, defining $y^a(q^2, z) = \partial_z \phi^a(q^2, z)/z$, to obtain [22]

$$\partial_z \left(\frac{z}{\beta^a(z)} \partial_z y^a(q^2, z) \right) + z \left(\frac{q^2}{\beta^a(z)} - 1 \right) y^a(q^2, z) = 0 \,. \tag{4.31}$$

In this notation, the boundary condition at the IR limit is given by $y^a(q^2, z_0) = 0$ which is nothing but $\partial_z \phi^a(q^2, z_0) = 0$. At the UV boundary, Eq. (4.30) and boundary conditions of π and ϕ, give $\varepsilon \partial_z y^a(q^2, \varepsilon)/\beta(\varepsilon) = 1$. Near the UV cut-off the profile function can be written as

$$y^a(q^2, \varepsilon) = \beta^a(\varepsilon) \ln(q\varepsilon) + c_2 (q\varepsilon)^2 \ln(q\varepsilon) + \dots \,. \tag{4.32}$$

Notice that although the above solution blows up logarithmically at UV, the profile functions $\phi(q^2, z)$ as well as $\pi(q^2, z)$ do not, because of a multiplication by z in their definition.

Pseudoscalar hadrons in the axial sector are pions, kaons and etas. Explicitly, π^a field can be written as follows

$$\pi^a t^a = \frac{1}{\sqrt{2}} \begin{pmatrix} \frac{\pi^0}{\sqrt{2}} + \frac{\eta^8}{\sqrt{6}} & \pi^+ & K^+ \\ \pi^- & -\frac{\pi^0}{\sqrt{2}} + \frac{\eta^8}{\sqrt{6}} & K^0 \\ K^- & \bar{K}^0 & -2\frac{\eta^8}{\sqrt{6}} \end{pmatrix} \,. \tag{4.33}$$

The corresponding normalizable modes, denoted by $y^a_n(z)$, satisfy Eq. (4.31). Their eigenvalues, $q^2 = m^{a2}_n$, are the squared mass of the corresponding hadrons. As in the
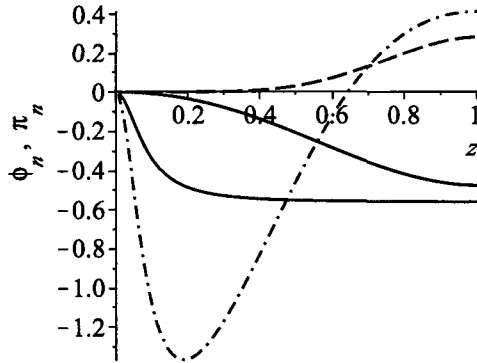
FIG. 4.2: Plot of π_1^a (lower solid curve, in red), and ϕ_1^a (upper solid curve, in blue) which correspond to $m_1^a = 139.6$ MeV, and π_2^a (dash-dot red curve), and ϕ_2^a (dashed blue curve) which correspond to $m_2^a = 1892.3$ MeV, for $a = 1, 2, 3$, with z in units of z_0. The units of ϕ_n^a and π_n^a are z_0^{-1}.

vector sector, the axial sector allows not a single mode but an infinite tower of KK modes. These modes satisfy $y_n^a(z_0) = 0$ at the IR boundary, consistent with $\partial_z \phi_n^a(z_0) = \partial_z \pi_n^a(z_0) = 0$, and $\varepsilon \partial_z y_n^a(\varepsilon)/\beta^a(\varepsilon) = 0$ at the UV brane, consistent with $\phi_n^a(\varepsilon) = \pi^a(\varepsilon) = 0$. Near the UV boundary, the normalizable mode behaves like

$$y_n(z) = a_0 + a_2 z^2 + \dots , \tag{4.34}$$

or equivalently $\phi_n \sim a_0 z^2/2$ and $\pi_n \sim m_n^2 a_0 z^2/(2\beta^a(\varepsilon))$. The coeffiecient a_0 is determined by the orthonormality condition

$$\int_\varepsilon^{z_0} dz \, \frac{z}{\beta^a(z)} y_n^a(z) y_m^a(z) = \frac{\delta_{nm}}{m_n^{a2}} . \tag{4.35}$$

These normalizable wave functions can be solved numerically. Using this normalization, the dimension of the normalizable modes is different from the dimension of the profile function. We use it because it is well behaved for the ground state in the chiral limit (despite the $1/m_n^{a2}$ on the right-hand-side). A plot of π_n and ϕ_n, for $n = 1$ and $n = 2$, is shown in Fig. 4.2.

Let us derive how the profile function, $y^a(q, z)$, can be written as sum over normalizable modes, $y_n^a(z)$. First, we write $y^a(q, z) = \sum c_n^a(q^2) y_n^a(z)$. Multiplying the left and

the right hand side of the equation by $z(q^2 - m_n^{a2})y_m(z)/\beta^a(z)$, then integrating over z, one obtains

$$c_m^a(q^2)\frac{(q^2 - m_m^{a\,2})}{m_m^{a\,2}} = -\frac{z}{\beta^a(z)}y_m^a(z)\partial_z y^a(q^2, z)\bigg|_\epsilon^{z_0} + \frac{z}{\beta^a(z)}y^a(q^2, z)\partial_z y_m^a(z)\bigg|_\epsilon^{z_0},$$

(4.36)

after integration by parts and imposing the equation of motion (4.31). The second term and the upper limit of the first term vanish by the boundary conditions of $y^a(q, z)$ and $y_n^a(z)$. Hence, ignoring the non-pole terms, the profile functions can be written as

$$y^a(q^2, \varepsilon) = \sum_n \frac{m_n^{a2}y_n^a(\varepsilon)y_n^a(z)}{q^2 - m_n^{a2}},$$

(4.37)

which can be integrated to obtain

$$\phi^a(q^2, z) = \sum_n \frac{-g_5 m_n^{a2} f_n^a \phi_n^a(z)}{q^2 - m_n^{a2}},$$

$$\pi^a(q^2, z) = \sum_n \frac{-g_5 m_n^{a2} f_n^a \pi_n^a(z)}{q^2 - m_n^{a2}},$$

(4.38)

where $f_n^a = -\partial_z \phi_n^a(\varepsilon)/(g_5\varepsilon)$.

Axial current-current correlators are analogous to Eq. (4.21),

$$i \int_x e^{iqx}\langle 0|\mathcal{T} J_{A\perp}^{\mu a}(x)J_{A\perp}^{\nu b}(0)|0\rangle = -P_T^{\mu\nu}\delta^{ab}\frac{\partial_z \mathcal{A}^a(q^2, \varepsilon)}{g_5^2\varepsilon},$$

$$i \int_x e^{iqx}\langle 0|\mathcal{T} J_{A\parallel}^{\mu a}(x)J_{A\parallel}^{\nu b}(0)|0\rangle = -P_L^{\mu\nu}\delta^{ab}\frac{\partial_z \phi^a(q^2, \varepsilon)}{g_5^2\varepsilon},$$

(4.39)

from which, one can identify f_n^a as the decay constant,

$$\langle 0 |J_{A\mu\parallel}^a(0)| \pi^b(q)\rangle = if_n^a q_\mu \delta^{ab}.$$

(4.40)

The experimental value of M^ρ gives the z_0 parameter. Parameters m_q and σ_q can be determined by fitting m_1^a and f_1^a, for $a = 1, 2, 3$, with the pion's mass and pion's decay constant respectively. In the $\sigma_q = \sigma_s$ limit, fitting m_1^a, for $a = 4, 5, 6, 7$, with the kaon's mass, m_K, gives m_s. We will call this parametrization as model A. Given experimental

data for $M_1^\rho = 775.5$, $m_\pi = 139.6$ MeV, $f_\pi = 92.4$ MeV, and $m_K = 495.7$ MeV, we obtain

$$
\begin{aligned}
z_0 &= (322.5 \, \text{MeV})^{-1}, \\
m_q &= (2\pi/\sqrt{3}) \, 2.29 \, \text{MeV} = 8.31 \, \text{MeV}, \\
\sigma_q &= \sigma_s = (\sqrt{3}/(2\pi)) \, (328.3 \, \text{MeV})^3 = (213.7 \, \text{MeV})^3, \\
m_s &= (2\pi/\sqrt{3}) \, 51.96 \, \text{MeV} = 188.5 \, \text{MeV}.
\end{aligned}
\tag{4.41}
$$

A global fit to fifteen observables, allowing $\sigma_q \neq \sigma_s$, yields,

$$
\begin{aligned}
z_0 &= (328.0 \, \text{MeV})^{-1}, \\
m_q &= (2\pi/\sqrt{3}) \, 2.16 \, \text{MeV} = 7.84 \, \text{MeV}, \\
\sigma_q &= (\sqrt{3}/(2\pi)) \, (312.2 \, \text{MeV})^3 = (203.2 \, \text{MeV})^3, \\
m_s &= (2\pi/\sqrt{3}) \, 56.81 \, \text{MeV} = 206.1 \, \text{MeV}, \\
\sigma_s &= (\sqrt{3}/(2\pi)) \, (322.8 \, \text{MeV})^3 = (210.1 \, \text{MeV})^3.
\end{aligned}
\tag{4.42}
$$

The fifteen obervables include eleven observable in Table 4.1 and the additional four observables are $f_+(0)$, λ'_+, λ''_+ and λ_0, from the kaon to pion transition form factor discussed in Sec.4.5. The quark masses given here include the normalization parameter suggested in [18, 19]. The AdS/QCD quark masses are renormalization scale independent. In QCD the quark masses do evolve with renormalization scale. We should compare our masses with experimental QCD values of the quark masses at a low renormalization scale, say 1 GeV or perhaps a bit below. The quark masses quoted by the particle data group [28] evolved to 1 GeV using their prescriptions are in the range 3.4–7 MeV for m_q and 95–175 MeV for m_s. Predictions of the model for masses and decay constants using terms up to second order expansion in the fields of the 5D action are summarized in Table 4.1. These may be compared to results in [37, 87, 88].

TABLE 4.1: Masses and decay constants. Model A is a four parameter fit to four observables as indicated in the Table, and maintains $\sigma_s = \sigma_q$. Model B is a five parameter fit to 15 observables (11 from this Table and 4 from the kaon to pion transition form factors discussed in the next section) with $\sigma_s \neq \sigma_q$. The values of the parameters are given in the text.

Observable	Model A $(\sigma_s = \sigma_q)$ (MeV)	Model B $(\sigma_s \neq \sigma_q)$ (MeV)	Measured (MeV)
m_π	(fit)	134.3	139.6
f_π	(fit)	86.6	92.4
m_K	(fit)	513.8	495.7
f_K	104	101	113 ± 1.4
$m_{K_0^*}$	791	697	672
$f_{K_0^*}$	28.	36	
m_ρ	(fit)	788.8	775.5
$F_\rho^{1/2}$	329	335	345 ± 8
m_{K^*}	791	821	893.8
$F_{K^*}^{1/2}$	329	337	
m_{a_1}	1366	1267	1230 ± 40
$F_{a_1}^{1/2}$	489	453	433 ± 13
m_{K_1}	1458	1402	1272 ± 7
$F_{K_1}^{1/2}$	511	488	

4.3.3 Massless pion limit

The AdS/QCD model has consequences of chiral symmetries, such as the Gell-Mann–Oakes–Renner relation (GOR), as shown in [13]. Here, we will present a slightly different derivation, starting from the normalization condition, Eq.(4.35). As noted in [13], the weight function $z/\beta(z)$ has significant support only for z close to $z_c = \sqrt{m_q/3\sigma}$, hence, the normalizable wave function y_n can be evaluated at $z \sim \varepsilon$ and moved outside the integral. Away from z_c, the weight function decays very fast, hence the upper limit integral can be replaced by infinity. Noting that from just after Eq. (4.38), $y_n(\varepsilon) = -g_5 f_\pi$, we obtain

$$g_5^2 f_1^{a2} m_1^{a2} \int_0^\infty dz \frac{z}{\beta^a(z)} = 1. \tag{4.43}$$

The GOR relations immediately follow, $f_\pi^2 m_\pi^2 = 2m_q\sigma_q$ for $a = 1, 2, 3$ and $f_K^2 m_K^2 = (m_q + m_s)(\sigma_q + \sigma_s)/2$ for $a = 4, 5, 6, 7$. However, for the kaon case, our results deviate by over 30 percent from the GOR relation.

As m_π approaches zero, the GOR relation becomes exact. Fixing f_π to experimental data, parameter σ_q approaches $(331.6\,\mathrm{MeV})^3$. In this limit, the $\pi_1(z)$ normalizable wave function becomes constant, $\pi_1(z) = -1/(g_5 f_\pi)$, throughout the region of interest with a step function-like jump near the UV boundary. The wave function of the lightest mode can be solved analytically in terms of modifed Bessel function. Defining $\eta = g_5\sigma/3$, one obtains

$$y_1 = Nz^2\left(-I_{-\frac{2}{3}}\left(\eta z^3\right) + \frac{I_{-\frac{2}{3}}\left(\eta z_0^3\right)}{I_{\frac{2}{3}}\left(\eta z_0^3\right)}I_{\frac{2}{3}}\left(\eta z^3\right) \right), \tag{4.44}$$

where,

$$N^2 = g_5^2\sigma^2\Gamma(2/3)\Gamma(1/3)\frac{I_{\frac{2}{3}}\left(\eta z_0^3\right)}{I_{-\frac{2}{3}}\left(\eta z_0^3\right)}. \tag{4.45}$$

Evaluating y_1 at UV boundary, we obtain an equation relating f_π and σ in the chiral limit which is in perfect agreement with previous result [23]. One should notice that $n > 1$ KK pions still present in the chiral limit.

4.4 Three point functions and form factors

The transition form factors for $K_{\ell 3}$ decay is defined from [28, 89]

$$\langle\pi^-(p)|J_\mu^{(|\Delta S|=1)}|K^0(k)\rangle$$
$$= f_+(q^2)(k + p)_\mu + f_-(q^2)(k - p)_\mu, \tag{4.46}$$

with $q = k - p$. By isospin, they could equally well be defined using the $K^+ \rightarrow \pi^0$ transition. Only the vector part of the current contributes. Further let

$$f_0(q^2) = f_+(q^2) + \frac{q^2}{m_K^2 - m_\pi^2}f_-(q^2), \tag{4.47}$$

so that f_+ and f_0 come from the transverse and longitudinal parts, respectively, of $J_\mu^{(|\Delta S|=1)}$. Unless $f_-(q^2)$ diverges as $q^2 \to 0$, one has $f_+(0) = f_0(0)$. One may also write

$$J_\mu^{(|\Delta S|=1)} = J_\mu^4 + iJ_\mu^5 , \qquad (4.48)$$

to show the SU(3) flavor indices.

In AdS/CFT or AdS/QCD, the three-point functions involving three currents are obtained by functionally differentiating the 5D action with respect to their sources, which are taken to be boundary values of the 5D fields that have the correct quantum numbers [17, 65, 21, 34]. To wit,

$$\langle 0|TJ_{A\|}^{\alpha a}(x)J_\perp^{\mu b}(y)J_{A\|}^{\beta b}(w)|0\rangle = \frac{(i/i^3)\,\delta S(V\pi\pi)}{\delta A_{\|\alpha}^{0a}(x)\,\delta V_{\perp\mu}^{0b}(y)\,\delta A_{\|\beta}^{0c}(w)} \qquad (4.49)$$

where $S(V\pi\pi)$ is the relevant part of the 5D action evaluated using classical fields that solve the equations of motion with $z = 0$ boundary values $A_{\|\alpha}^{0a}(x)$ or $V_{\perp\mu}^{0b}(y)$.

Matrix elements of the current are obtained from the three-point functions using [21, 34],

$$\langle \pi_n^a(p)|J_\perp^{\mu b}(0)|\pi_k^c(k)\rangle = \lim_{\substack{p^2 \to m_n^{a\,2} \\ k^2 \to m_k^{c\,2}}} \frac{p_\alpha k_\beta}{p^2 k^2} \frac{(p^2 - m_n^{a\,2})(k^2 - m_k^{c\,2})}{f_{\pi_n^a} f_{\pi_k^c}}$$

$$\times \int d^4x\, d^4w\, e^{ipx - ikw}\, \langle 0|TJ_{A\|}^{\alpha a}(x)J_\perp^{\mu b}(0)J_{A\|}^{\beta c}(w)|0\rangle , \qquad (4.50)$$

from which we obtain the form factor f_+.

A similar expression for the longitudinal part of the current $J_\|^{\mu b}(0)$ using $V_{\|\mu}^{0b}(y)$, allowing us to obtain the scalar form factor f_0.

The relevant part of the action receives contributions both from the gauge terms and the chiral terms. Keeping only terms that have one vector field and two pion fields (either

81

$\phi^a(x,z)$ or $\pi^a(x,z)$) one obtains

$$
\begin{aligned}
S(V\pi\pi) &= \int d^5x \left\{ \frac{1}{2g_5^2 z} f^{abc} \left(\partial^\mu \phi^a V_{\mu\nu}^b \partial^\nu \phi^c + 2\partial_z \partial_\nu \phi^a V_z^b \partial^\nu \phi^c \right) \right. \\
&+ \frac{1}{z^3} \left[g^{abc} \left(\partial^\mu \pi^a - \partial^\mu \phi^a \right) V_\mu^b \pi^c - h^{abc} \left(\frac{1}{2} \partial^\mu \left(\pi^a \pi^c \right) - \partial^\mu \phi^a \pi^c \right) V_\mu^b \right] \\
&\left. - \frac{1}{z^3} \left[g^{abc} \partial_z \pi^a V_z^b \pi^c - h^{abc} \frac{1}{2} \partial_z \left(\pi^a \pi^c \right) V_z^b \right] \right\}
\end{aligned}
\tag{4.51}
$$

The f^{abc} terms come from the gauge part of the original action, and the other terms come from the chiral part. We have defined

$$
g^{abc} = -2i\,\mathrm{Tr}\,\{t^a, X_0\}\left[t^b, \{t^c, X_0\}\right]
$$

$$
h^{abc} = -2i\,\mathrm{Tr}\,\left[t^b, X_0\right]\{t^a, \{t^c, X_0\}\}
\tag{4.52}
$$

If none of a, b, or c is equal to "8", these become

$$
g^{abc} = f^{abc} v_a v_c\,,
$$

$$
h^{abc} = f^{abc}(v_c - v_a)v_c\,,
\tag{4.53}
$$

where for $X_0 = \frac{1}{2}c_0 + c_8 t^8$,

$$
v_a = c_0 + c_8 d^{aa8} = \begin{cases} v_q\,, & a = 1, 2, 3 \\ \frac{1}{2}\left(v_q + v_s\right)\,, & a = 4, 5, 6, 7\,. \end{cases}
\tag{4.54}
$$

The derivatives indicated in Eq. (4.49) are facilitated by going to Fourier transform space and using the relations [23, 35],

$$
\phi^a(p, z) = \phi^a(p^2, z)\phi^{0a}(p) = \phi^a(p^2, z)\frac{ip^\alpha}{p^2}A_{\|\alpha}^{0a}(p)\,,
$$

$$
\pi^a(p, z) = \pi^a(p^2, z)\frac{ip^\alpha}{p^2}A_{\|\alpha}^{0a}(p)\,,
$$

$$
V_{\perp\mu}^b(q, z) = \mathcal{V}^b(q^2, z)\,V_{\perp\mu}^{0b}(q)\,,
$$

$$
V_{\|\mu}^b(q, z) = \left(\tilde{\phi}^b(q^2, z) - \tilde{\pi}^b(q^2, z)\right)V_{\|\mu}^{0b}(q)\,,
$$

$$
V_z^b(q, z) = -\partial_z \tilde{\pi}^b(q^2, z)\,\frac{iq^\alpha}{q^2}V_{\|\mu}^{0b}(q)\,,
$$

$$
\partial^\mu \rightarrow -i\,(\text{relevant momentum})^\mu\,.
\tag{4.55}
$$

With experience, one can use the above translation dictionary to obtain form factor results quite quickly. Incidentally, in the limit of having the same quark condensate parameter σ for all flavors of quarks, one can show that the bulk-to-boundary propagator $\mathcal{V}^b(q^2, z)$ for the transverse case is identical to $\tilde{\phi}^b(q^2, z) - \tilde{\pi}^b(q^2, z)$.

For the transverse form factor, the V_z terms in the action, Eq. (4.51), do not contribute. One obtains,

$$f_+(q^2) = \int_0^{z_0} dz \, \mathcal{V}^4(q^2, z) \left\{ \frac{1}{z} \partial_z \phi^1(z) \partial_z \phi^7(z) \right. \tag{4.56}$$
$$\left. + \frac{g_5^2}{2z^3} v_q (v_q + v_s) \left(\phi^1(z) - \pi^1(z) \right) \left(\phi^7(z) - \pi^7(z) \right) \right\},$$

where ϕ^a and π^a are now ground state normalizable eigenmodes, with subscript "1" tacit. The superscripts on ϕ^a, π^a, and $\mathcal{V}^b$ are the flavor indices for quantities with pion or kaon quantum numbers. We are working in the isospin conserving limit, so that the ϕ^a are the same for $a = 1, 2, 3$ and again the same for the set $a = 4, 5, 6, 7$, and similarly for π^a and $\mathcal{V}^b$.

As a check, in the equal mass limit, $v_s = v_q = v$, the transverse $K_{\ell 3}$ form factor should by SU(3) symmetry be the same as the electromagnetic form factor. One obtains in this limit

$$f_+(q^2) \stackrel{\text{SU(3) limit}}{=} \int_0^{z_0} dz \, \mathcal{V}(q^2, z) \left\{ \frac{1}{z} (\partial_z \phi(z))^2 + \frac{g_5^2 v^2(z)}{z^3} (\phi(z) - \pi(z))^2 \right\}, \tag{4.57}$$

which indeed is the same as $F_\pi(q^2)$ as found in Eq. (3.5) in [22] or to Eq. (38) in [23], allowing for the fact that those authors wrote the results using the profile functions and the massless pion limit, whereas we used the normalizable eigensolutions [34] and nonzero mass.

The longitudinal form factor is

$$f_0(q^2) = \int_0^{z_0} dz$$

$$\times \left((\tilde{\phi}^4(q^2, z) - \tilde{\pi}^4(q^2, z)) \left\{ \frac{1}{z} \partial_z \phi^1 \partial_z \phi^7 + \frac{g_5^2 v_q (v_q + v_s)}{2z^3} (\phi^1 - \pi^1)(\phi^7 - \pi^7) \right. \right.$$

$$+ \frac{q^2}{2z} \phi^1 \phi^7 + \frac{g_5^2 q^2}{8z^3(m_K^2 - m_\pi^2)} \left[(v_s - v_q)(3v_q + v_s)(\phi^1 - \pi^1)(\phi^7 - \pi^7) \right.$$

$$\left. \left. - 4v_q v_s \phi^1 (\phi^7 - \pi^7) + (v_q + v_s)(3v_q - v_s)(\phi^1 - \pi^1)\phi^7 \right] \right\}$$

$$+ \frac{\partial_z \tilde{\pi}^4(q^2, z)}{(m_K^2 - m_\pi^2)} \left\{ \frac{m_k^2 + m_\pi^2 - q^2}{2z} \left(\partial_z \phi^1 \ \phi^7 - \phi^1 \partial_z \phi^7 \right) + \frac{g_5^2(v_s - v_q)(3v_q + v_s)}{8z^3} \partial_z(\pi^1 \pi^7) \right.$$

$$\left. + \frac{g_5^2 v_q(v_q + v_s)}{2z^3} \left(\pi^1 \partial_z \pi^7 - \partial_z \pi^1 \ \pi^7 \right) - \frac{m_K^2 - m_\pi^2}{2z} \frac{\partial_z \alpha^4(z)}{\alpha^4(z)} \phi^1 \phi^7 \right\} \right). \tag{4.58}$$

The identity $f_0(0) = f_+(0)$ is apparent after noting that $\partial_z \tilde{\pi}^b(0, z) = 0$ and considering the $q^2 = 0$ normalizations of the profile functions.

4.5 Numerical Results for $K_{\ell 3}$ Form Factors

We obtain numerical solutions for the bulk-to-boundary propagators and the normalizable eigenfunctions in the massive quark case using Mathematica or Maple, and then use the numerical solutions to obtain $f_+(q^2)$ and $f_0(q^2)$. We present a plot of the results in Fig. 4.3. Of particular interest for comparison to data [28, 89] and to chiral perturbation theory [77, 78, 79, 80] or lattice gauge theory [81, 82, 83, 84, 85] are the values of $f_+(0)$, the slopes of f_+ and f_0, and the curvature of f_+.

Our results from models A ($\sigma_s = \sigma_q$) and B (σ_s independently fit), as well as the results from lattice gauge theory, chiral perturbation theory, and experiment are listed in Table 4.2.

Experiments measure $f_+(0)$ times the Cabibbo-Kobayashi-Maskawa (CKM) matrix element V_{us}. If the CKM matrix element is gotten from elsewhere, for example from the
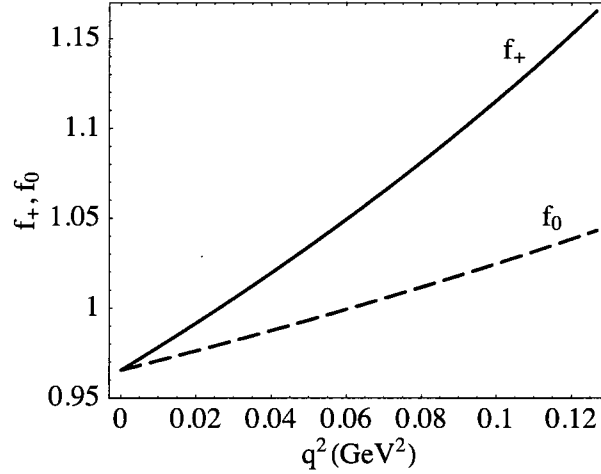
FIG. 4.3: The $K_{\ell 3}$ form factors f_+ (solid red line) and f_0 (dashed blue line) plotted vs. q^2 over the physical range pertinent to $K \to \pi e \nu$. The plot is based on the "Model A" parameters, where $\sigma_s = \sigma_q$.

unitarity relation, then all the above values of $f_+(0)$ are in agreement with experimental data. More usually, the calculations are taken to be accurate within the stated limits, and are used to extract the most precise available values of $|V_{us}|$ from the data.

Experiments also measure the slope and curvature of the $K_{\ell 3}$ form factors. For f_+, both the slope and curvature can be fit, and are parameterized as [28]

$$f_+(q^2) = f_+(0) \left(1 + \lambda'_+ \left(q^2/m_{\pi+}^2 \right) + \frac{1}{2} \lambda''_+ \left(q^2/m_{\pi+}^2 \right)^2 \right), \qquad (4.59)$$

while for $f_0(q^2)$ there is a linear fit

$$f_0(q^2) = f_0(0) \left(1 + \lambda_0 \left(q^2/m_{\pi+}^2 \right) \right). \qquad (4.60)$$

Values for the parameters are given in the Table. For the experimental data in Table 4.2, we took the numbers from the FlaviaNet Working Group on Kaon Decays [89].

Additionally, [84] quotes a result $f_-(0) = -0.113(12)$. The intercept $f_-(0)$ can be related to the slope parameters,

$$f_-(0) = \frac{m_K^2 - m_\pi^2}{m_{\pi+}^2} f_+(0) \left(\lambda_0 - \lambda'_+ \right), \qquad (4.61)$$

TABLE 4.2: Results from our models, compared to lattice gauge theory, chiral perturbation theory, and experimental data.

Observable	Model A	Model B	Lattice	χPT	Data [89]
$f_+(0)$	0.965	0.936	0.968(11) [82] 0.9742(41) [84] 0.9560(84) [85]	0.961(8) [77] 0.978(10) [78] 0.984(12) [79] 0.974(11) [80]	
λ'_+	0.0249	0.0227	0.0237(23)(21) [85]		0.0249(11)
λ''_+	0.0021	0.0016			0.0016(5)
λ_0	0.0123	0.0140	0.0128(22)(45) [85]		0.0134(12)

which leads to $f_-(0) = -0.141$ for model A and $f_-(0) = -0.110$ for model B obtained here or $f_-(0) = -0.129(18)$ using the FlaviaNet fits to experimental data for λ_0 and λ'_+.

4.6 Conclusions

We have extended the AdS/QCD model of Ref. [13, 14] to $SU(3)_L \times SU(3)_R$ model with a broken flavor symmetry. In order to introduce quarks with differing masses, we write the X field with the exponentials of the pseudoscalar field split symmetrically about the classical expectation value X_0. We find that neither the longitudinal part of the vector field nor V_z can be gauged away for $a = 4, 5, 6, 7$. If instead of using the symmetric form, one expands $X = \exp(i2\pi^a t^a)X_0$, as can certainly be done when X_0 is a multiple of the identity, the longitudinal part of the vector field and V_z will in general mix with the π field, hence with the longitudinal part of the axial-vector field, and give a parity violating term in the Lagrangian.

We have done both a four parameter and a five parameter fit. The four parameter fit constrains the condensate parameter to be flavor symmetric, $\sigma_s = \sigma_q$, and the other four parameters are fit to the rho meson's mass, pion's mass, pion's decay constant and kaon's mass. Predictions of the model for the non-dynamical properties of mesons such as

masses and decay constants are within 20% of the experimental data. There is an infinite KK tower of pions present, just as there is for vector and axial vector mesons. For three-point functions, we have calculated kaon-to-pion transition form factors, f_+ and f_0 and obtain excellent agreement with experiment for the slope as well as for the curvature. We further find that the intercept, $f_+(0)$, agrees very well with lattice and chiral perturbation theory calculations.

The five parameter fit allows σ_s to vary from σ_q, and we performed a global fit to fifteen observables, including the intercept, slope, and curvature of the K to π transition form factors. The results were again good, comparable to though somewhat improved as expected compared to the four parameter fit. The best value of the strange condensate parameter was close to the value in the non-strange sector.

We could perhaps add that we found the intercept $f_+(0)$ to be somewhat touchy. A drift of either m_s or σ_s away from the best values could lead to a significant decrease in its value. On the technical side, in the chiral limit, $f_+(0)$ becomes normalized to unity. This is because the profile functions $\mathcal{V}^b(q^2, z)$ in the chiral limit are unity at $q^2 = 0$ for all z and all b, so that $f_+(0)$ becomes just a wave function normalization integral. However, when differing quark masses and differing condensate parameters are used, the profile function at $q^2 = 0$ is unity only for $z = 0$ and can drift quite far from unity as z approaches the IR cutoff, particularly if σ_s gets far from σ_q.

A lack within the AdS/QCD framework is the absence of error estimates. On the other hand, in the present context, it should be remembered that the form factor at $q^2 = 0$ is fixed by a normalization requirement in the equal quark mass limit, so what is really being calculated for $f_{+,0}(0)$ is the difference away from unity. Here a 10–20% error suffices match the error estimates quoted from other methods.

Possible extensions of present work include calculations of four-point functions to obtain the B_K parameter and $K_{\pi 2}$ decay amplitudes [44], to consider isospin breaking in the context of the present model, and to use AdS/QCD as a method to study how differing

quark mass and hence differing pion mass affects the calculated results, and compare the trends that are found to lattice gauge theory. We hope to return to these topics in future work.

CHAPTER 5

Hadronic Momentum Densities in the Transverse Plane

5.1 Introduction

Mapping the distribution of matter inside the nucleon is a goal of hadron structure physics. For example, one can relate the density of charged and magnetically polarized material inside a nucleon to Fourier transforms of charge and magnetic form factors. This old area has seen interesting and notable improvement lately, by way of finding relativistically exact relations between form factor data and two-dimensional line-of-sight projections of the charge density and polarization density [90, 91, 92].

In a related fashion, as we study here, one can map out the distribution of momentum within a hadron. Here too there is old information, in particular that (at some resolution scale) the momentum in a hadron is carried in about equal measures by quarks and gluons. More precisely, one reports the fraction x of the light-front longitudinal momentum, $p^+ \equiv p^0 + p^3$, that is carried by individual constituents. In an extended object, one can further ask how the total momentum is distributed point by point, either in three-dimensions, or

as we shall do here, in a two-dimensional line-of-sight projection.

We will study the spatial distribution of the momentum component p^+, finding relativistically exact connections to Fourier transforms of gravitational form factors. Gravitational form factors are directly related to empirical data, in that they are matrix elements of the stress (or energy-momentum) tensor which can be obtained as second Mellin moments of generalized parton distributions (GPDs) [54, 34]. The GPDs are accessible from deeply virtual Compton scattering experiments and can be loosely defined as the amplitude for replacing a parton in a hadron with one of a different light-front momentum. In the forward limit, GPDs reduce to ordinary parton distribution functions, and the first Mellin moments give the electromagnetic form factors; for reviews, see e.g. [93, 94, 55, 95, 96, 97].

In a light-front formalism, one can kinematically connect the wave functions of any hadrons of relevant momentum. Conventionally, the longitudinal direction is the z-direction, chosen to point along the vector direction of $p = (p_1 + p_2)/2$, where $p_1(p_2)$ is the momentum of the initial(final) hadron. Further, one chooses the frame so that the momentum transfer $q = p_2 - p_1$ has $q^+ = 0$, and satisfies $q^2 = -\vec{q}_\perp^2 = -Q^2$. Within the light-front formalism, one can project the probability density into transverse plane [98] and show that it is obtained from the 2-dimensional Fourier transform of a form factor.

Transverse charge densities have been calculated for nucleons [90, 91, 92] and deuterons [99], using empirical electromagnetic form factors. Similar to the charge density, one can observe that the T^{++} component of the stress or energy-momentum tensor is the density corresponding to the p^+ component of the 4-momentum,

$$P^+ = \int T^{++} d^2 x_\perp dx_+ .$$
(5.1)

In the transverse plane in position space, the density of momentum p^+ can be defined from expectation value of the local operator $T^{++}(x^+, x^-, x_\perp)$,

$$\rho^+(\vec{b}_\perp) = \frac{1}{2p^{+2}} \left\langle \Psi | T^{++}(0, 0, \vec{b}_\perp) | \Psi \right\rangle ,$$
(5.2)

such that $\int d^2\vec{b}_\perp \rho^+(\vec{b}_\perp) = 1$. The state $|\Psi\rangle$ is localized with its transverse center of momentum located at the origin, and is formed by linear superposition of light-front helicity eigenstates $|p^+, \mathbf{p}_\perp, \lambda\rangle$,

$$|\Psi\rangle \equiv |p^+, \vec{R}_\perp = 0, \lambda\rangle = \mathcal{N} \int \frac{d^2\vec{p}_\perp}{(2\pi)^2} |p^+, \vec{p}_\perp, \lambda\rangle. \tag{5.3}$$

Normalization factor $\mathcal{N}$ satisfies $|\mathcal{N}|^2 \int d^2\vec{p}_\perp/(2\pi)^2 = 1$.

The matrix elements of the stress tensor between momentum eigenstates can be written as

$$\left\langle p^+, \frac{\vec{q}_\perp}{2}, \lambda_2 \middle| T^{++}(0) \middle| p^+, -\frac{\vec{q}_\perp}{2}, \lambda_1 \right\rangle = 2(p^+)^2 \, e^{i(\lambda_1 - \lambda_2)\phi_q} \, \mathcal{T}^{+}_{\lambda_2\lambda_1}(Q^2), \tag{5.4}$$

where $\lambda_1(\lambda_2)$ denotes the initial (final) light-front helicity, and $\vec{q}_\perp = Q(\cos\phi_q \hat{e}_x + \sin\phi_q \hat{e}_y)$. The p^+ momentum density can be written in terms of 2-dimensional Fourier transform of the form factor

$$\rho^+_\lambda(\vec{b}_\perp) = \int \frac{d^2\vec{q}_\perp}{(2\pi)^2} e^{-i\vec{q}_\perp \cdot \vec{b}} \mathcal{T}^{+}_{\lambda\lambda}(Q^2). \tag{5.5}$$

We will calculate the spatial distribution of p^+ in the transverse plane for spin-1/2 and spin-1 hadrons, specifically the nucleons and the rho mesons.

5.2 Spin-1/2 (Nucleons from GPD's)

The momentum density results for nucleons will be semi-empirical. We use matrix elements of the stress tensor obtained from second moments of GPDs [54]. "Semi" in semi-empirical is a reminder that the GPDs are not yet measured in detail. However, the models are constrained to accurately represent measured parton distribution functions in one limit and to give measured electromagnetic form factors in another.

For spin-1/2 particles, matrix elements of the stress tensor involve three gravitational

form factors,

$$\langle p_2, \lambda_2 | T^{\mu\nu}(0) | p_1, \lambda_1 \rangle = \bar{u}_{\lambda_2}(p_2) \left(A(Q^2) \gamma^{(\mu}p^{\nu)} + B(Q^2) \frac{p^{(\mu}i\sigma^{\nu)\alpha}q_\alpha}{2m} \right. \tag{5.6}$$
$$\left. + C(Q^2) \frac{q^\mu q^\nu - q^2 g^{\mu\nu}}{m} \right) u_{\lambda_1}(p_1),$$

where $\gamma^{(\mu}p^{\nu)} = (\gamma^\mu p^\nu + p^\nu \gamma^\mu)/2$ and $p_{1,2} = p \mp q/2$.

For the vector GPDs for spin-1/2 particles, the quarkic contribution is defined by

$$p^+ \int \frac{dy^-}{2\pi} e^{ixp^+y^-} \langle p_2, \lambda_2 | \bar{\psi}_q(-\frac{y}{2}) \gamma^\mu \psi_q(\frac{y}{2}) | p_1, \lambda_1 \rangle_{y^+, y_\perp=0} =$$

$$\bar{u}(p_2, \lambda_2) \left[H^q(x, \xi, t) \gamma^\mu + E^q(x, \xi, t) \frac{i}{2m} \sigma^{\mu\nu} q_\nu \right] u(p_1, \lambda_1). \tag{5.7}$$

(In the frame we use, $\xi \equiv -2q^+/p^+ = 0$.) We also have H^g and E^g due to gluons. From the definitions,

$$A(Q^2) = \sum_{a=g,q} \int_{-1}^1 x \, dx \, H^a(x, \xi, Q^2),$$

$$B(Q^2) = \sum_{a=g,q} \int_{-1}^1 x \, dx \, E^a(x, \xi, Q^2). \tag{5.8}$$

For the GPDs we use the "modified Regge model" of Ref. [100]. There we find,

$$H^q(x, 0, Q^2) = q_v(x) x^{\alpha'(1-x)Q^2},$$

$$E^q(x, 0, Q^2) = \frac{\kappa^q}{N^q}(1-x)^{\eta_q} q_v(x) x^{\alpha'(1-x)Q^2}, \tag{5.9}$$

with

$$\alpha' = 1.105 \text{ GeV}^{-2}, \qquad \eta_u = 1.713, \qquad \eta_d = 0.566,$$

$$\kappa_u = 1.673, \qquad N_u = 1.475,$$

$$\kappa_d = -2.033, \qquad N_d = 0.9083. \tag{5.10}$$

The values of $\kappa^{u,d}$ are obtained from $\kappa_p = (2/3)\kappa_u - (1/3)\kappa_d$ and $\kappa_n = -(1/3)\kappa_u + (2/3)\kappa_d$.

For the momentum density we need sea and gluon distributions. The gluon GPD $H^g(x, 0, Q^2)$ is discussed in [101]. For applications, they give two forms, each of which is a gluon parton distribution multiplied by either a dipole form or a gaussian form for the Q^2 dependence. The results from these two forms are very close to each other. A third possibility is to use the same Q^2 dependence as for the valence quarks, Eq. (5.9). This gives a result in between the results from the two choices in [101], so will be the choice we use in this chapter. We follow a similar procedure for the sea quark contributions.

All quark and gluon distributions are taken from the MRST2002 global NNLO fit [102] at input scale $\mu^2 = 1\ \mathrm{GeV}^2$,

$$u_v(x) = 0.262x^{-0.69}(1 - x)^{3.50} \left(1 + 3.83x^{0.5} + 37.65x\right),$$

$$d_v(x) = 0.061x^{-0.65}(1 - x)^{4.03} \left(1 + 49.05x^{0.5} + 8.65x\right),$$

$$S(x) = 0.759x^{-1.12}(1 - x)^{7.66}(1 - 1.34x^{0.5} + 7.40x),$$

$$g(x) = 0.669x^{-1}(1 - x)^{3.96}(1 + 6.98x^{0.5} - 3.63x) - 0.23x^{-1.27}(1 - x)^{8.7}. \tag{5.11}$$

With these definitions, we calculate

$$\rho_{1/2}^+(b) = \int_0^\infty \frac{dQ}{2\pi}\, Q J_0(bQ)\, A(Q^2), \tag{5.12}$$

where, J_0 is the Bessel function, $b = |\vec{b}_\perp|$, and $Q = |\vec{q}_\perp|$.

Results for $\rho_{1/2}^+(b)$ are shown in Fig. 5.1, both as a contour plot and along a line through the center of the nucleon. The result is the same for the proton and neutron, assuming isospin symmetry. For comparison, the charge density of the proton is also shown.

The RMS radius of the p^+ density is 0.61 fm, notably smaller than the Dirac radius of 0.80 fm (corresponding to charge radius 0.87 fm) in this parametrization.

Nucleons can also display density shifts due to polarization. We polarize the nucleons in the transverse plane, and denote the polarization direction by $\hat{S}_\perp = \cos\phi_S\, \hat{e}_x + \sin\phi_S\, \hat{e}_y$. The state with spin projection $s_\perp = 1/2$ in this direction will be $|p^+, \vec{q}_\perp/2, s_\perp\rangle$.
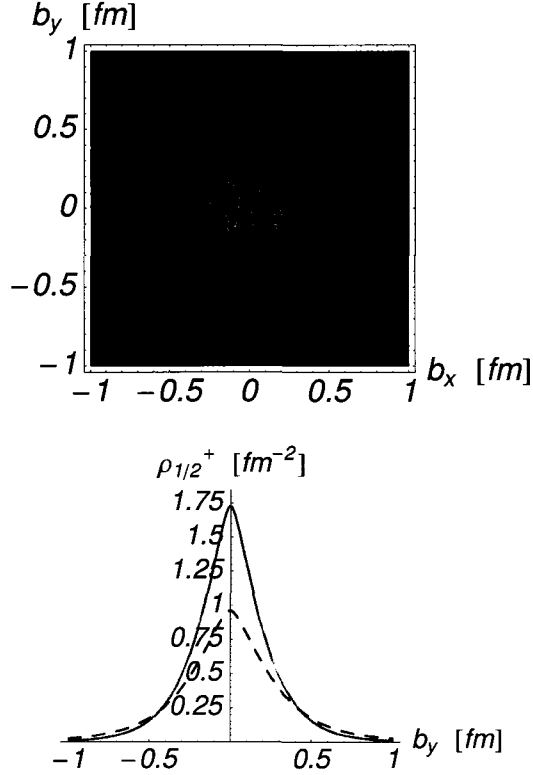
FIG. 5.1: Upper panel: Momentum density (for "p^+") of the nucleon, $\rho_{1/2}^+$, projected onto the transverse plane. Lower panel: The solid red line is $\rho_{1/2}^+$ for the nucleon, along an axis through the nucleon's center. For comparison, the proton charge density is also shown, as a dashed green line. The charge density spreads out more than the momentum density.

The impact parameter direction is denoted by $\hat{b}_\perp = \cos\phi_b\,\hat{e}_x + \sin\phi_b\,\hat{e}_y$. The p^+ density of the transversely polarized state is

$$
\rho_{Ts_\perp}^+(\vec{b}_\perp) = \frac{1}{2p^{+2}} \int \frac{d^2 q_\perp}{(2\pi)^2} e^{-i\vec{q}_\perp\cdot\vec{p}_\perp} \langle p^+, \frac{\vec{q}_\perp}{2}, s_\perp | T^{++}(0) | p^+, -\frac{\vec{q}_\perp}{2}, s_\perp\rangle
$$

$$
= \rho_{1/2}^+(b_\perp) + \sin(\phi_b - \phi_S) \int_0^\infty \frac{dQ}{2\pi} \frac{Q^2}{2m} J_1(bQ)\, B(Q^2).
$$

For the valence quarks, $B(0) \approx -0.02$, and $\rho_{Ts_\perp}^+$ is essentially the same as $\rho_{1/2}^+$, in contrast to the corresponding electromagnetic case [91, 92], and we show no plots.

5.3   Spin-1(Rho Mesons from AdS/QCD)

For spin-1 particles, the stress tensor matrix elements can be expanded in term of six Lorentz structures multiplying six gravitational form factors,

$$
\begin{aligned}
\langle p_2, \lambda_2 | T^{\mu\nu} | p_1, \lambda_1 \rangle = \varepsilon_{2\alpha}^* \varepsilon_{1\beta} \Big\{ & - 2A(q^2)\eta^{\alpha\beta} p^\mu p^\nu - 4\big(A(q^2) + B(q^2)\big) q^{[\alpha}\eta^{\beta](\mu} p^{\nu)} \\
& + \frac{1}{2} C(q^2)\eta^{\alpha\beta}\big(q^\mu q^\nu - q^2\eta^{\mu\nu}\big) + D(q^2)\big[q^\alpha q^\beta \eta^{\mu\nu} - 2q^{(\alpha}\eta^{\beta)(\mu} q^{\nu)} + q^2\eta^{\alpha(\mu}\eta^{\nu)\beta}\big] \\
& + E(q^2)\frac{q^\alpha q^\beta}{m^2} p^\mu p^\nu + F(q^2)\frac{q^\alpha q^\beta}{m^2}\big(q^\mu q^\nu - q^2\eta^{\mu\nu}\big) \Big\} .
\end{aligned}
\tag{5.13}
$$

where $a^{[\alpha}b^{\beta]} = (a^\alpha b^\beta - a^\beta b^\alpha)/2$.

The two independent helicity conserving form factors T_{11}^+, and T_{00}^+, defined by Eq. (5.4), can be expressed in terms of the above form factors,

$$
T_{11}^+ = A + \eta E = Z_2(Q^2) ,
\tag{5.14}
$$

$$
T_{00}^+ = \big((1 + 2\eta) A + 4\eta B - 2\eta D - 2\eta^2 E\big) = Z_1(Q^2) ,
$$

where $\eta = Q^2/(4m^2)$. The first equality in each line above is generic; the second uses an AdS/QCD model worked out for rho (and other) mesons in [34, 35], where

$$
\begin{aligned}
Z_1(Q^2) &= \frac{1}{m_\rho^2} \int \frac{dz}{z} e^{-\Phi} \mathcal{H}(Q, z) \partial_z \psi(z) \partial_z \psi(z) , \\
Z_2(Q^2) &= \int \frac{dz}{z} e^{-\Phi} \mathcal{H}(Q, z) \psi(z) \psi(z) .
\end{aligned}
\tag{5.15}
$$

We obtain the densities

$$
\begin{aligned}
\rho_1^+(\vec{b}_\perp) &= \int_0^\infty \frac{dQ}{2\pi} Q J_0(bQ) Z_2(Q^2) , \\
\rho_0^+(\vec{b}_\perp) &= \int_0^\infty \frac{dQ}{2\pi} Q J_0(bQ) Z_1(Q^2) .
\end{aligned}
\tag{5.16}
$$

In the hard-wall model [13], $\Phi(z) = 0$ and the z-integration in Eq. (5.15) is from 0 to z_0. The profile function $\mathcal{H}(Q, z)$ and wave functions $\psi(z)$ are

$$
\begin{aligned}
\mathcal{H}(Q, z) &= \frac{1}{2} Q^2 z^2 \left(\frac{K_1(Qz_0)}{I_1(Qz_0)} I_2(Qz) + K_2(Qz) \right) , \\
\psi_n(z) &= \frac{\sqrt{2}}{z_0 J_1(m_n z_0)} z J_1(m_n z) .
\end{aligned}
\tag{5.17}
$$

They satisfy the boundary conditions $\mathcal{H}(Q,0) = 1$, $\partial_z \mathcal{H}(Q, z_0) = 0$, $\psi(0) = 0$, and $\partial_z \psi(z_0) = 0$. The value of $z_0 = (323\text{MeV})^{-1}$ is fixed by the rho meson's mass, such that $J_0(m_n z_0) = 0$, where the lightest mass (labeled $n = 1$) corresponds to the rho meson. See also [21, 41]

For the soft-wall model [31], $\Phi(z) = \kappa^2 z^2$. The mass eigenvalues are given by $m_n^2 = 4(n + 1)\kappa^2$, with now $n = 0$ corresponding to the rho meson. The integration region in Eq. (5.15) spans from 0 to infinity. Instead of boundary conditions at the upper limit, we require a normalizable wave function, $\int (dz/z) e^{-\kappa^2 z^2} \psi^2 = 1$, and finiteness of $\mathcal{H}$ at infinity. Using results of H. Grigoryan [103],

$$\mathcal{H}(Q, z) = \Gamma(4\eta + 2)\, U(4\eta, -1, z^2)$$
$$\psi_n(z) = \kappa^2 z^2 \sqrt{\frac{2}{n+1}} L_n^{(1)}(\kappa^2 z^2). \tag{5.18}$$

where $L_n^{(\alpha)}$ is the generalized Laguerre polynomial and $U(a, b, w)$ is the 2nd Kummer function.

An analytic form can be obtained for density $\rho_0^+(\vec{b}_\perp)$,

$$\rho_0^+(\vec{b}_\perp) = \frac{m_\rho^2}{\pi} K_0(\sqrt{2} m_\rho b). \tag{5.19}$$

The other densities can be calculated numerically. They are shown in Fig.(5.2), along with the charge density [99].

Light-front longitudinal densities as well as charge densities, for helicity-0 rho-meson are logarithmically divergent at the origin for both hard-wall and soft-wall model, which is evident in (5.19) for the soft-wall model. The hard-wall model is more compact than the soft-wall model and the helicity-0 rho mesons are more compact than the helicity-1 rho mesons. Overall, the distribution of longitudinal momentum in position space is more compact than that of the charge.

The two independent helicity flip form factors are

$$\mathcal{T}_{10}^+ = \sqrt{2\eta}\,(-B + \eta E)\ , \qquad \mathcal{T}_{-1,1}^+ = -\eta E. \tag{5.20}$$
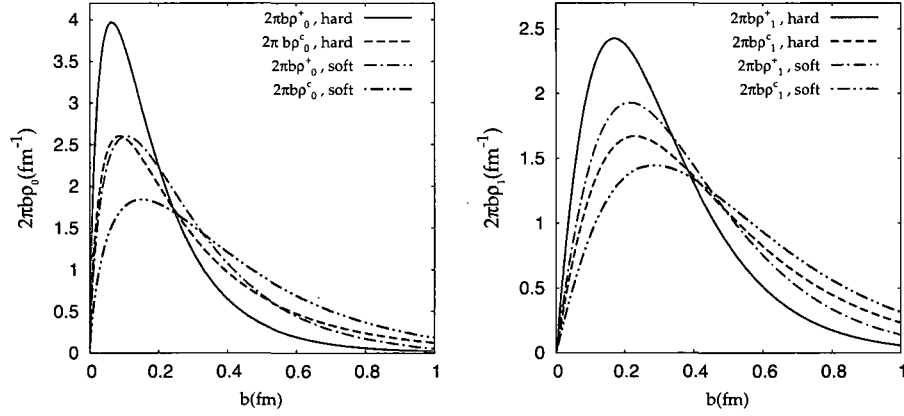
FIG. 5.2: Upper panel: The red solid line is $2\pi b$ times $\rho_0^+(b)$, the p^+ density of helicity-0 ρ-mesons in the hard-wall AdS/QCD model, while the purple dash-dotted line is the corresponding result in the soft-wall model. The blue dashed line is $2\pi b$ times $\rho_0^c(b)$, the charge density of helicity-0 ρ-mesons in the hard-wall model, while the green dash-dot-dotted line is the corresponding result in the soft-wall model. Lower panel: the same but for $\rho_1^+(b)$ and $\rho_1^c(b)$.

However, both B and E vanish in the AdS/QCD model.

5.4 Conclusions

In conclusion, we have studied the distribution within extended objects of the matter that carries the component p^+ of the momentum, in a light front viewpoint.

The examples we used were real nucleons, where we used semi-empirical models of the nucleon GPDs as underlying input, and spin-1 particles, where the underlying input came from AdS/QCD studies of these states. The crucial gravitational form factors can be obtained as second moments of the GPDs. There are conceptual similarities to the light-front relations of charge distribution in the transverse plane to Fourier transforms of the electromagnetic form factors. Differences include using the gravitational instead of electromagnetic form factors and weighting the GPDs with x instead of charge.

We presented plots that showed the p^+ density in the entire transverse plane. A qualitative result is that the hadrons we study are all more compact when looking at the

p^+ momentum density than when looking at the charge (or magnetic) density. We had earlier calculated "gravitational radii" from the slope of the gravitational form factors obtained for several species of mesons in an AdS/QCD model [34, 35]. In addition, we have learned that the phenomenon of compactness of the momentum distribution and the corresponding smaller root-mean-square radius is not limited to mesons which are studied using a purely theoretical AdS/QCD correspondence, but is also seen in nucleon distributions based on real data.

CHAPTER 6

Nucleon electromagnetic and gravitational form factors from holography

6.1 Introduction

The anti de Sitter space/conformal field theory (AdS/CFT) correspondence [8, 17, 65] is a conjecture which holds the possibility of obtaining accurate results in the strong coupling limit of gauge theories from classical calculations of gravitationally interacting fields in a higher dimensional space. The original correspondence was between a paricular string theory in 10D and a particular conformal field theory in 4D, namely the large N_C limit of $\mathcal{N} = 4$ super Yang-Mills theory.

A particular implementation motivated by the original AdS/CFT correspondence is the "bottom-up" approach, introduced in [13, 14], which is a way of using the AdS/CFT correspondence as motivation for modeling QCD starting from a 5D space. One may think that one has reached the point where the 10D string theory of the original AdS/CFT

correspondence has been reduced to a gravitational theory on AdS_5, and one then asks what terms should exist in the Lagrangian. The terms are chosen based on simplicity, symmetries, and relevance to the problems one wishes to study.

QCD is not a conformal field theory, so one also needs to break a corresponding symmetry in the AdS space, in order to obtain, for example, discrete hadron masses. Two schemes which have the virtue of being analytically tractable are the hard-wall model, where the AdS space is sharply cutoff and a boundary condition imposed, and the soft-wall model where extra interactions are introduced which have an effect akin to warping the metric and suppressing long distance propagation in the fifth dimension.

Having chosen a Lagrangian and a cutoff scheme, one can study the phenomeno-logical consequences for the 4D correspondent theory, and compare the results to data. Much of the work has focused on the bosonic sector [63, 72, 39, 45, 40, 41, 36, 31, 21, 32, 23, 43, 73, 22, 74, 66, 49, 34, 35]. The works include studies of spin-1 vector and axial states, pseudoscalars, and glueballs. Masses, decay constants, and charge radii that can be compared to experimental data agree with experimental data at the roughly 10% level.

Studying fermions with the AdS/CFT correspondence is technically more compli-cated than studying bosons. Two approaches have been pursued. One approach is to fol-low upon the bosonic studies, and treat the fermions as Skyrmions within the model [104, 46, 47]. The other approach is to begin with a theory in the 5D sector that has fundamen-tal fermion fields interacting with an AdS gravitational background [105, 106, 107, 108]. One can also consider a hybrid of the two approaches, where one begins with fermions as Skyrmions of a 5D model, and uses the Skyrmion model to obtain parameters and interac-tion terms of another 5D Lagrangian where the fermion fields appear as explicit degrees of freedom [109, 110, 111].

We here pursue the AdS/CFT correspondence within a model where the fermion stands as an explicit field in the 5D Lagrangian. We will particularly be interested in

obtaining results for the electromagnetic and gravitational form factors. For the electro-magnetic form factors, there is already work reported in the literature, particularly for the hard-wall model, and we will quote some results from this material, adding some useful detail. The derivation of the tensor or gravitational form factors is new.

One point in mapping fermion fields from a 5D theory to a 4D theory is that not all components of the fermion spinor are independent. In both theories, for massive fermions, one can obtain the (ill-named) right handed part of the field from the left handed part of the field, or *vice-versa*. An early 4D discussion of this is in [112]. Thus, as one begins by finding exact solutions for fermions in an AdS background, one can only choose boundary conditions for the independent components, which one can choose to be the left handed ones. The left handed 5D fermions on the boundary are sources for right handed fermionic currents in the 4D theory, and the corresponding left handed fermion currents can either be obtained from these, or can be consistently obtained from the derived right handed fermions in AdS space.

When we study the soft wall model for fermions, the usual procedure of producing a "soft wall" by inserting an interaction with a background dilation field via an overall exponential factor does not by itself lead to normalizable solutions. (Indeed, it is possible to remove the overall exponential factor in the fermion case by rescaling the field.) We will introduce an additional interaction with the background field by using an analog of a scalar potential, that is, by adding a dilation interaction to the mass term. The resulting equations describing the interaction with both AdS gravity and the soft-wall potential can be solved exactly in the classical limit, with the normalizable solutions having the fea-ture common to soft-wall models that their functional dependence in the extra dimension contains a generalized Laguerre polynomial.

Our presentation will focus on the soft-wall model. It is easy to switch our equations to the hard-wall model just by dropping the soft-wall interaction term and using a suitable boundary condition. We will comment on this and show hard-wall as well as soft-wall re-

sults. We will obtain expressions for both electromagnetic and gravitational form factors, and present the result for the nucleon radii as well as for general momentum transfer. We will find that radii obtained from the gravitational momentum form factor is smaller than radii obtained electromagnetically, as is also the case for the meson sector [34, 35].

The model, focusing on the baryonic degrees of freedom, is outlined in Sec. 6.2, and the two-point functions are worked out in Sec. 6.3. The form factors, both electromagnetic and gravitational are discussed in Sec. 6.4, and a summary is given in Sec. 6.5.

6.2 The Model

In a d-dimensional field theory, the generating function is given by

$$\mathscr{Z}_{CFT}[\Phi^0] = \left\langle \exp\left(i \int d^d x \mathcal{O}(x) \Phi^0(x) \right) \right\rangle, \tag{6.1}$$

The precise statement of the AdS/CFT correspondence is that the generating function of a d-dimensional CFT is equal to the partition function of a field theory in AdS$_{d+1}$

$$Z_{CFT}[\Phi^0] = e^{iS_{AdS}(\Phi_{cl})}. \tag{6.2}$$

On the right hand side of the above equation, $S_{AdS}(\Phi_{cl})$ is the classical action evaluated on the solution of the equation of motion with boundary condition

$$\lim_{z \to 0} \Phi_{cl}(x, z) = z^\Delta \Phi^0(x). \tag{6.3}$$

The constant Δ depends on the nature of operator $\mathcal{O}$.

The metric of $d + 1$-dimensional AdS space is given by

$$ds^2 = g_{MN} dx^M dx^N = \frac{1}{z^2} \left(\eta_{\mu\nu} dx^\mu dx^\nu - dz^2 \right), \tag{6.4}$$

where $\eta_{\mu\nu} = diag(1, -1, -1, -1)$, $\mu, \nu = 0, 1, 2, ..., d - 1$ and we will set $d = 4$. The z variable extend from $\varepsilon \to 0$, which is called the UV-boundary, to ∞, which is the

IR-boundary. In order to simulates confinement, one can use a hard-wall model [13, 14, 45, 21], by cutting off the AdS geometry at z_0. The mass spectrum is found to be approximately linear at large mass, $m_n \sim n$. Alternatively, one can use the soft-wall model [31, 32], where the geometry is smoothly cut-off by a background dilaton field $\Phi(z)$. A choice for the dilaton field solution, $\Phi(z) = \kappa^2 z^2$, gives the mass spectrum that is in agreement with Regge trajectory, $m_n^2 \sim n$.

Consider a Dirac field coupled to a vector field in the $d + 1$-dimensional AdS space with the following action

$$S_F = \int d^{d+1}x \sqrt{g}\, e^{-\Phi} \left[\frac{i}{2} \bar{\Psi} e_A^N \Gamma^A D_N \Psi - \frac{i}{2}(D_N \Psi)^\dagger \Gamma^0 e_A^N \Gamma^A \Psi - (M + \Phi)\bar{\Psi}\Psi \right], \quad (6.5)$$

where for the AdS space, $e_A^N = z\delta_A^N$ is the inverse vielbein. Covariant derivative $D_N = \partial_N + \frac{1}{8}\omega_{NAB}[\Gamma^A, \Gamma^B] - iV_N$ ensure that the action satisfies gauge invariance and diffeomorphism invariance. The non-vanishing components of the spin connection are $\omega_{\mu z\nu} = -\omega_{\mu\nu z} = \frac{1}{z}\eta_{\mu\nu}$. The Dirac gamma matrices have been defined in such a way that they satisfy anti-commutation relation $\{\Gamma^A, \Gamma^B\} = 2\eta^{AB}$, that is for $d = 4$, we have $\Gamma^A = (\gamma^\mu, -i\gamma^5)$. We implement the soft-wall model by adding $\Phi(z) = \kappa^2 z^2$ to the mass term. Both the Dirac and the vector fields have an $U(2)$ isospin structure. In particular, $V_N = \frac{1}{2}V_N^s + V_N^a t^a$, where t^a is an $SU(2)$ generator normalized by $\text{Tr}(t^a t^b) = \delta^{ab}/2$.

The Dirac field satisfies the following equation of motion

$$\left[ie_A^N \Gamma^A D_N - \frac{i}{2}(\partial_N \Phi)\, e_A^N \Gamma^A - (M + \Phi(z)) \right] \Psi = 0. \quad (6.6)$$

Evaluating the action on the solution, we obtain

$$\begin{aligned} S_F[\Psi_{cl}] &= \int d^d x \left(-\frac{i}{2}\sqrt{g}\, e^{-\kappa^2 z^2} \bar{\Psi} z \Gamma^z \Psi \right)_\epsilon^{z_{IR}} \\ &= \int d^d x\, \frac{-1}{2z^d} e^{-\kappa^2 z^2} \left(\bar{\Psi}_L \Psi_R - \bar{\Psi}_R \Psi_L \right) \Big|_\epsilon^{z_{IR}}, \quad (6.7) \end{aligned}$$

where $\Psi_{R,L} = (1/2)(1 \pm \gamma^5)\Psi$. For hard-wall model the IR boundary is located at finite $z_{IR} = z_0$, while for the soft-wall model the z variable extends to infinity, $i.e.$, $z_{IR} = \infty$.

In the case of hard-wall model, the IR boundary term can be removed by requiring that either $\Psi_L(z_{IR}) = 0$ or $\Psi_R(z_{IR}) = 0$.

Following [105, 106, 107], we add extra term in the UV-boundary

$$\frac{1}{2} \int d^d x \sqrt{-g^{(d)}} \left(\bar{\Psi}_L \Psi_R + \bar{\Psi}_R \Psi_L \right)_\varepsilon . \tag{6.8}$$

This term preserves the $O(d + 1, 1)$ isometry group of the original action and does not change the equation of motion. The action becomes

$$S_F = \int d^d x \left(\frac{1}{z^d} \bar{\Psi}_L \Psi_R \right)_\varepsilon \tag{6.9}$$

The Dirac field $\Psi_{R,L}$ in momentum space can be written in terms of a product of d-dimensional boundary fields $\Psi^0_{R,L}$ and profile functions or the bulk-to-boundary propagators $f_{R,L}$, i.e., $\Psi_{R,L}(p, z) = z^\Delta f_{R,L}(p, z) \Psi^0(p)_{R,L}$, where p is the momentum in d-dimensions. We choose $\Psi^0_L(p)$ as the independent source field which corresponds to the spin-$\frac{1}{2}$ baryon operator $\mathcal{O}_R$ in the d-dimensional field theory. Hence, Δ is chosen such that the equation of motion allows $f_L(p, \varepsilon) = 1$.

The left handed and the right handed components of the spin-$\frac{1}{2}$ field operators in d-dimensional flat space are not independent, since they are related by the Dirac equation. This is realized by the relationship between Ψ^0_L and Ψ^0_R, chosen to satisfies $\not{p} \Psi^0_R(p) = p \Psi^0_L(p)$. Ignoring the interaction term with the vector field, the equation of motion for the Dirac field becomes (for $\Phi = \kappa^2 z^2$),

$$\left(\partial_z - \frac{d/2 + M - \Delta + 2\Phi}{z} \right) f_R = -p f_L,$$
$$\left(\partial_z - \frac{d/2 - M - \Delta}{z} \right) f_L = p f_R, \tag{6.10}$$

where $p \equiv \sqrt{p^2}$.

In addition to (6.5) or (6.9), we have the kinetic term of the vector field

$$S_V = \int d^{d+1} x \, e^{-\Phi} \sqrt{g} \mathrm{Tr} \left(-\frac{F_V^2}{2g_5^2} \right), \tag{6.11}$$

where $F_{MN}^V = \partial_M V_N - \partial_N V_M$. The transverse part of the vector field can be written as

$V_\mu(p, z) = V(p, z) V_\mu^0(p)$. At the UV-boundary, the bulk-to-boundary propagator satisfies

$V(p, \varepsilon) = 1$. According to the AdS/CFT dictionary, the $V_\mu^0(p)$ is the source for the 4D

current operator J_μ^V. The equation of motion in the $V_z = 0$ gauge is given by [32]

$$\left[\partial_z \left(\frac{e^{-\Phi}}{z} \partial_z \right) + \frac{e^{-\Phi}}{z} p^2 \right] V(p, z) = 0. \tag{6.12}$$

The normalizable mode, is a solution of the above equation with eigenvalue $p^2 = M_n^2$

which corresponds to the mass of the n-th Kaluza Klein mode of vector meson [13]. For

the soft-wall model [32], the mass eigenvalues are $M_n^2 = 4\kappa^2(n+1)$, where $n = 0, 1, \ldots$.

For the hard-wall model the mass eigenvalues are $M_n = \gamma_{0,n+1}/z_0$, where $\gamma_{0,n+1}$ is the

$n + 1$-th zeros of the Bessel function J_0.

6.3 Two-point function

6.3.1 Soft-wall Model

To have $f_L(p, \varepsilon) = 1$ for $\Phi(0) = 0$ and f_R not singular requires $\Delta = \frac{d}{2} - M$. The

equation of motions of the profile functions (6.10), with $\Phi(z) = \kappa^2 z^2$, become

$$\left[\partial_z^2 - \frac{2(M + \kappa^2 z^2)}{z} \partial_z + \frac{2(M - \kappa^2 z^2)}{z^2} + p^2 \right] f_R = 0,$$

$$\left[\partial_z^2 - \frac{2(M + \kappa^2 z^2)}{z} \partial_z + p^2 \right] f_L = 0. \tag{6.13}$$

The general solution is given by Kummer's functions of the first and the second kind.

Requiring that the profile functions vanish at infinity, we obtain

$$f_L(p, z) = N_L U\left(-\frac{p^2}{4\kappa^2}, \frac{1}{2} - M; \xi \right), \tag{6.14}$$

$$f_R(p, z) = N_R \xi^{\frac{1}{2}} U\left(1 - \frac{p^2}{4\kappa^2}, \frac{3}{2} - M; \xi \right), \tag{6.15}$$

where $\xi = \kappa^2 z^2$. From the UV-boundary condition we obtain

$$N_L = \frac{\Gamma\left(\alpha - \frac{p^2}{4\kappa^2} \right)}{\Gamma(\alpha)}, \tag{6.16}$$

where $\alpha = M + \frac{1}{2}$ and we have $N_R = N_L \frac{p}{2\kappa}$ from Eq. (6.10).

The normalizable wave function $\psi_{L,R}^{(n)}$ for the n-th Kaluza Klein mode can be obtained from Eq. (6.13), by requiring that $p^2 = m_n^2$. One find that solutions exist in terms of Laguerre polynomial when $m_n^2 = 4\kappa^2(n + \alpha)$

$$\psi_L^{(n)}(z) = n_L \xi^\alpha L_n^{(\alpha)}(\xi),\tag{6.17}$$

$$\psi_R^{(n)}(z) = n_R \xi^{\alpha-\frac{1}{2}} L_n^{(\alpha-1)}(\xi).\tag{6.18}$$

Imposing the normalization condition,

$$\int dz \, \frac{e^{-\kappa^2 z^2}}{z^{2M}} \psi_L^{(n)} \psi_L^{(m)} = \delta_{nm},\tag{6.19}$$

one obtains the normalization factors,

$$n_L = \frac{1}{\kappa^{\alpha-1}} \sqrt{\frac{2\Gamma(n+1)}{\Gamma(\alpha+n+1)}},\tag{6.20}$$

$$n_R = n_L\sqrt{\alpha+n},\tag{6.21}$$

For the right handed wave function $\psi_R^{(n)}$, the normalization factor can be obtained either by using Eq. (6.10) or by imposing the above normalization condition.

For the time-like region $p^2 > 0$, the profile functions have infinite number of poles which correspond to the tower of infinite Kaluza-Klein mode. To show this, we write the profile functions in different forms utilizing the Kummer transformation ([113], p.505),

$$f_L(p, z) = N_L \, \xi^\alpha U\left(\alpha - \frac{p^2}{4\kappa^2}, \alpha + 1; \xi\right),\tag{6.22}$$

$$f_R(p, z) = N_R \, \xi^{\alpha-\frac{1}{2}} U\left(\alpha - \frac{p^2}{4\kappa^2}, \alpha; \xi\right).\tag{6.23}$$

The Kummer function can be written in integral representations,

$$f_L(p, z) = \frac{\xi^\alpha}{\Gamma(\alpha)} \int_0^1 dx \frac{x^{\alpha+a-1}}{(1-x)^{\alpha+1}} \exp\left(-\frac{x}{1-x}\xi\right),\tag{6.24}$$

where $a = -p^2/(4\kappa^2)$. The integrand contains generating function for Laguerre polynomial ([113], p.784)

$$\frac{1}{(1-x)^{\alpha+1}} \exp\left(-\frac{x}{1-x}\xi\right) = \sum_{n=0}^{\infty} L_n^{(\alpha)}(\xi) x^n.\tag{6.25}$$

Performing the integrals, one obtains

$$f_L(p,z) = \frac{-4\kappa^2\xi^\alpha}{\Gamma(\alpha)} \sum_{n=0}^{\infty} \frac{L_n^{(\alpha)}(\xi)}{p^2 - 4\kappa^2(n+\alpha)}, \tag{6.26}$$

which show that the mass square of the n-th Kaluza-Klein mode is $4\kappa^2(n+\alpha)$, as expected. Similar expansion for the right handed profile function yields

$$f_R(p,z) = \frac{-2\kappa\,p\,\xi^{\alpha-\frac{1}{2}}}{\Gamma(\alpha)} \sum_{n=0}^{\infty} \frac{L_n^{(\alpha-1)}(\xi)}{p^2 - 4\kappa^2(n+\alpha)}. \tag{6.27}$$

Notice that the Laguerre polynomials which appears in the expansion precisely match the normalizable modes. Defining $f_n = 2\kappa/(\Gamma(\alpha)\,n_R) = \psi_R^{(n)}(\varepsilon)/\varepsilon^{2M}$, the profile functions become

$$f_L(p,z) = \sum_{n=0}^{\infty} \frac{f_n m_n \psi_L^{(n)}(z)}{p^2 - m_n^2}, \tag{6.28}$$

$$f_R(p,z) = \sum_{n=0}^{\infty} \frac{f_n p\,\psi_R^{(n)}(z)}{p^2 - m_n^2}. \tag{6.29}$$

The 5D fermion action (6.9) can now be written in terms of sum over modes

$$S_F = \int \frac{d^dp}{(2\pi)^d} \bar{\Psi}_L^0(p) \frac{f_R(p,\varepsilon)\,\not{p}}{\varepsilon^{2M}p} \Psi_L^0(p) = \sum_n \int \frac{d^dp}{(2\pi)^d} \bar{\Psi}_L^0(p) \left[\frac{-f_n^2 P_R\,\not{p}}{p^2 - m_n^2}\right] \Psi_L^0(p), \tag{6.30}$$

where $P_R = (1+\gamma^5)/2$ is the right handed chirality projector. From the AdS/CFT correspondence and the appropriate functional derivatives, we have

$$\int d^dx\, e^{iqx} \langle 0 | \mathcal{T}\mathcal{O}_R(x)\bar{\mathcal{O}}_R(0) | 0 \rangle = \sum_n \frac{if_n^2 P_R\,\not{q}}{q^2 - m_n^2}. \tag{6.31}$$

One may also define the decay constant f_n from $\langle 0 | \mathcal{O}_R(0) | p \rangle = f_n u_R(p)$ and obtain the same result by inserting a set of intermediate states. In order to obtain the complete two-point function $\langle \mathcal{O}\bar{\mathcal{O}} \rangle$, one also needs the left handed chirality operator $\mathcal{O}_L$, which can be obtained from the right handed one using $\mathcal{O}_L(p) = (\not{p}/p)\mathcal{O}_R(p)$.

6.3.2 Hard-wall Model

For the hard-wall model $\kappa = 0$, and IR boundary is at $z_{IR} = z_0$. The mass eigenvalue of the Kaluza Klein mode depends on which propagator vanish at IR boundary. We will

set $f_R(z_0) = 0$, such that there is no massless mode. Requiring that $f_L(p, \varepsilon) = 1$, the solution can be written in terms of Bessel function

$$
\begin{aligned}
f_L &= \frac{\pi}{\Gamma(\alpha)} \left(\frac{pz}{2}\right)^\alpha \left(\frac{Y_{\alpha-1}(pz_0)}{J_{\alpha-1}(pz_0)} J_\alpha(pz) - Y_\alpha(pz)\right), & (6.32) \\
f_R &= \frac{\pi}{\Gamma(\alpha)} \left(\frac{pz}{2}\right)^\alpha \left(\frac{Y_{\alpha-1}(pz_0)}{J_{\alpha-1}(pz_0)} J_{\alpha-1}(pz) - Y_{\alpha-1}(pz)\right).
\end{aligned}
$$

The normalizable mode, again, setting $p^2 = m_n^2$ on Eq. (6.13) with Dirichlet boundary condition $\phi_R^{(n)}(z_0) = 0$ and $\phi_L^{(n)}(\varepsilon) = 0$ gives

$$
\begin{aligned}
\phi_L^{(n)}(z) &= \frac{\sqrt{2} z^\alpha J_\alpha(m_n z)}{z_0 J_\alpha(m_n z_0)}, \\
\phi_R^{(n)}(z) &= \frac{\sqrt{2} z^\alpha J_{\alpha-1}(m_n z)}{z_0 J_\alpha(m_n z_0)}. & (6.33)
\end{aligned}
$$

Both satisfy normalization condition given in Eq. (6.19). The mass eigenvalue determined by $J_{\alpha-1}(m_n z_0) = 0$. One can easily see that the location of the pole of the profile function $f_{R,L}(p, z)$, in the time-like region $p^2 > 0$, are precisely at the mass eigenstates m_n^2.

As in the soft-wall model, the bulk-to-boundary propagators can be written in terms of sum over normalizable modes given in Eq. (6.28) and (6.29), where for the hard-wall model

$$
f_n = \frac{\sqrt{2}(\frac{m_n}{2})^{\alpha-1}}{\Gamma(\alpha) z_0 J_\alpha(m_n z_0)}. \tag{6.34}
$$

6.4 Form factors

6.4.1 Electromagnetic Form Factors

For spin-$\frac{1}{2}$ particles, the electromagnetic current matrix element can be written in terms of two independent form factors

$$
\langle p_2, s_2 | J^\mu(0) | p_1, s_1 \rangle = u(p_2, s_2) \left(F_1(Q)\gamma^\mu + F_2(Q)\frac{i\sigma^{\mu\nu} q_\nu}{2m_n}\right) u(p_1, s_1), \tag{6.35}
$$

where $q = p_2 - p_1$ and $Q^2 = -q^2$. In this chapter, our interest is on the electromagnetic current operator of nucleons which can be written in terms of isoscalar and isovector currents

$$J_{p,n}^\mu = \chi_i \left(\frac{1}{2} J_S^\mu \delta_{ij} + J_V^{a,\mu} t_{ij}^a \right) \chi_j, \tag{6.36}$$

where $\chi = (1,0)$ for proton, and $\chi = (0,1)$ for neutron. According to the AdS/CFT dictionary, the 4D isoscalar J_S^μ and isovector $J_V^{a,\mu}$ current operators correspond to the isoscalar and isovector part of the 5D gauge field respectively. In the simplest model, the profile function of both satisfy Eq. (6.12).

The isovector matrix element can be extracted from the 3-point function by the following relation

$$\lim_{p_{1,2}^0 \to E_{1,2}^n} (p_1^2 - m_n^2)(p_2^2 - m_n^2) \int d^4x d^4y e^{i(p_2 x - qy - p_1 w)} \left\langle 0 \left| \mathcal{T} \mathcal{O}_R^i(x) J^{a\mu}(y) \bar{\mathcal{O}}_R^j(w) \right| 0 \right\rangle$$
$$= f_n^2 \chi^i u(p_2, s_2) \left\langle p_2, s_2 \left| J^{a\mu}(0) \right| p_1, s_1 \right\rangle \bar{u}(p_1, s_1) \chi^j \delta^{(4)}(p_2 - p_1 - q), \tag{6.37}$$

and analogously for the isoscalar current.

Relevant term in the action (6.5) which contribute to the 3-point function is given by

$$S_F = \int d^5x \sqrt{g} e^{-\Phi} \bar{\Psi} e_A^M \Gamma^A V_M \Psi. \tag{6.38}$$

However the above term only provides the F_1 form factor. Hence, we should add the following gauge invariant term to the action

$$\eta_{S,V} \int d^5x \sqrt{g} e^{-\Phi} i \frac{1}{2} \bar{\Psi} e_A^M e_B^N [\Gamma^A, \Gamma^B] F_{MN}^{(S,V)} \Psi. \tag{6.39}$$

We shall use different parameters: η_S for the isoscalar component and η_V for the isovector component of the vector field. They are fixed by the experimental values of the proton and the neutron magnetic moments.
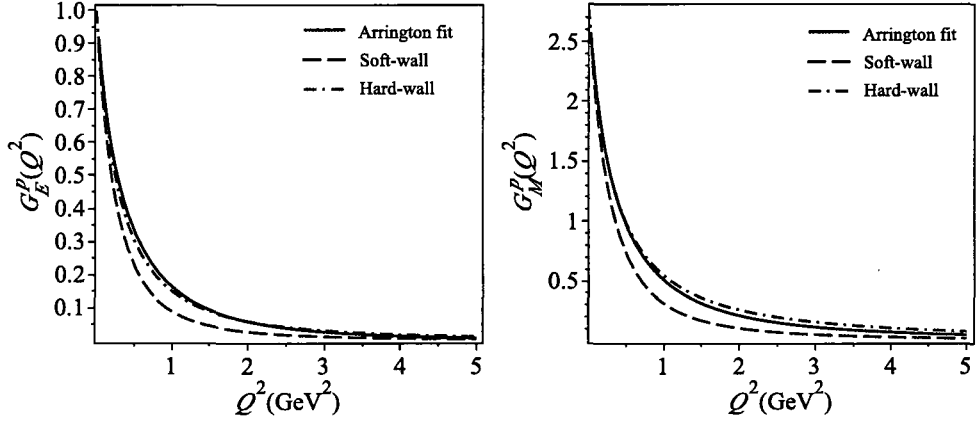
FIG. 6.1: The red dashed line and the purple dot-dashed line are the electromagnetic form factors of proton from the soft-wall and the hard-wall model of AdS/QCD respectively. The solid blue line is the corresponding form factor from the Arrington empirical fit [114]

Defining invariant functions

$$C_1(Q) = \int dz\, e^{-\Phi} \frac{V(Q,z)}{2z^{2M}} \left(\psi_L{}^2(z) + \psi_R{}^2(z) \right) , \tag{6.40}$$

$$C_2(Q) = \int dz\, e^{-\Phi} \frac{\partial_z V(Q,z)}{2z^{2M-1}} \left(\psi_L{}^2(z) - \psi_R{}^2(z) \right) , \tag{6.41}$$

$$C_3(Q) = \int dz\, e^{-\Phi} \frac{2m_n V(Q,z)}{z^{2M-1}} \psi_L(z)\psi_R(z), \tag{6.42}$$

where $Q^2 = -q^2 > 0$, we obtain the electromagnetic form factors for the proton

$$F_1^{(P)}(Q) = C_1(Q) + \eta_P C_2(Q), \tag{6.43}$$

$$F_2^{(P)}(Q) = \eta_P C_3(Q). \tag{6.44}$$

For the neutron, the F_1 and the F_2 form factors are solely come from (6.39). We have

$$F_1^{(N)}(Q) = \eta_N C_2(Q), \tag{6.45}$$

$$F_2^{(N)}(Q) = \eta_N C_3(Q), \tag{6.46}$$

with parameters η_P and η_N are defined by $\eta_{P,N} = (\eta_V \pm \eta_S)/2$.

In the soft-wall model, the bulk-to-boundary propagator of the vector field is given by[32]

$$V(Q,z) = \Gamma(1 + a)\, U(a, 0; \xi) = a \int_0^1 dx\, x^{a-1} \exp\left(-\frac{x}{1-x}\xi \right) . \tag{6.47}$$

where again $a = Q^2/(4\kappa^2)$. Integral in Eq.(6.40-6.42) can be evaluated analytically. For the lowest state $n = 0$, we obtain

$$C_1(Q) \;=\; \frac{\frac{1}{2}\left(2 + \frac{a}{a+1}\right)}{\left(\frac{a}{a+1} + 1\right)\left(\frac{a}{a} + 1\right)\ldots(a+1)}, \qquad (6.48)$$

$$C_2(Q) \;=\; \frac{-a(1 - \alpha a)\,(\alpha + 2)^{-1}\,(\alpha + 1)^{-1}}{\left[\left(\frac{a}{a+2} + 1\right)\ldots(a+1)\right]}, \qquad (6.49)$$

$$C_3(Q) \;=\; \frac{4\alpha}{\left(\frac{a}{a+1} + 1\right)\left(\frac{a}{a} + 1\right)\ldots(a+1)}. \qquad (6.50)$$

One can check that $F_1^{(P)}(0) = 1$ and $F_1^{(N)}(0) = 0$.

In the limit of large momentum transverse, the electromagnetic form factors for the proton becomes

$$F_1^{(P)}(Q) \;=\; \frac{\alpha!(2\kappa)^{2\alpha}}{2Q^{2\alpha}}\,(1 + 2\eta_P\,\alpha), \qquad (6.51)$$

$$F_2^{(P)}(Q) \;=\; \frac{4\alpha(\alpha + 1)!\,(2\kappa)^{2\alpha+2}}{Q^{2\alpha+2}}. \qquad (6.52)$$

Hence, $M = \frac{3}{2}$ which corresponds to $\alpha = 2$ gives the correct large momentum scaling. The constant κ, was simultaneously fixed to the proton's and the ρ-meson's mass. The best fit, given by $\kappa = 0.350\,\mathrm{GeV}$, gives the proton's mass $0.990\,\mathrm{GeV}$ and ρ-meson's mass $0.700\,\mathrm{GeV}$.

Parameters η_P and η_N can be determined by matching the value of $F_2(0)$ with the experimental data: 1.793 for proton and -1.913 for neutron. One obtain, for $\alpha = 2$, $\eta_P = 0.224$ and $\eta_N = -0.239$.

The charge radius for the proton is defined by

$$\langle r_C^2\rangle_p \;=\; -\frac{6}{G_E(0)}\frac{dG_E(0)}{dQ^2}, \qquad (6.53)$$

where $G_E(Q) = F_1(Q) - Q^2 F_2(Q)/(4m_p^2)$. One obtains

$$\langle r_C^2\rangle_p \;=\; \frac{5}{2\kappa^2} + \frac{\eta_P}{8\kappa^2} + \frac{6F_2^{(P)}(0)}{4m_p^2} = (0.961\,\mathrm{fm})^2, \qquad (6.54)$$

which, in terms of rms-radius, is about 10 percent larger than the experimental result $\langle r_C\rangle = (0.877\,\mathrm{fm})$.
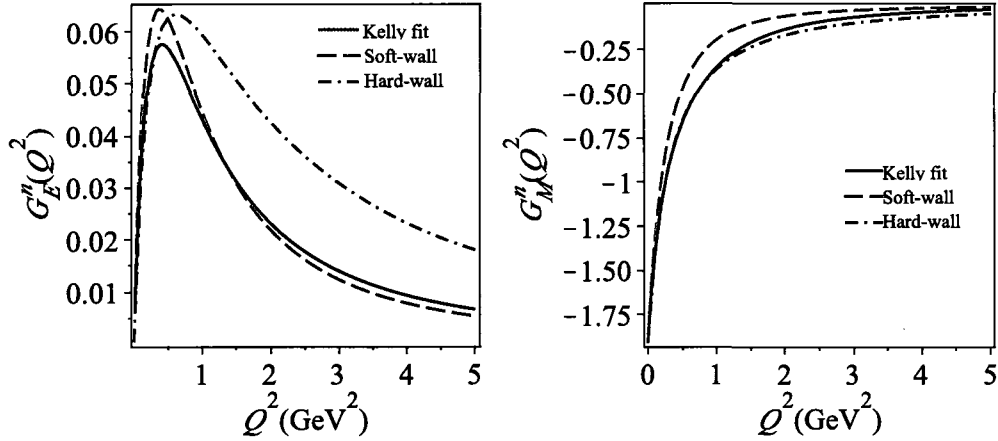
FIG. 6.2: The red dashed line and the purple dot-dashed line are the electromagnetic form factors of neutron from the soft-wall and the hard-wall model of AdS/QCD respectively. The solid blue line is the corresponding form factor from the Kelly empirical fit [115]

For the neutron, the charge radius is defined by

$$\langle r_C^2 \rangle_n = -6 \frac{dG_E(0)}{dQ^2}. \tag{6.55}$$

One obtains

$$\langle r_C^2 \rangle_n = \frac{\eta_N}{8\kappa^2} + \frac{6F_2^{(N)}(0)}{4m_p^2} = (-0.136\,\text{fm}^2), \tag{6.56}$$

which is an acceptably well result compared to the experiment $\langle r_C^2 \rangle = (-0.112\,\text{fm}^2)$.

For the hard-wall model, the bulk-to-boundary propagator is given by [21]

$$V(Q, z) = Qz \left(\frac{K_0(Qz_0)}{I_0(Qz_0)} I_1(Qz) + K_1(Qz) \right). \tag{6.57}$$

The parameter z_0 determines both the mass of the nucleon and ρ-meson. We set $z_0 = (0.245\,\text{GeV})^{-1}$, which fits the measured proton's mass.

In the large Q^2 region, $V(Q, z) \rightarrow QzK_1(Qz)$, which behaves like exponential. It has significant support near $z = 0$ only. Therefore, one can replace $\phi_R^2(z) \pm \phi_L^2(z)$ by its

approximate form near ε, that is, $\pm f_n^2 z^{4\alpha-2}$. One obtains

$$C_1(Q) = \frac{f_n^2}{2Q^{2\alpha}} \int_0^\infty dw\, w^{2\alpha} K_1(w), \tag{6.58}$$

$$C_2(Q) = \frac{f_n^2}{2Q^{2\alpha}} \int_0^\infty dw\, w^{2\alpha+1} K_0(w), \tag{6.59}$$

$$C_3(Q) = \frac{2m_n^2 f_n^2}{\alpha Q^{2\alpha+2}} \int_0^\infty dw\, w^{2\alpha+2} K_1(w), \tag{6.60}$$

where the integral can be solved analytically to obtain

$$C_1(Q) = 2^{\alpha-2}\alpha!(\alpha-1)!\frac{f_n^2}{Q^{2\alpha}}, \tag{6.61}$$

$$C_2(Q) = 2^{\alpha-1}(\alpha!)^2 \frac{f_n^2}{Q^{2\alpha}}, \tag{6.62}$$

$$C_2(Q) = 2^{\alpha+2}(\alpha-1)!(\alpha+1)!\, m_n^2 \frac{f_n^2}{Q^{2\alpha+2}} \tag{6.63}$$

Just as in the soft-wall model, the F_1 form factor falls off correctly like Q^{-4}, when $\alpha = 2$. Fixing the $F_2^{(P)}(0)$ to the experimental value 1.793, one obtains $\eta_P = 0.448$. Hence, for the proton

$$F_1^{(P)}(Q) = \frac{3.64}{Q^4}, \qquad F_2^{(P)}(Q) = \frac{12.37}{Q^6}. \tag{6.64}$$

For the neutron, fixing $F_2^{(N)}(0)$ to the experimental value -1.913, we have $\eta_N = -0.478$.

In the limit where $Q^2 \to 0$, the bulk-to-boundary propagator of the vector field can be expanded as

$$V(Q, z) = 1 - \frac{Q^2 z^2}{4}\left(1 - 2\ln\left(\frac{z}{z_0}\right)\right), \tag{6.65}$$

hence, in this limit,

$$\partial_z V(Q, z) = Q^2 z \ln\left(\frac{z}{z_0}\right). \tag{6.66}$$

Substituting Eq.(6.65) and Eq.(6.66) to Eq.(6.40-6.42) and taking the derivative with respect to Q^2, we obtain the Dirac radius for the proton $\langle r_1^2 \rangle_p = (0.843 \text{ fm})^2$, which corresponds to the charge radius $\langle r_C^2 \rangle_p = (0.910 \text{ fm})^2$. For the neutron, we obtain $\langle r_C^2 \rangle_n = (-0.125 \text{ fm}^2)$. These calculated charge radius are in better agreement with experimental results compared to the soft-wall model.

In Fig. 6.1 we show plots of G_E and G_M form factors using AdS/QCD model and compare it with empirical fit given in [114]. Figure 6.2 shows the corresponding plots for the neutron with the empirical fit given in [115].

6.4.2 Gravitational Form Factors

The most general structure of stress tensor matrix element for spin-$\frac{1}{2}$ particles can be written in terms of three form factors

$$\langle p_2, s_2 | T^{\mu\nu}(0) | p_1, s_1 \rangle = u(p_2, s_2) \left(A(Q) \gamma^{(\mu} p^{\nu)} + B(Q) \frac{ip^{(\mu} \sigma^{\nu)\alpha} q_\alpha}{2m_n} \right. \qquad (6.67)$$
$$\left. + C(Q) \frac{q^\mu q^\nu - q^2 \eta^{\mu\nu}}{m} \right) u(p_1, s_1),$$

where $p = (p_1 + p_2)/2$. This matrix element can be extracted from the following 3-point function

$$\langle 0 | \mathcal{T} \mathcal{O}_R^i(x) T^{\mu\nu}(y) \bar{\mathcal{O}}_R^j(w) | 0 \rangle . \qquad (6.68)$$

Stress tensor operator in 4D strongly coupled theory correspond to the metric perturbation in the bulk.

Consider a gravity-dilaton-tachyon action [42, 116], in addition to (6.5). The metric is perturb from its static solution according to $\eta_{\mu\nu} \rightarrow \eta_{\mu\nu} + h_{\mu\nu}$. The action in the second order perturbation becomes

$$S_{GR} = - \int d^5 x \, \frac{e^{-2\kappa^2 z^2}}{4z^3} \left(h_{\mu\nu,z} h^{\mu\nu}{}_{,z} + h_{\mu\nu} \Box h^{\mu\nu} \right) \qquad (6.69)$$

where the transverse-traceless gauge conditions, $\partial^\mu h_{\mu\nu} = 0$, and $h_\mu^\mu = 0$, have been imposed. The profile function of the metric perturbation satisfies the following linearized Einstein equation

$$\left[\partial_z \left(\frac{e^{-2\kappa^2 z^2}}{z^3} \partial_z \right) + \frac{e^{-2\kappa^2 z^2}}{z^3} p^2 \right] h(p, z) = 0, \qquad (6.70)$$

For the soft-wall model, the non-normalizable solution is given by

$$
\begin{aligned}
H(Q, z) &= \Gamma(a' + 2)U(a', -1; 2\xi), \\
&= a'(a' + 1) \int_0^1 dx \, x^{a'-1}(1 - x) \exp\left(\frac{-2\xi x}{1 - x}\right),
\end{aligned}
\tag{6.71}
$$

where $H(Q, z) \equiv h(q^2 = -Q^2, z)$ and $a' = a/2$. It satisfies $H(p, \varepsilon) = 1$ and vanishes at infinity. For the hard-wall model, imposing Neumann boundary condition $\partial_z H(p, z_0) = 0$, we have [34]

$$
H(Q, z) = \frac{(Qz)^2}{2}\left(\frac{K_1(Qz_0)}{I_1(Qz_0)}I_2(Qz) + K_2(Qz)\right).
\tag{6.72}
$$

In order to calculate (6.68), we will need terms in the 5D action in the form of $h\bar{\Psi}\Psi$. The vielbeins are modified according to $e^\mu{}_\alpha \to e^\mu{}_\alpha - zh^\mu_\alpha/2$. In the transverse-traceless gauge, the determinant of the metric is unchanged from the static solution. It can be shown that the following factor in the 5D action (6.5) is unchanged under perturbation

$$
\frac{1}{8}e^M{}_C \Gamma^C \omega_{MAB}[\Gamma^A, \Gamma^B].
\tag{6.73}
$$

Hence, remaining terms in the 5D action (6.5) relevant in calculating (6.68) are

$$
S_F^{(G)} = \int \frac{d^5x}{z^5}\left(\frac{-izh_{\mu\nu}}{4}\right)\left(\bar{\Psi}\Gamma^\mu \overleftrightarrow{\partial}^\nu \Psi\right).
\tag{6.74}
$$

Fourier transforming the fields

$$
\begin{aligned}
S_F^{(G)} &= \int \frac{dz}{z^{2M}}e^{-\kappa^2 z^2} \int \frac{d^4p_2 d^4q d^4p_1}{(2\pi)^{12}}(2\pi)^4\delta^4(p_2 - q - p_1)\,\bar{\Psi}_L^0(p_2)h^0_{\mu\nu}(q)H(q, z) \\
&\quad \times \frac{-1}{2}\left(f_L(p_2, z)f_L(p_1, z)\gamma^\mu p^\nu + f_R(p_2, z)f_R(p_1, z)\frac{\slashed{p}_2}{p_2}\gamma^\mu p^\nu \frac{\slashed{p}_1}{p_1}\right)\Psi_L(p_1),
\end{aligned}
\tag{6.75}
$$

where $H(Q, z)$ is the bulk-to-boundary propagator defined by $h_{\mu\nu}(q, z) = H(q, z)h^0_{\mu\nu}(q)$ and $h^0_{\mu\nu}(q)$ acts as a source for the 4D stress tensor operator.

Lorentz structure of Eq.(6.75) shows that only A form factor present. We obtain

$$
A(Q) = \int dz \, \frac{e^{-\kappa^2 z^2}}{2z^{2M}}H(Q, z)\left(\psi_L^2(z) + \psi_R^2(z)\right).
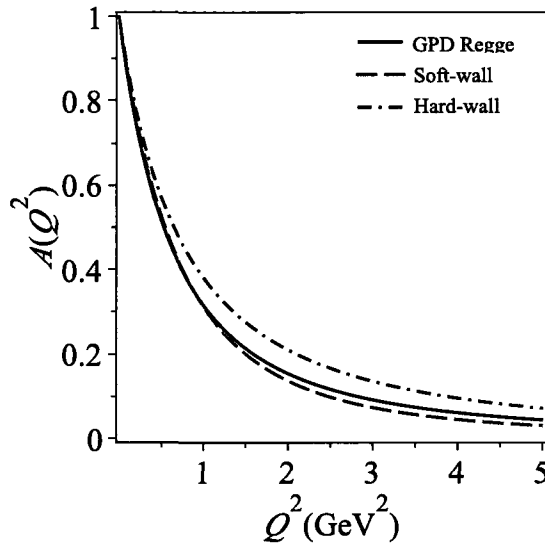\tag{6.76}
$$

FIG. 6.3: The red dashed line is the gravitational form factor from the soft-wall model, while the solid blue line is the corresponding form factor from the integral of a GPD model [100], and the purple dot-dash line is for the hard-wall model.

For the soft-wall model, an analytical solution can be obtained. In particular, for $n = 0$

$$A(Q^2) = (a' + 1)\left[- \left(1 + a' + 2a'^2\right) + 2\left(a' + 2a'^3\right)\Phi(-1, 1, a')\right], \qquad (6.77)$$

where $\Phi(-1, 1, a')$ is the LerchPhi function. Results are shown graphically in Fig. 6.3 for both the hard-wall and soft-wall models, and compared to results obtained by integrating a model for the nucleon GPDs [100].

The corresponding gravitational radius is

$$\left\langle r_G^2 \right\rangle = -\frac{6}{A(0)}\frac{dA(0)}{dQ^2} = \frac{3\ln(2)}{2\kappa^2} = (0.575\,\text{fm})^2, \qquad (6.78)$$

which is slightly smaller than the gravitational radius obtained from the second moment integral of the modified Regge GPD model, *i.e.*, 0.608 fm, and notably smaller than the proton charge radius.

6.5 Conclusions

We have studied baryon form factors using the AdS/QCD correspondence, and have modeled the baryons using fundamental fermions in the extra dimensional theory. We have given results for both the soft-wall and hard-wall models for both electromagnetic form factors and for the gravitational form factor $A(Q^2)$, the momentum form factor.

The soft-wall model has extra interactions whose effect is to effectively cut off propagation as one gets deeply into the extra dimension. Originally, the soft-wall exponential modifications were simply inserted [31] in order to obtain an excited hadron spectrum more in accord with observation, but it has been shown [42, 116] how to obtain the exponential factors in a dynamical model including kinetic terms and a scalar potential for explicit dilaton and tachyon degrees of freedom. We have followed the latter implementation here, noting that it leads to different numerical coefficients in the argument of the exponential for the vector and graviton sectors. For the baryon sector, we implemented the soft-wall model by including also a harmonic oscillator-like scalar potential added to the mass term [116].

In the bottom-up approach to modeling QCD via 5D theories and the AdS/CFT correspondence, the terms in the 5D Lagrangian are chosen based on simplicity, symmetries, and relevance to the quantities under study. However, the most simple vector-fermion interaction yields only a Dirac form factor, so a Pauli term must be introduced in the 5D action. This means that the overall normalization of the F_2 form factors is not determined *ab initio*, but the shape of the form factors is fixed.

Our results for the form factors were presented both algebraically and graphically over some Q^2 range, with the radii corresponding to each form factor given explicitly. In all cases, radii measured from gravitational form factors are smaller that radii measured from electromagnetic form factors. This accords with similar observations from lattice gauge theory [117], and one may attribute it to the fact that higher momentum fraction

matter, quarks or gluons, is more heavily weighted in the momentum sum rule, and high momentum fraction partons tend to have a narrower transverse size distribution [118].

CHAPTER 7

Conclusions

Quantum Chromodynamics (QCD) has been generally accepted as the correct description of strong interaction. However, the non-perturbative aspect of QCD is far from being understood. The gauge/gravity or AdS/CFT correspondence offers the possibility of relating nonperturbative quantities in theories akin to QCD in four dimensions to weakly coupled five dimensional gravitational theories.

A bottom-up AdS/QCD approach has been used, by constructing five dimensional Lagrangian with field contents that match four dimensional operators. Many aspects of QCD can be reproduced such as chiral symmetry breaking, confinement. Quantitatively, the results obtained from the AdS/QCD model agrees up to 20% with experimental data, or other methods (when available).

In Chapter 2, the gravitational form factors of rho mesons are calculated. These provide restrictions on the generalized parton distributions of vector mesons, via the sum rules connecting stress tensor form factors to generalized parton distributions. We concentrate on the traceless part of the stress tensor, which suffices to fix the momentum and angular momentum sum rules. The vector mesons appear noticeably more compact measured by the gravitational form factors than by the charge form factor.

118

In Chapter 3, the gravitational form factors of pions and $a1$ mesons are calculated. One (of the two) pion gravitational form factors is directly related to the second moment of the pion generalized parton distribution, thus providing a sum rule for the latter. As was also the case for vector mesons, both the pion and the axial-vector mesons appear strikingly more compact measured by the gravitational form factor than by the electro-magnetic form factor.

Generalization of the AdS/QCD model to include the strange quark is performed in Chapter 4. We present a calculation of the K_{l3} transition form factors using the AdS/QCD correspondence. The normalization of the form factors is a crucial ingredient for extract-ing $|V_{us}|$ from data, and the results obtained here agree well with results from chiral pertur-bation theory and lattice gauge theory. The slopes and curvature of the form factors agree well with the data, and with what results are available from other methods of calculation.

In Chapter 5, we examine the spatial density within extended objects of the momen-tum component p^+, and find relativistically exact connections to Fourier transforms of gravitational form factors. We apply these results to obtain semiempirical momentum density distributions within nucleons, and similar distributions for spin-1 objects based on theoretical results from the AdS/QCD correspondence. We find that the momentum density in the transverse plane is more compact than the charge density.

Finally in Chapter 6, we have studied electromagnetic and gravitational form factors for baryons, in a scheme where the baryons are treated as independent particles in AdS space. The form factors were calculated both in the case of so called hard-wall and soft-wall model. The simplest fermion Lagrangian for the five dimensional curved space does not contribute to the F_2 form factor unless one add a Pauli term which also contributes to the F_1 form factor.

BIBLIOGRAPHY

[1] M. Gell-Mann, Phys. Rev. **125**, 1067 (1962).

[2] J. D. Bjorken, Phys. Rev. **179**, 1547 (1969).

[3] G. Ecker, Prog. Part. Nucl. Phys. **35**, 1 (1995), `hep-ph/9501357`.

[4] G. 't Hooft, Nucl. Phys. **B72**, 461 (1974).

[5] J. F. Donoghue, E. Golowich, and B. R. Holstein, Camb. Monogr. Part. Phys. Nucl. Phys. Cosmol. **2**, 1 (1992).

[6] A. V. Manohar (1998), `hep-ph/9802419`.

[7] J. Polchinski, Phys. Rev. Lett. **75**, 4724 (1995), `hep-th/9510017`.

[8] J. M. Maldacena, Adv. Theor. Math. Phys. **2**, 231 (1998), `hep-th/9711200`.

[9] A. Karch and E. Katz, JHEP **06**, 043 (2002), `hep-th/0205236`.

[10] J. Babington, J. Erdmenger, N. J. Evans, Z. Guralnik, and I. Kirsch, Phys. Rev. **D69**, 066007 (2004), `hep-th/0306018`.

[11] M. Kruczenski, D. Mateos, R. C. Myers, and D. J. Winters, JHEP **07**, 049 (2003), `hep-th/0304032`.

[12] T. Sakai and S. Sugimoto, Prog. Theor. Phys. **113**, 843 (2005), `hep-th/0412141`.

[13] J. Erlich, E. Katz, D. T. Son, and M. A. Stephanov, Phys. Rev. Lett. **95**, 261602 (2005), hep-ph/0501128.

[14] L. Da Rold and A. Pomarol, Nucl. Phys. **B721**, 79 (2005), hep-ph/0501218.

[15] J. Hirn and V. Sanz, JHEP **12**, 030 (2005), hep-ph/0507049.

[16] M. E. Peskin and D. V. Schroeder (1995), reading, USA: Addison-Wesley (1995) 842 p.

[17] E. Witten, Adv. Theor. Math. Phys. **2**, 253 (1998), hep-th/9802150.

[18] L. Da Rold and A. Pomarol, JHEP **01**, 157 (2006), hep-ph/0510268.

[19] A. Cherman, T. D. Cohen, and E. S. Werbos, Phys. Rev. **C79**, 045203 (2009), 0804.1096.

[20] J. I. Kapusta, T. M. Kelley, and T. Gherghetta (2009), 0908.0725.

[21] H. R. Grigoryan and A. V. Radyushkin, Phys. Lett. **B650**, 421 (2007), hep-ph/0703069.

[22] H. J. Kwee and R. F. Lebed, JHEP **01**, 027 (2008), 0708.4054.

[23] H. R. Grigoryan and A. V. Radyushkin, Phys. Rev. **D76**, 115007 (2007), 0709.0500.

[24] S. R. Amendolia et al., Phys. Lett. **B138**, 454 (1984).

[25] V. Tadevosyan et al. (Jefferson Lab F(pi)), Phys. Rev. **C75**, 055205 (2007), nucl-ex/0607007.

[26] T. Horn et al. (Jefferson Lab F(pi)-2), Phys. Rev. Lett. **97**, 192001 (2006), nucl-ex/0607005.

[27] B. G. Lasscock, J. Hedditch, D. B. Leinweber, and A. G. Williams, PoS **LAT2006**, 114 (2006), hep-lat/0611029.

[28] C. Amsler et al. (Particle Data Group), Phys. Lett. **B667**, 1 (esp. pp. 717ff for the $K_{\ell 3}$ form factors), (2008).

[29] S. J. Brodsky and J. R. Hiller, Phys. Rev. **D46**, 2141 (1992).

[30] P. L. Chung, W. N. Polyzou, F. Coester, and B. D. Keister, Phys. Rev. **C37**, 2000 (1988).

[31] A. Karch, E. Katz, D. T. Son, and M. A. Stephanov, Phys. Rev. **D74**, 015005 (2006), hep-ph/0602229.

[32] H. R. Grigoryan and A. V. Radyushkin, Phys. Rev. **D76**, 095007 (2007), 0706.1543.

[33] J. Hirn, N. Rius, and V. Sanz, Phys. Rev. **D73**, 085005 (2006), hep-ph/0512240.

[34] Z. Abidin and C. E. Carlson, Phys. Rev. **D77**, 095007 (2008), 0801.3839.

[35] Z. Abidin and C. E. Carlson, Phys. Rev. **D77**, 115021 (2008), 0804.0214.

[36] S. J. Brodsky and G. F. de Teramond, Phys. Rev. **D78**, 025032 (2008), 0804.0452.

[37] J. P. Shock and F. Wu, JHEP **08**, 023 (2006), hep-ph/0603142.

[38] Z. Abidin and C. E. Carlson, Phys. Rev. **D80**, 115010 (2009), 0908.2452.

[39] S. J. Brodsky and G. F. de Teramond, Phys. Lett. **B582**, 211 (2004), hep-th/0310227.

[40] S. J. Brodsky and G. F. de Teramond, Phys. Rev. Lett. **96**, 201601 (2006), hep-ph/0602252.

[41] S. J. Brodsky and G. F. de Teramond, Phys. Rev. **D77**, 056007 (2008), 0707.3859.

[42] B. Batell and T. Gherghetta, Phys. Rev. **D78**, 026002 (2008), 0801.4383.

[43] H. R. Grigoryan and A. V. Radyushkin, Phys. Rev. **D77**, 115024 (2008), 0803.1143.

[44] T. Hambye, B. Hassanain, J. March-Russell, and M. Schvellinger, Phys. Rev. **D76**, 125017 (2007), hep-ph/0612010.

[45] G. F. de Teramond and S. J. Brodsky, Phys. Rev. Lett. **94**, 201601 (2005), hep-th/0501022.

[46] A. Pomarol and A. Wulzer, JHEP **03**, 051 (2008), 0712.3276.

[47] A. Pomarol and A. Wulzer, Nucl. Phys. **B809**, 347 (2009), 0807.0316.

[48] C. P. Herzog, Phys. Rev. Lett. **98**, 091601 (2007), hep-th/0608151.

[49] C. A. Ballon Bayona, H. Boschi-Filho, N. R. F. Braga, and L. A. Pando Zayas, Phys. Rev. **D77**, 046002 (2008), 0705.1529.

[50] N. Arkani-Hamed, M. Porrati, and L. Randall, JHEP **08**, 017 (2001), hep-th/0012148.

[51] T. Schafer, Phys. Rev. **D77**, 126010 (2008), 0711.0236.

[52] N. Evans and A. Tedder, Phys. Rev. Lett. **100**, 162003 (2008), 0711.0300.

[53] J. Erdmenger, N. Evans, I. Kirsch, and E. Threlfall, Eur. Phys. J. **A35**, 81 (2008), 0711.4467.

[54] X.-D. Ji, Phys. Rev. Lett. **78**, 610 (1997), hep-ph/9603249.

[55] M. Diehl, Phys. Rept. **388**, 41 (2003), hep-ph/0307382.

[56] E. R. Berger, F. Cano, M. Diehl, and B. Pire, Phys. Rev. Lett. **87**, 142302 (2001), hep-ph/0106192.

[57] S. J. Brodsky, D. S. Hwang, B.-Q. Ma, and I. Schmidt, Nucl. Phys. **B593**, 311 (2001), hep-th/0003082.

[58] R. G. Arnold, C. E. Carlson, and F. Gross, Phys. Rev. **C21**, 1426 (1980).

[59] M. S. Bhagwat and P. Maris, Phys. Rev. **C77**, 025203 (2008), nucl-th/0612069.

[60] J. N. Hedditch et al., Phys. Rev. **D75**, 094504 (2007), hep-lat/0703014.

[61] C. E. Carlson and F. Gross, Phys. Rev. Lett. **53**, 127 (1984).

[62] C. E. Carlson and C.-R. Ji, Phys. Rev. **D67**, 116002 (2003), hep-ph/0301213.

[63] J. Polchinski and M. J. Strassler, Phys. Rev. Lett. **88**, 031601 (2002), hep-th/0109174.

[64] S. J. Brodsky and G. R. Farrar, Phys. Rev. **D11**, 1309 (1975).

[65] S. S. Gubser, I. R. Klebanov, and A. M. Polyakov, Phys. Lett. **B428**, 105 (1998), hep-th/9802109.

[66] H. Boschi-Filho, N. R. F. Braga, and H. L. Carrion, Phys. Rev. **D73**, 047901 (2006), hep-th/0507063.

[67] M. V. Polyakov and C. Weiss, Phys. Rev. **D60**, 114017 (1999), hep-ph/9902451.

[68] D. T. Son and A. O. Starinets, Ann. Rev. Nucl. Part. Sci. **57**, 95 (2007), 0704.0240.

[69] J. Garriga and T. Tanaka, Phys. Rev. Lett. **84**, 2778 (2000), hep-th/9911055.

[70] W. M. Yao et al. (Particle Data Group), J. Phys. **G33**, 1 (2006).

[71] M. V. Polyakov, Fizika **B8**, 335 (1999), hep-ph/9901315.

[72] J. Polchinski and M. J. Strassler, JHEP **05**, 012 (2003), hep-th/0209211.

[73] H. R. Grigoryan and A. V. Radyushkin, Phys. Rev. **D78**, 115008 (2008), 0808.1243.

[74] H. J. Kwee and R. F. Lebed, Phys. Rev. **D77**, 115007 (2008), 0712.1811.

[75] Z. Abidin and C. E. Carlson, Phys. Rev. **D78**, 071502 (2008), 0808.3097.

[76] Z. Abidin and C. E. Carlson, Phys. Rev. **D79**, 115003 (2009), 0903.4818.

[77] H. Leutwyler and M. Roos, Z. Phys. **C25**, 91 (1984).

[78] J. Bijnens and P. Talavera, Nucl. Phys. **B669**, 341 (2003), hep-ph/0303103.

[79] V. Cirigliano et al., JHEP **04**, 006 (2005), hep-ph/0503108.

[80] M. Jamin, J. A. Oller, and A. Pich, Phys. Rev. **D74**, 074009 (2006), hep-ph/0605095.

[81] D. Becirevic et al., Nucl. Phys. **B705**, 339 (2005), hep-ph/0403217.

[82] C. Dawson, T. Izubuchi, T. Kaneko, S. Sasaki, and A. Soni, Phys. Rev. **D74**, 114502 (2006), hep-ph/0607162.

[83] P. A. Boyle et al., Phys. Rev. Lett. **100**, 141601 (2008), 0710.5136.

[84] J. M. Flynn et al. (2008), 0812.4265.

[85] V. Lubicz, F. Mescia, S. Simula, C. Tarantino, and f. t. E. Collaboration (2009), 0906.4728.

[86] M. Gell-Mann, R. J. Oakes, and B. Renner, Phys. Rev. **175**, 2195 (1968).

[87] E. Katz and M. D. Schwartz, JHEP **08**, 077 (2007), 0705.0534.

[88] J. Erlich, PoS **CONFINEMENT8**, 032 (2008), 0812.4976.

[89] M. Antonelli et al. (FlaviaNet Working Group on Kaon Decays) (2008), 0801.1817.

[90] M. Burkardt, Int. J. Mod. Phys. **A18**, 173 (2003), hep-ph/0207047.

[91] G. A. Miller, Phys. Rev. Lett. **99**, 112001 (2007), 0705.2409.

[92] C. E. Carlson and M. Vanderhaeghen, Phys. Rev. Lett. **100**, 032004 (2008), 0710.0835.

[93] X.-D. Ji, J. Phys. **G24**, 1181 (1998), hep-ph/9807358.

[94] K. Goeke, M. V. Polyakov, and M. Vanderhaeghen, Prog. Part. Nucl. Phys. **47**, 401 (2001), hep-ph/0106012.

[95] A. V. Belitsky and A. V. Radyushkin, Phys. Rept. **418**, 1 (2005), hep-ph/0504030.

[96] S. Boffi and B. Pasquini, Riv. Nuovo Cim. **30**, 387 (2007), 0711.2625.

[97] M. V. Polyakov, Phys. Lett. **B555**, 57 (2003), hep-ph/0210165.

[98] M. Burkardt, Phys. Rev. **D62**, 071503 (2000), hep-ph/0005108.

[99] C. E. Carlson and M. Vanderhaeghen, Eur. Phys. J. **A41**, 1 (2009), 0807.4537.

[100] M. Guidal, M. V. Polyakov, A. V. Radyushkin, and M. Vanderhaeghen, Phys. Rev. **D72**, 054013 (2005), hep-ph/0410251.

[101] L. Frankfurt, C. E. Hyde, M. Strikman, and C. Weiss, Phys. Rev. **D75**, 054009 (2007), hep-ph/0608271.

[102] A. D. Martin, R. G. Roberts, W. J. Stirling, and R. S. Thorne, Phys. Lett. **B531**, 216 (2002), hep-ph/0201127.

[103] H. R. Grigoryan, Unpublished (2008).

[104] H. Hata, T. Sakai, S. Sugimoto, and S. Yamato, Prog. Theor. Phys. **117**, 1157 (2007), hep-th/0701280.

[105] M. Henningson and K. Sfetsos, Phys. Lett. **B431**, 63 (1998), hep-th/9803251.

[106] W. Mueck and K. S. Viswanathan, Phys. Rev. **D58**, 106006 (1998), hep-th/9805145.

[107] R. Contino and A. Pomarol, JHEP **11**, 058 (2004), hep-th/0406257.

[108] D. K. Hong, T. Inami, and H.-U. Yee, Phys. Lett. **B646**, 165 (2007), hep-ph/0609270.

[109] D. K. Hong, M. Rho, H.-U. Yee, and P. Yi, Phys. Rev. **D76**, 061901 (2007), hep-th/0701276.

[110] D. K. Hong, M. Rho, H.-U. Yee, and P. Yi, JHEP **09**, 063 (2007), 0705.2632.

[111] D. K. Hong, M. Rho, H.-U. Yee, and P. Yi, Phys. Rev. **D77**, 014030 (2008), 0710.4615.

[112] L. M. Brown, Phys. Rev. **111**, 957 (1958).

[113] S. I. A. Abramowitz, M. (1972).

[114] J. Arrington, W. Melnitchouk, and J. A. Tjon, Phys. Rev. **C76**, 035205 (2007), 0707.1861.

[115] J. J. Kelly, Phys. Rev. **C70**, 068202 (2004).

[116] B. Batell, T. Gherghetta, and D. Sword, Phys. Rev. **D78**, 116011 (2008), 0808.3977.

[117] P. Hagler et al. (LHPC), Phys. Rev. **D77**, 094502 (2008), 0705.4295.

[118] M. Burkardt, Phys. Rev. **D66**, 114005 (2002), hep-ph/0209179.

VITA

Zainul Abidin

Zainul was born on December 19, 1981 in Parepare, South Sulawesi, Indonesia. He began his formal education in 1988 at SDN 35 Elementary School in Parepare. Six years later, he entered SMPN 01 Junior High School in Parepare. In 1997, he leave his hometown to entered SMUN 02 High School in Tinggimoncong, South Sulawesi, Indonesia. In 2000, he participated in the International Physics Olympiad in Leicester, England, and won an Honorable Mention. Later, in the same year, he attended Institut Teknologi Bandung, in West Java, Indonesia. He graduated in 2004 with bachelor degree in Physics. Afterward, he worked as a trainer for the Indonesian Physics Olympiad Team. He attended College of William and Mary, in Virginia, in the fall of 2005 and in the following year started to work with Prof. Carl Carlson.